MINIMIZING THE UNCERTAINTIES IN DEPTH PREDICTION OF CARBONATE STRUCTURE IN CENTRAL LUCONIA PROVINCE, OFFSHORE SARAWAK

MAZLAN BIN MD TAHIR

PETROLEUM GEOSCIENCE
UNIVERSITI TEKNOLOGI PETRONAS
JANUARY 2008

STATUS OF THESIS

MINIMIZING THE UNCERTAINTIES IN DEPTH PREDICTION OF CARBONATE STRUCTURE IN CENTRAL LUCONIA PROVINCE, OFFSHORE SARAWAK

I, **MAZLAN BIN MD TAHIR** hereby allow my thesis to be placed at the Information Resource Center (IRC) of Universiti Teknologi PETRONAS (UTP) with the following conditions:

1. The thesis becomes the property of UTP
2. The IRC of UTP may make copies of the thesis for academic purposes only
3. The thesis is classified as

[X] Confidential

[ ] Non-confidential

If this thesis is confidential, please state the reason:

As instructed by Petroleum Management Unit (PMU), PETRONAS

The contents of the thesis will remain confidential for _____ years.

Remarks on disclosure:

Endorse by

Petroleum Resource Assessment
and Marketing,
Petroleum Management Unit,
Petroliam Nasional Berhad,
Level 22, Tower 2,
PETRONAS Twin Towers,
Kuala Lumpur City Centre,
50088 Kuala Lumpur

Date: 18th February 2008

Petroleum Resource Assessment
and Marketing,
Petroleum Management Unit,
Petroliam Nasional Berhad,
Level 22, Tower 2,
PETRONAS Twin Towers,
Kuala Lumpur City Centre,
50088 Kuala Lumpur

Date: 18th February 2008

APPROVAL PAGE

UNIVERSITI TEKNOLOGI PETRONAS

Approval by Supervisor (s)

The undersigned certify that they have read, and recommend to The Postgraduate Studies Programme for acceptance, a thesis entitled "**Minimizing the Uncertainties in Depth Prediction of Carbonate Structure in Central Luconia Province, Offshore Sarawak**" submitted by **Mazlan bin Md Tahir** for the fulfilment of the requirements for the degree of master of science in Petroleum Geoscience.

Date: 18th February 2008

Signature : _____

Main Supervisor : En. Che Shaari Abdullah

Date : 18th February 2008

Co-Supervisor 1 : _____

Co-Supervisor 2 : _____

TITLE PAGE

UNIVERSITI TEKNOLOGI PETRONAS

MINIMIZING THE UNCERTAINTIES IN DEPTH PREDICTION OF CARBONATE STRUCTURE IN CENTRAL LUCONIA PROVINCE, OFFSHORE SARAWAK

By

MAZLAN BIN MD TAHIR

A THESIS

SUBMITTED TO THE POSTGRADUATE STUDIES PROGRAMME

AS A REQUIREMENT FOR THE

DEGREE OF MASTER OF SCIENCE

IN PETROLEUM GEOSCIENCE

BANDAR SERI ISKANDAR,

PERAK

JANUARY, 2008

DECLARATION

I hereby declare that the thesis is based on my original work except for quotations and citations which have been duly acknowledged. I also declare that it has not been previously or concurrently submitted for any other degree at UTP or other institutions.

Signature : 

Name : Mazlan bin Md Tahir

Date : 18th February 2008

ACKNOWLEDGEMENT

I am very grateful to my supervisor, En. Che Shaari Abdullah (Staff Geoscientist, PRAM, PMU, PETRONAS) for his interesting insight and invaluable guidance. Also, I would like to thank Mr. Mike Brumby (Director and Asian Regional Manager, Petrosys), Mr. Ji Ping (Manager, PRAM, PMU, PETRONAS) and Mr. Alwyn Chung Kwang Tjet (Geoscientist, PRAM, PMU, PETRONAS) for their constructive criticism and fruitful discussion as well as to my colleagues for their support.

ABSTRACT

The objective of this case study is to reduce the uncertainties in depth prediction of the target carbonate reservoir by mapping optimum interval velocities in the overlying sequences. Lithology facies variations have very significant impact on the lateral and vertical velocity behaviour of geologic formation. The area covering Block SK316 and SK310, offshore Sarawak, East Malaysia where the carbonate pinnacle structure is the target reservoir has been chosen for the study. Five major horizons had been identified and interpreted which are Seabed, Near Cycle VII, Near Cycle VI, Near Cycle V and Near Cycle IV (Top of carbonate) using the seismic line vintage 1994. Two softwares had been used in this case study which are SeisWorks, Landmark Graphic software (for interpretation purposes) and Petrosys software (for mapping purposes). By finding the interval velocity models for the major stratigraphic sequences and depth structure map of the target reservoir, we can improve the depth structure map of the carbonate pinnacle reservoir and reduce the uncertainties in hydrocarbon volume estimation.

ABSTRAK

Objektif kajian kes ini adalah untuk mengurangkan ketidakpastian didalam meramalkan kedalaman sasaran takungan karbonat. Ini dapat dilakukan dengan proses pemetaan halaju selang yang optimum bagi setiap lapisan. Variasi terhadap fasies litologi memberi kesan yang penting bagi sifat atau tingkah laku halaju secara menegak dan sisian didalam pembentukan geologi. Kawasan Blok SK316 dan SK310 di luar persisiran Sarawak telah dipilih dalam kajian kes ini di mana sasaran takungan adalah merupakan karbonat yang mempunyai struktur berbentuk puncak. Lima lapisan tanah telah dikenalpasti dan ditafsirkan adalah *"Seabed"*, *"Near Cycle VII"*, *"Near Cycle VI"*, *"Near Cycle V"* dan *"Near Cycle IV"* (Kemuncak karbonat) dengan menggunakan garisan seismos 1994. Dua perisian komputer telah digunakan didalam kajian kes ini iaitu perisian SeisWorks, Landmark Graphic (digunakan untuk tujuan pentafsiran) dan perisian Petrosys (digunakan untuk tujuan pemetaan). Dengan mencari model halaju selang bagi setiap susunan stratigrafik utama dan peta struktur kedalaman sasaran takuangan, kita dapat memperbaiki peta struktur kedalaman bagi takungan karbonat berbentuk puncak dan juga dapat mengurangkan ketidakpastian didalam membuat anggaran isipadu hidrokarbon.

LIST OF CONTENTS

LIST OF TABLES

LIST OF FIGURES

LIST OF SYMBOLS

km	kilometer
m	meter
Ma	million years
msec or ms	millisecond
sec or s	second
V	velocity
&	and
°	degree
′	minutes
″	second

LIST OF ABBREVIATIONS

2D	Two dimension
GR	Gamma Ray
Int	Interval
INTVEL	Interval velocity
KB	Kelly Bushing
Max	Maximum
MD	Measured depth
Min	Minimum
MSL	Mean Sea Level
NE	North West
NNE	North North East
OK/NG	OK/Not Good
OWT	One way time
SS	Subsea
SSW	South South West
TD	Total depth
TVD	True vertical depth
TWT	Two-way-time
T-Z	Time-Depth
UTM	Universal Transverse Mercator
VSP	Vertical Seismic profile
WDF	Petrosys Well Data Editor File

CHAPTER 1

INTRODUCTION

1.1 OBJECTIVE

The objective of this case study is to reduce the uncertainties in depth prediction by finding optimum velocity on each layer. This is because of variations of vertical and lateral velocity. The vertical and lateral velocity variations introduce significant uncertainties in reservoir depth prediction and depth structure mapping of carbonate pinnacle in Central Luconia province, offshore Sarawak. By finding optimum velocity model, it can refine the accuracy.

1.2 FOCUS AREA

The area of this case study is in East Central Luconia province, offshore Sarawak in Block SK316 and SK310 (Fig. 1.1 and Fig. 1.2). The area size is approximately 2820 km^2 with water depths ranging from 70 m to 118 m and the main reservoirs here are carbonates of Miocene age.

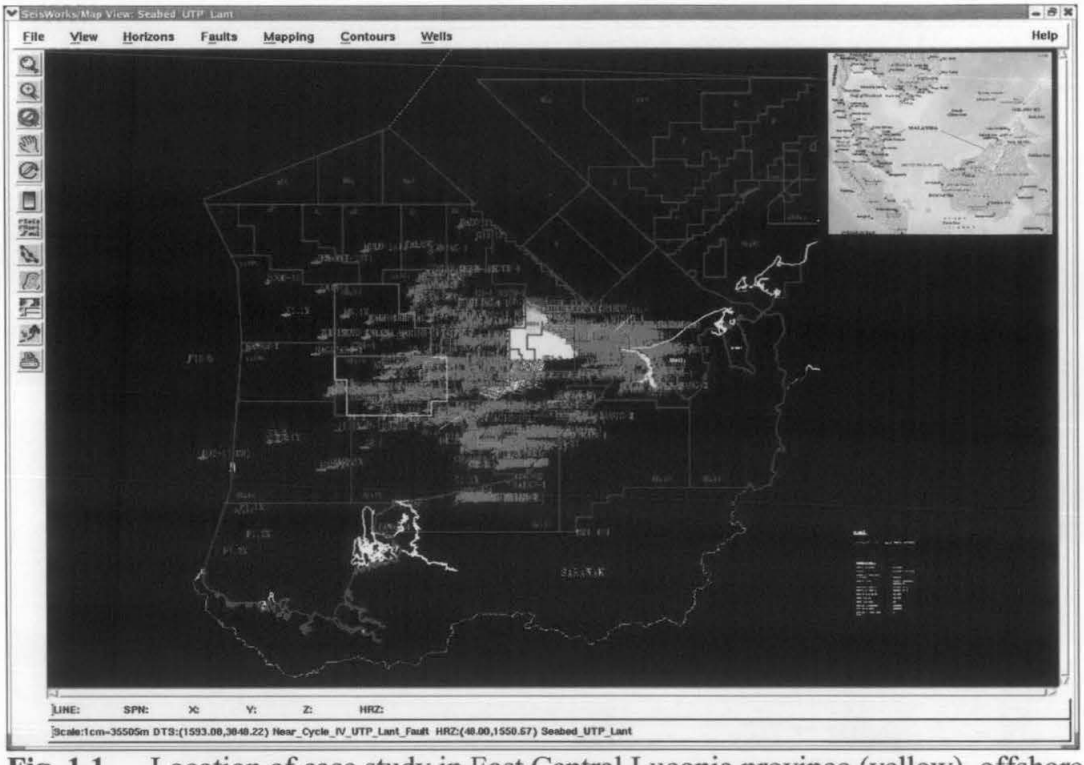

Fig. 1.1 Location of case study in East Central Luconia province (yellow), offshore Sarawak in Block SK316 and SK310. Small map at the upper right corner is a map of Malaysia.

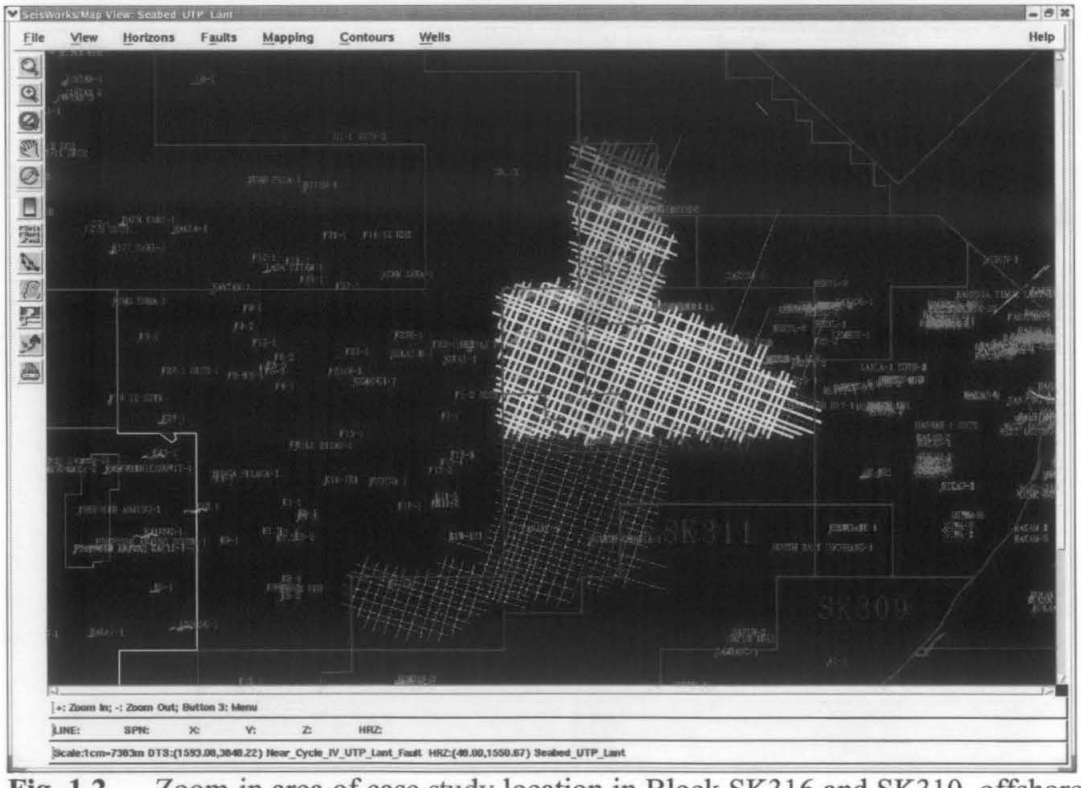

Fig. 1.2 Zoom-in area of case study location in Block SK316 and SK310, offshore Sarawak.

1.3 DATABASE

1.3.1 SEISMIC DATA

Seismic data (2D) vintage 88, 94 and 93 have been used is this case study (Fig. 1.3). But, interpreted horizons tracking is based only on seismic line vintage 94. Seismic line vintage 88 and vintage 93 have seismic misties problems due to difference in acquisition and processing parameters.

The seismic line vintage 94, data quality is considered good from seabed down to top of carbonate (Near Cycle IV) and seismic markers are relatively easy to correlate. But in NE of Block SK316, the seismic data is poor because of major fault zone. Below the carbonate layer (Near Cycle IV), the seismic quality deteriorates (Fig 1.6).

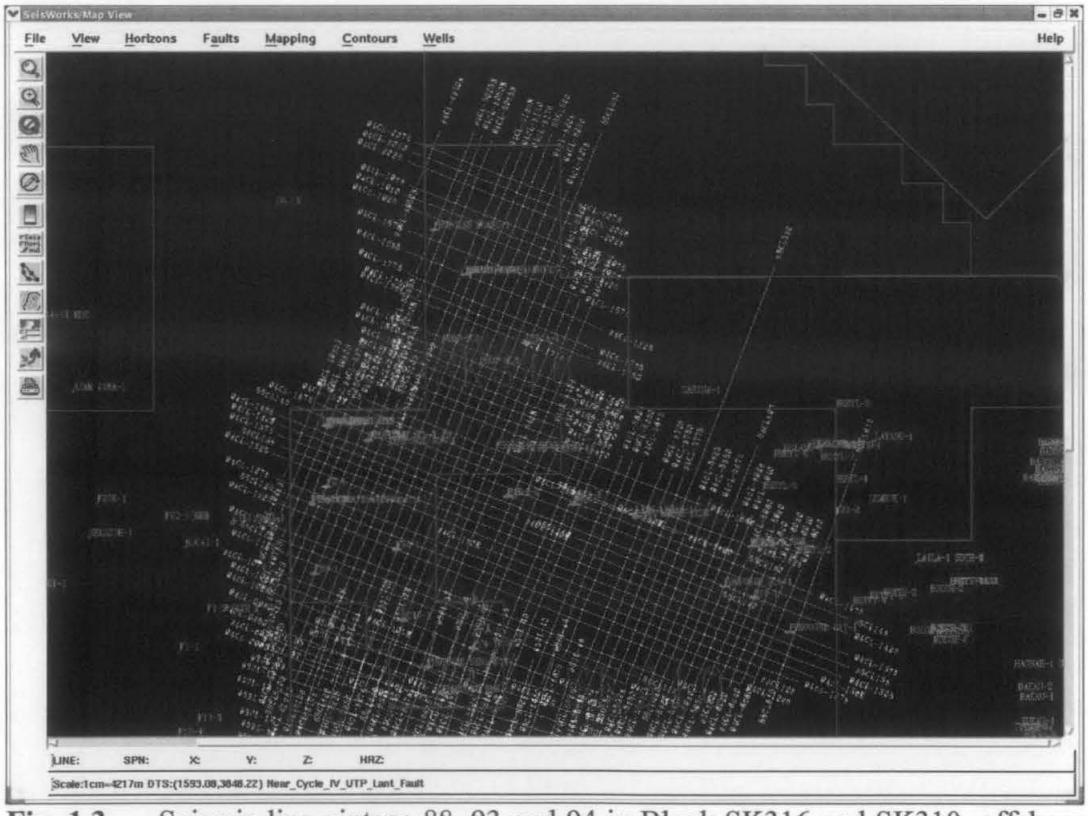

Fig. 1.3 Seismic line vintage 88, 93 and 94 in Block SK316 and SK310, offshore Sarawak.

1.3.2 WELL DATA

Eight wells, Kenari-1, NC4-1, F2-1, F39-1, F38-1, NC10-1, PC4-1 and B16-1 have been chosen as well control for this case study. Below are locations of those wells (Fig. 1.4)

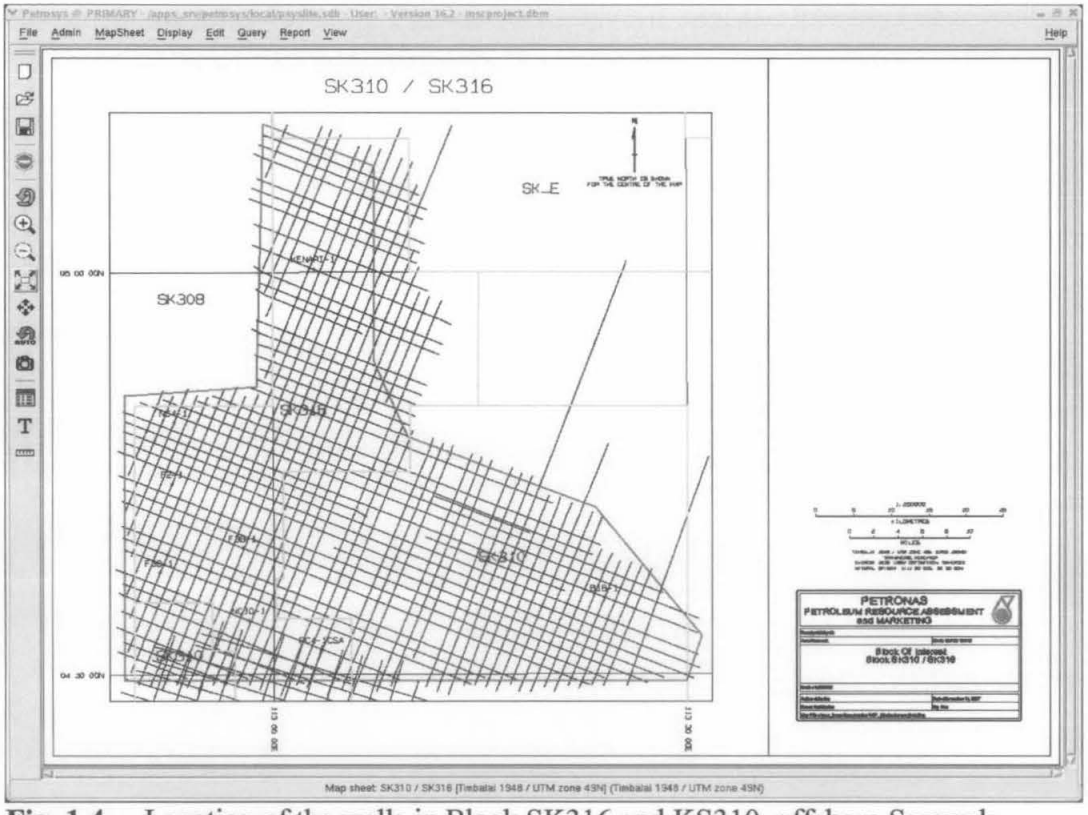

Fig. 1.4 Location of the wells in Block SK316 and KS310, offshore Sarawak.

The distance between these wells in Block SK316 and SK310 has been identified (Table 1.1). From the table, the nearest well is about 8 km between NC4-1 and F2-1 and the furthest is about 62 km between F2-1 and B16-1.

Distance (m)	PC4-1	NC10-1	F39-1	F38-1	F2-1	NC4-1	KENARI-1	B16-1
PC4-1		10814	24235	17842	30610	37290	52532	38527
NC10-1	10814		13557	9906	21341	28934	49040	47896
F39-1	24235	13557		11606	12347	20736	46570	59780
F38-1	17842	9906	11606		12938	19525	39545	49058
F2-1	30610	21341	12347	12938		8419	35078	60092
NC4-1	37290	28934	20736	19525	8419		28215	62570
KENARI-1	52532	49040	46570	39545	35078	28215		59745
B16-1	38527	47896	59780	49058	60092	62570	59745	

Table 1.1 Distance between wells in Block SK316 and SK310, offshore Sarawak.

1.3.3 WIRELINE DATA

Wireline data such as *GR* and Sonic data of each well are also used for interpretation purposes.

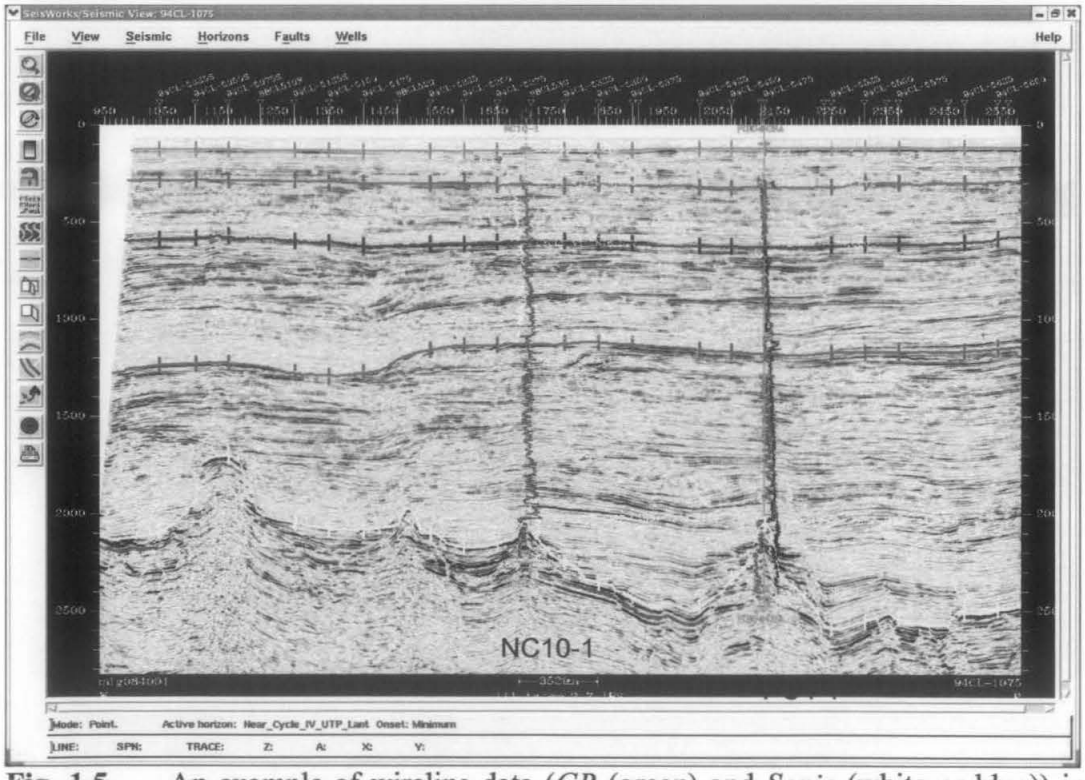

Fig. 1.5 An example of wireline data (*GR* (green) and *Sonic* (white or blue)) in NC10-1 and PC4-1 well that have been used to identify and to help in each horizon interpretation.

1.4 COMPETENCIES

The competencies required are as follows:

i. Proficiency in velocity concept and wireline sonic data analysis.
ii. Familiarity in using workstation based seismic interpretation – SeisWorks, Landmark Graphic software.
iii. Skill in using mapping software – Petrosys software.

CHAPTER 2

LITERATURE REVIEW

2.1 GENERAL GEOLOGICAL SETTING OF CENTRAL LUCONIA PROVINCE

Central Luconia province in offshore Sarawak lies immediately North of Balingian Province and is flanked by the clastic depocenters of the Baram Delta to the East and the West Luconia Province to the west (Fig. 2.1). Relatively stable conditions have prevailed since early Middle Miocene time.

The area is characterised by fairly continuous subsidence and is unaffected by strong folding. The most important features of the Province are the Middle Miocene carbonate reef buildups. The tops of the main carbonates form a diachronous horizon, younger in the North and older to the South. The reefs are flanked and overlain by clastic sequences of the same or younger age, resulting from an overall northwards regional regression during the Middle Miocene (Ho, 1978; Doust, 1981).

The Central Luconia province is a broad and stable continental shelf platform, characterised by extensive development of Late Miocene carbonates. More than 2000 carbonate buildups have been seismically mapped and some 65 buildups have been tested (M. Yamin, 1999; Abolins P., 1999)

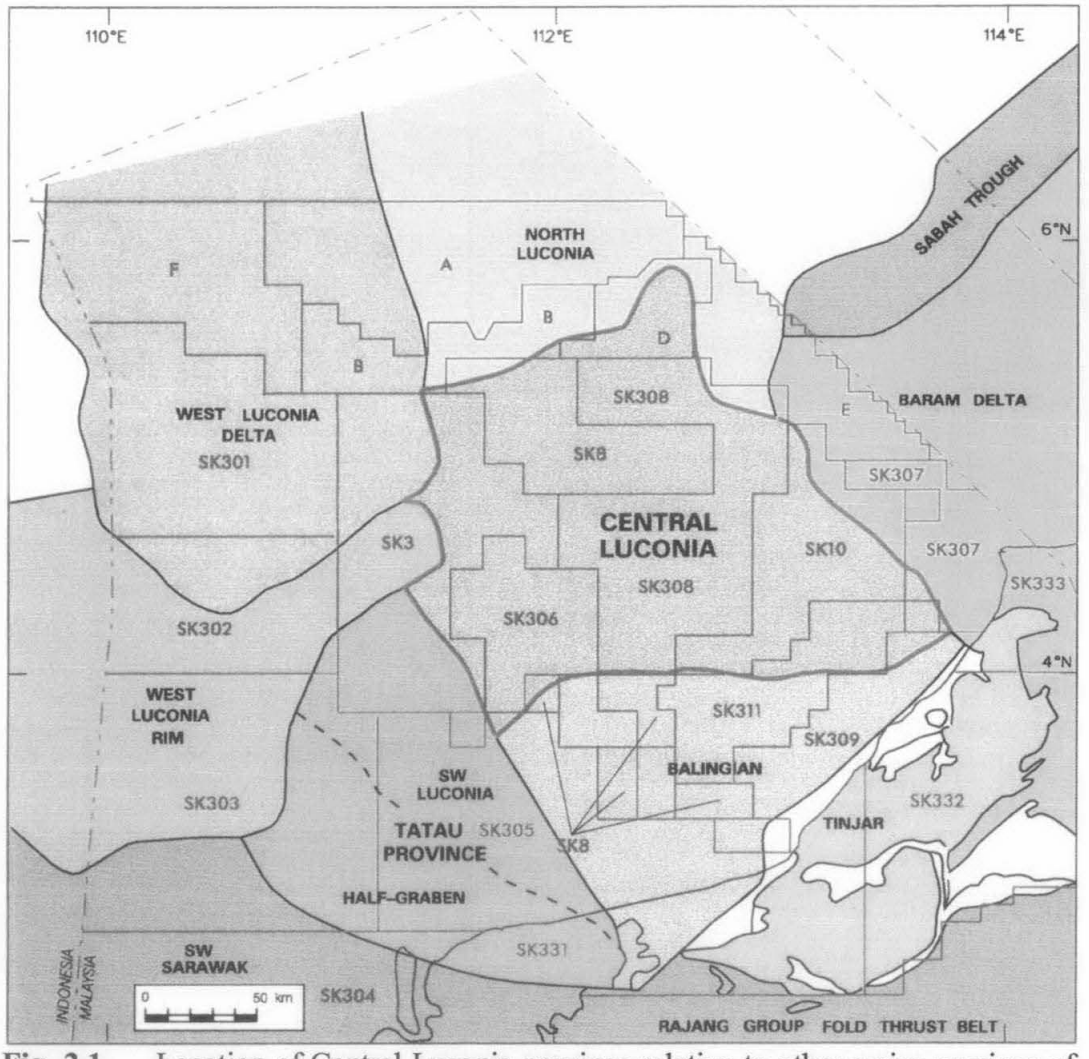

Fig. 2.1 Location of Central Luconia province relative to other major province of Northern Borneo (M. Yamin 1999; Abolins P., 1999).

2.2 STRUCTURAL FRAMEWORK

The province is characterised by a network of NNE – SSW trending faults which divide the zone into a somewhat elevated central block with flanking depressions and basinal areas. To the East and West, the basin floor descends below younger deltaic sediments associated with the Baram Delta and the East Natuna area.

The principal localised structures are associated with the pinnacles and the flat-topped mounds and platform.

2.3 STRATIGRAPHY

Carbonate deposition began during the widespread subsidence of the Middle Miocene (Cycle IV) at a time when this part of the shelf lay well away from the coastline and in an open marine environment. Bank deposits to thickness of 200-300 meters were developed on areas of structural elevation. Maximum transgression took place during the Middle to Upper Miocene (Cycle V) and widespread reefs and reef-associated carbonates were developed (Epting, 1980).

Some carbonate buildups exceed 20 kilometers in length and 1.5 kilometers in thickness. During this period, the Baram and Rajang-Lupar deltas began to prograde offshore and by the end of Near Cycle V had extended over much of Balingian and the Southern part of Luconia, burying several of the smaller buildups in their path (M. Yamin, 1999; Abolins P., 1999). Below is the stratigraphic section of this case study (Fig. 2.2).

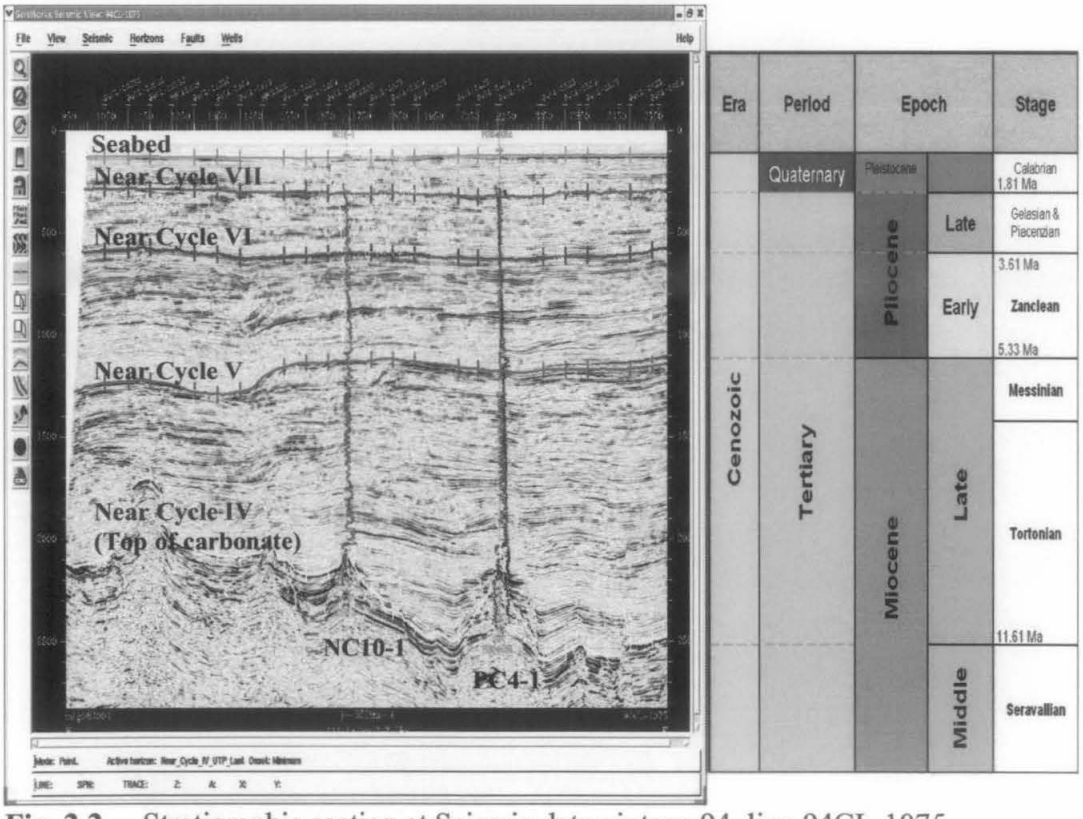

Fig. 2.2 Stratigraphic section at Seismic data vintage 94, line 94CL-1075.

CHAPTER 3

METHODOLOGY

3.1 DATA COLLECTION / PREPARATION

Data gathering started from the first week of August. The data included the reports from PETRONAS UDRS, well data, paper review, etc. All seismic lines were already loaded in the workstation as this is a continuation of the project that was done in 2005 by Petroleum Management Unit (PMU), PETRONAS.

3.2 WORKFLOW

Below is the general workflow of this case study (Fig. 3.1). Inputs such as seismic data (vintage 88, 93 and 94), wells data (Kenari-1, NC4-1, F2-1, F39-1, F38-1, NC10-1, PC4-1 and B16-1) and wireline data (*GR* and Sonic) were loaded into the server workstation. Well to seismic tie was done on each well. This is to tie on seismic lines (time domain) and the top of geological formations identified on the wireline well logging interpretation (depth domain) by using time-depth relationship.

By knowing the time-depth relationship from the VSP or checkshot of each well, we can estimate the depth of each horizon interpreted. From here, we can do the gridding and contouring process to generate the interval velocity map and depth structure map.

Workflow 1 shows precise detail to generate the interval velocity map (Fig. 3.2). Workflow 2 shows the detail to generate depth map of each horizon (Fig. 3.3).

General Workflow:

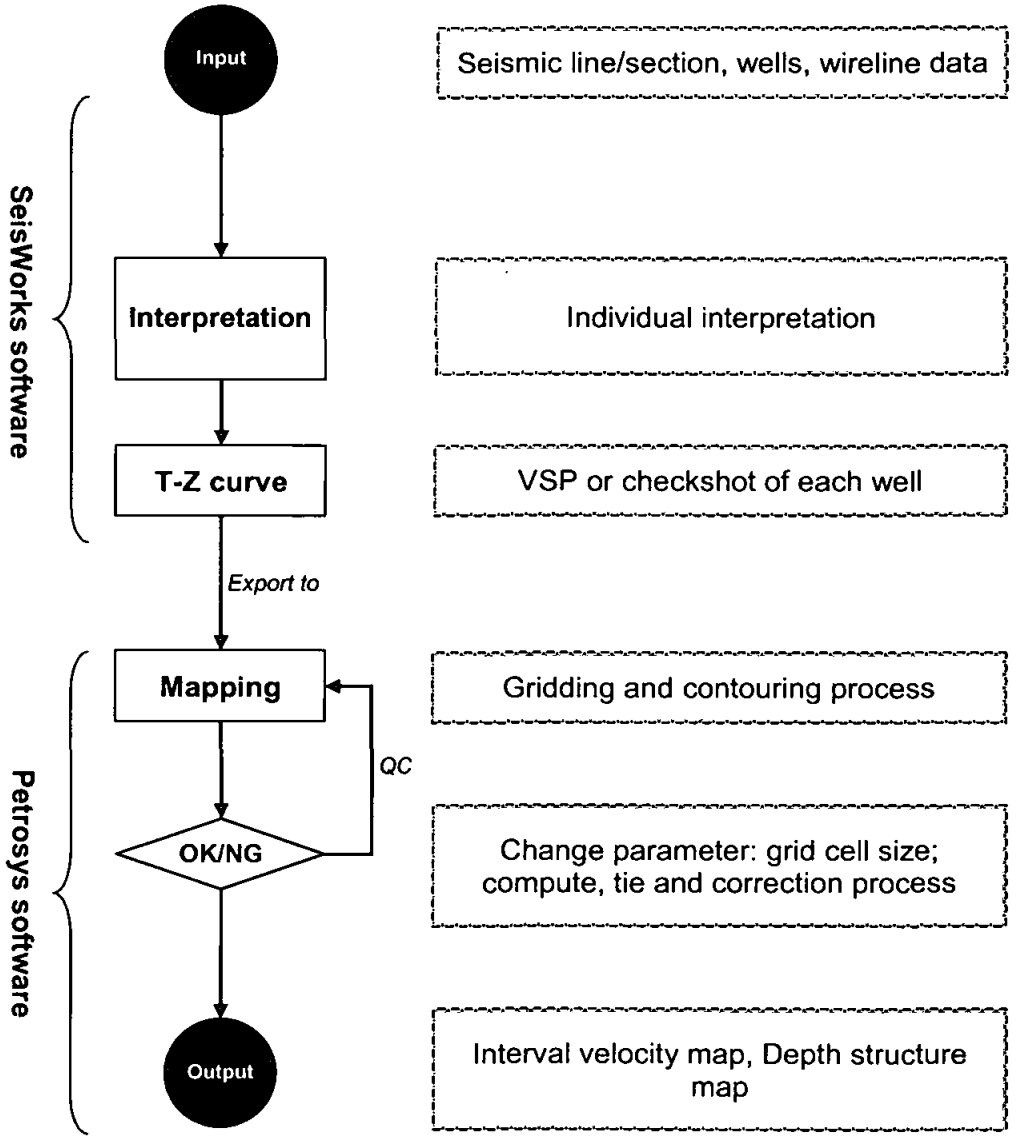

Fig. 3.1 General workflow of case study.

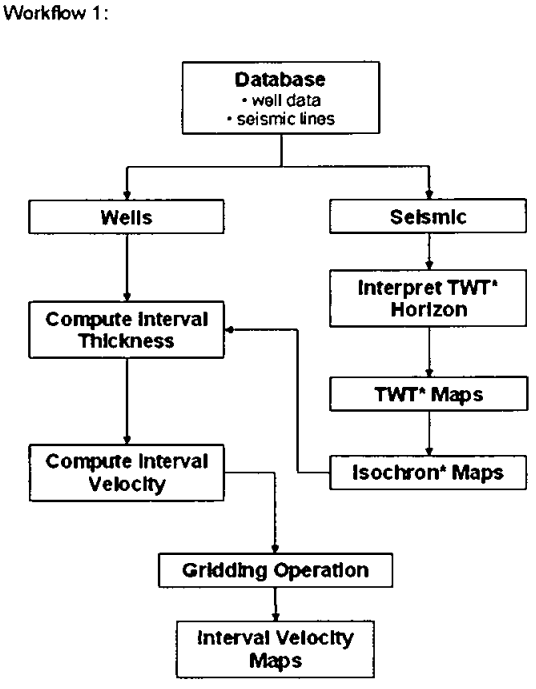

Fig. 3.2 Workflow to generate the interval velocity map on each layer.

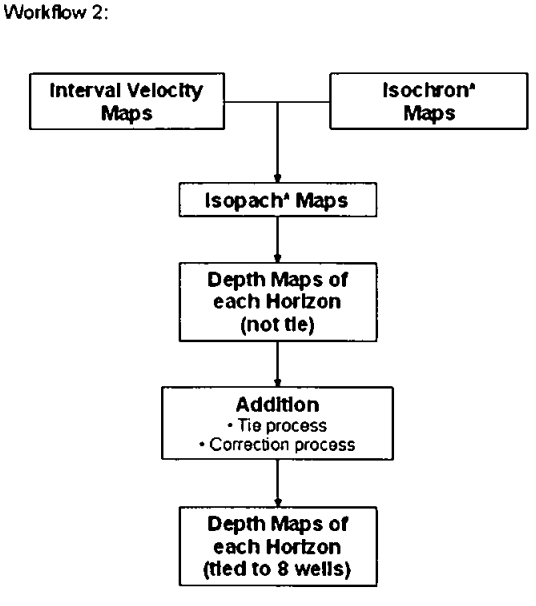

Fig. 3.3 Workflow to generate depth contour map of each horizon.

3.3 SEISMIC INTERPRETATION

The seismic interpretation was done using SeisWorks, Landmark Graphic software. It took about 2 months to interpret all horizons (Seabed, Near Cycle VII, Near Cycle VI, Near Cycle V, Near Cycle IV). The interpreted horizons are based on the unconformity picking on the seismic section (Homewood, 1999), *GR* and Sonic curve of each well (Schlumberger, 1989). In this case study, five (5) horizons as follows had been identified and interpreted (Fig. 3.4):

i. Seabed
ii. Near Cycle VII
iii. Near Cycle VI
iv. Near Cycle V
v. Near Cycle IV (Top of carbonate)

Each horizon tracking is based on seismic line vintage 94 only. Seismic line vintage 93 and vintage 88 have seismic misties problems due to difference in acquisition and processing. Interpretation was not attempted in NE of block SK316 due to poor seismic data, results of major fault zone.

Well NC10-1 and PC4-1 are used as main well control (Fig. 3.4).

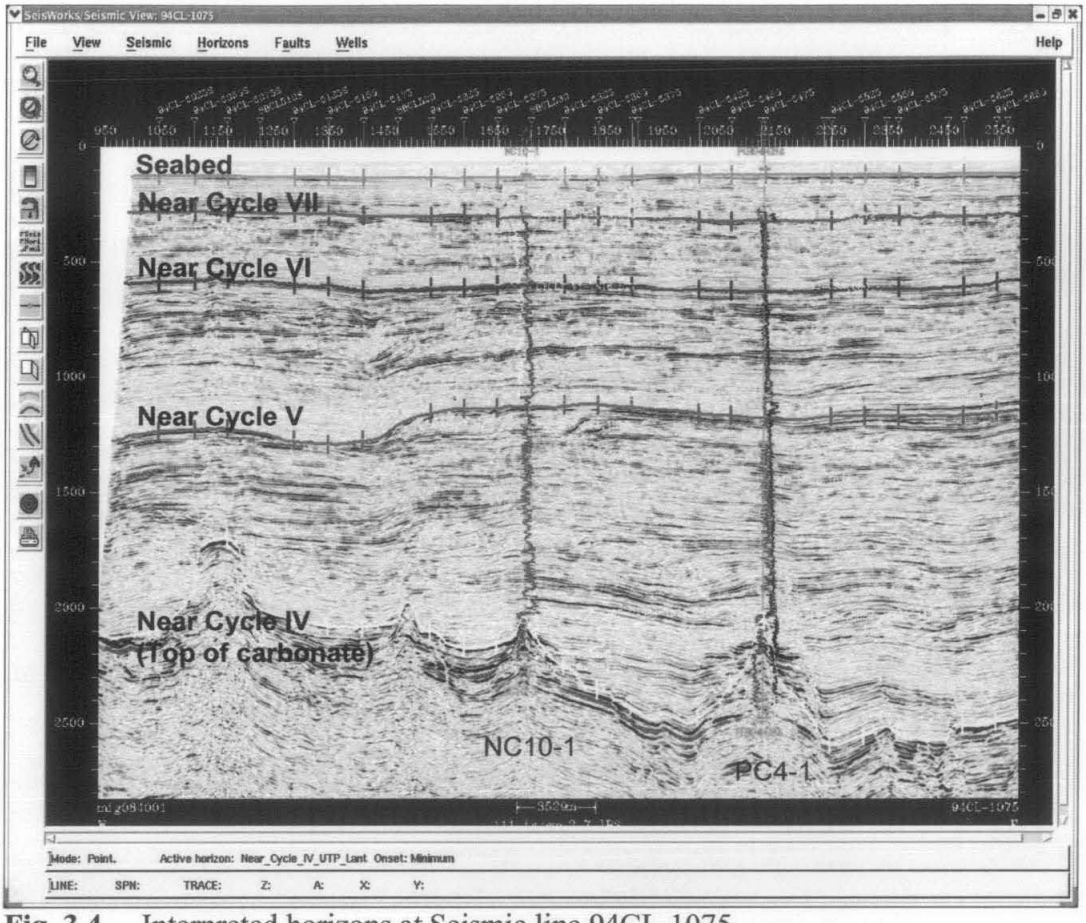

Fig. 3.4 Interpreted horizons at Seismic line 94CL-1075.

3.4 TIME-DEPTH RELATIONSHIP MODELING

Interpretation was done on seismic section in time domain. But, in real life, wells are drilled in depth domain. Here, we need to know the time-depth relationship. Thus, we can estimate and know the prediction depth of the horizon interpreted. Below are 2 examples of Vertical Seismic Profile (VSP) and checkshot taken at well NC10-1 and well PC4-1 (Fig. 3.5 and Fig. 3.6).

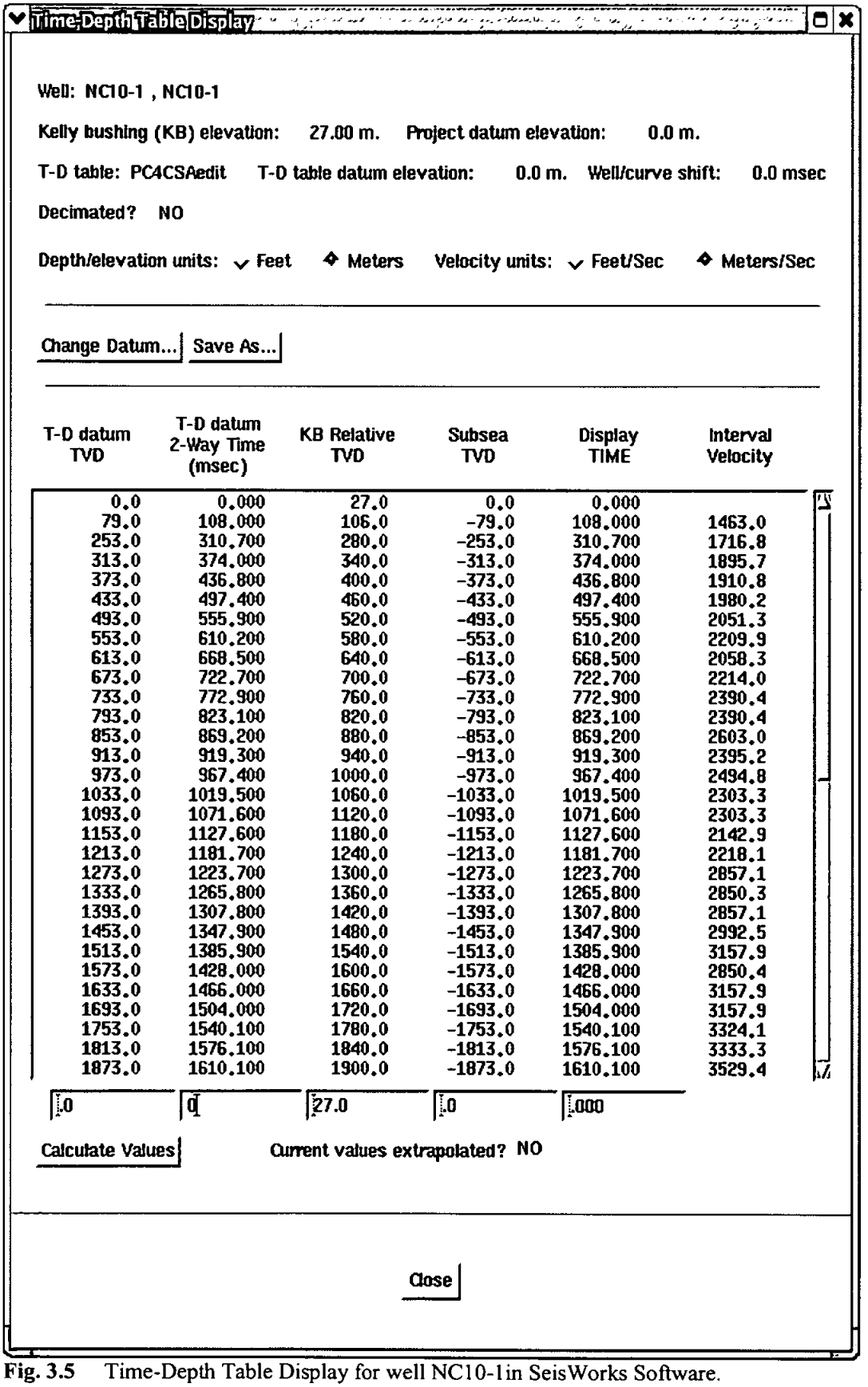

Fig. 3.5 Time-Depth Table Display for well NC10-1in SeisWorks Software.

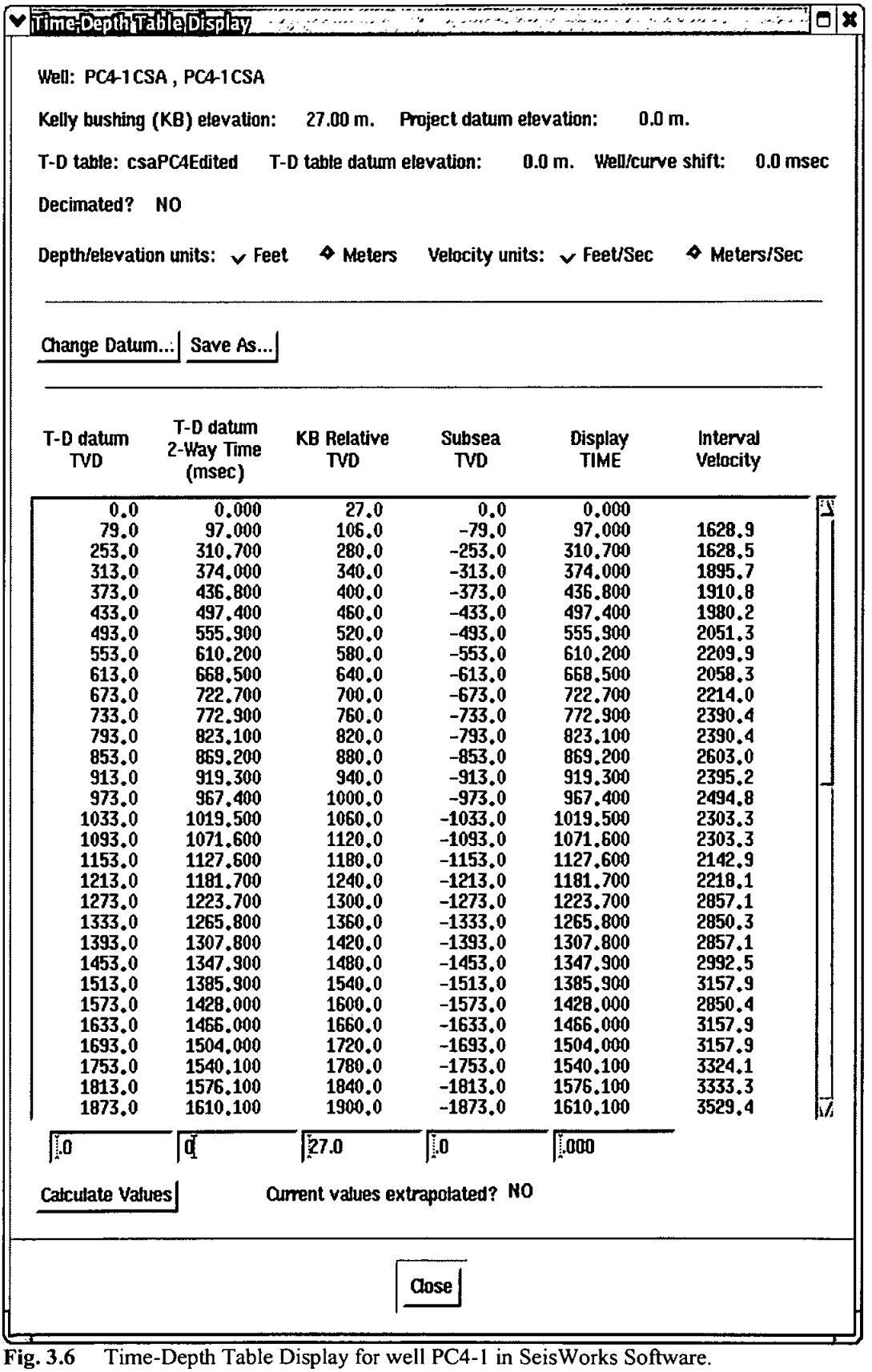

T-D datum TVD	T-D datum 2-Way Time (msec)	KB Relative TVD	Subsea TVD	Display TIME	Interval Velocity
0.0	0.000	27.0	0.0	0.000	
79.0	97.000	106.0	-79.0	97.000	1628.9
253.0	310.700	280.0	-253.0	310.700	1628.5
313.0	374.000	340.0	-313.0	374.000	1895.7
373.0	436.800	400.0	-373.0	436.800	1910.8
433.0	497.400	460.0	-433.0	497.400	1980.2
493.0	555.900	520.0	-493.0	555.900	2051.3
553.0	610.200	580.0	-553.0	610.200	2209.9
613.0	668.500	640.0	-613.0	668.500	2058.3
673.0	722.700	700.0	-673.0	722.700	2214.0
733.0	772.900	760.0	-733.0	772.900	2390.4
793.0	823.100	820.0	-793.0	823.100	2390.4
853.0	869.200	880.0	-853.0	869.200	2603.0
913.0	919.300	940.0	-913.0	919.300	2395.2
973.0	967.400	1000.0	-973.0	967.400	2494.8
1033.0	1019.500	1060.0	-1033.0	1019.500	2303.3
1093.0	1071.600	1120.0	-1093.0	1071.600	2303.3
1153.0	1127.600	1180.0	-1153.0	1127.600	2142.9
1213.0	1181.700	1240.0	-1213.0	1181.700	2218.1
1273.0	1223.700	1300.0	-1273.0	1223.700	2857.1
1333.0	1265.800	1360.0	-1333.0	1265.800	2850.3
1393.0	1307.800	1420.0	-1393.0	1307.800	2857.1
1453.0	1347.900	1480.0	-1453.0	1347.900	2992.5
1513.0	1385.900	1540.0	-1513.0	1385.900	3157.9
1573.0	1428.000	1600.0	-1573.0	1428.000	2850.4
1633.0	1466.000	1660.0	-1633.0	1466.000	3157.9
1693.0	1504.000	1720.0	-1693.0	1504.000	3157.9
1753.0	1540.100	1780.0	-1753.0	1540.100	3324.1
1813.0	1576.100	1840.0	-1813.0	1576.100	3333.3
1873.0	1610.100	1900.0	-1873.0	1610.100	3529.4
.0	0	27.0	.0	.000	

Fig. 3.6 Time-Depth Table Display for well PC4-1 in SeisWorks Software.

3.5 INTERVAL VELOCITY CALCULATION

In this case study, 8 wells are been used as the well control. From formula below, we can easily calculate the interval velocity between horizons.

$$V_{\text{int}}(ms^{-1}) = \frac{Depth_{\text{int}}(m)}{Time(OWT)_{\text{int}}(s)} \tag{1}$$

Using Petrosys software, this interval velocity values can be calculate using WDF spreadsheet (Fig 3.7).

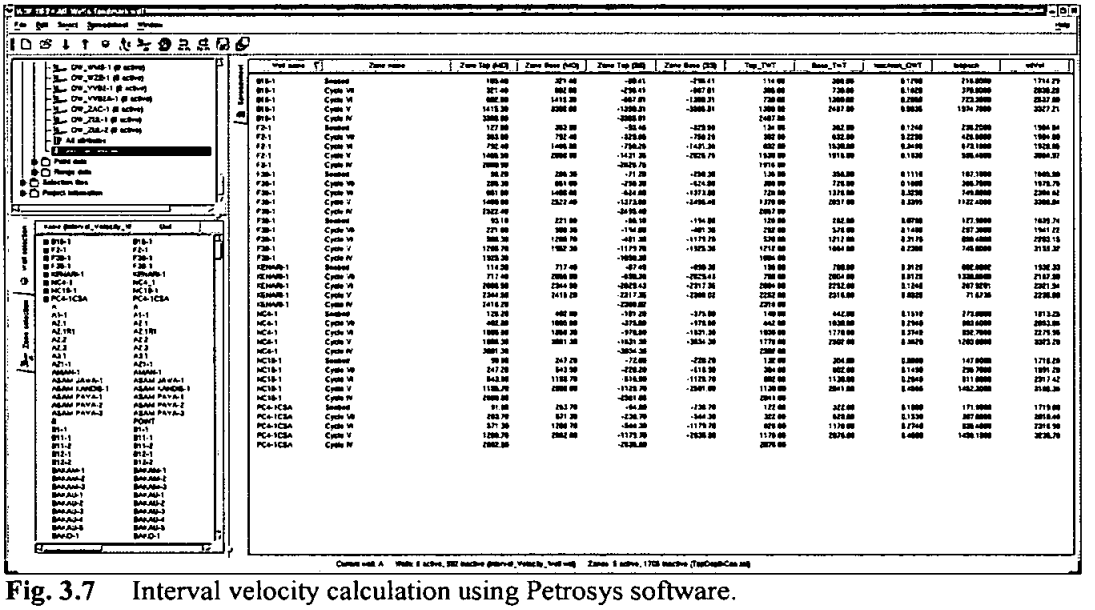

Fig. 3.7 Interval velocity calculation using Petrosys software.

3.6 MAPPING

All the horizons in SeisWorks have been transferred to Petrosys software to continue with mapping process. Details of the mapping projection are listed below:

Projection	:	Universal Transverse Mercator
UTM Zone	:	49N (EPSG 29849)
Spheroid	:	Everest 1830 (1967 Definition)
Hemisphere	:	Northern
Natural origin	:	[111° 00'00''E, 00° 00' 00''N]

Five horizons had been mapped in the Petrosys software. Several types of map that had been done such as TWT contour maps, isochron contour maps, isopach contour maps, depth contour maps and some depth correction maps.

CHAPTER 4

RESULTS & DISCUSSION

4.1 STUDY AREA EXTENT

The following figures are the area extent of each interpreted horizons in Block SK316 and SK310 by using seismic lines vintage 94 in SeisWorks (Fig. 4.1 – Fig. 4.5).

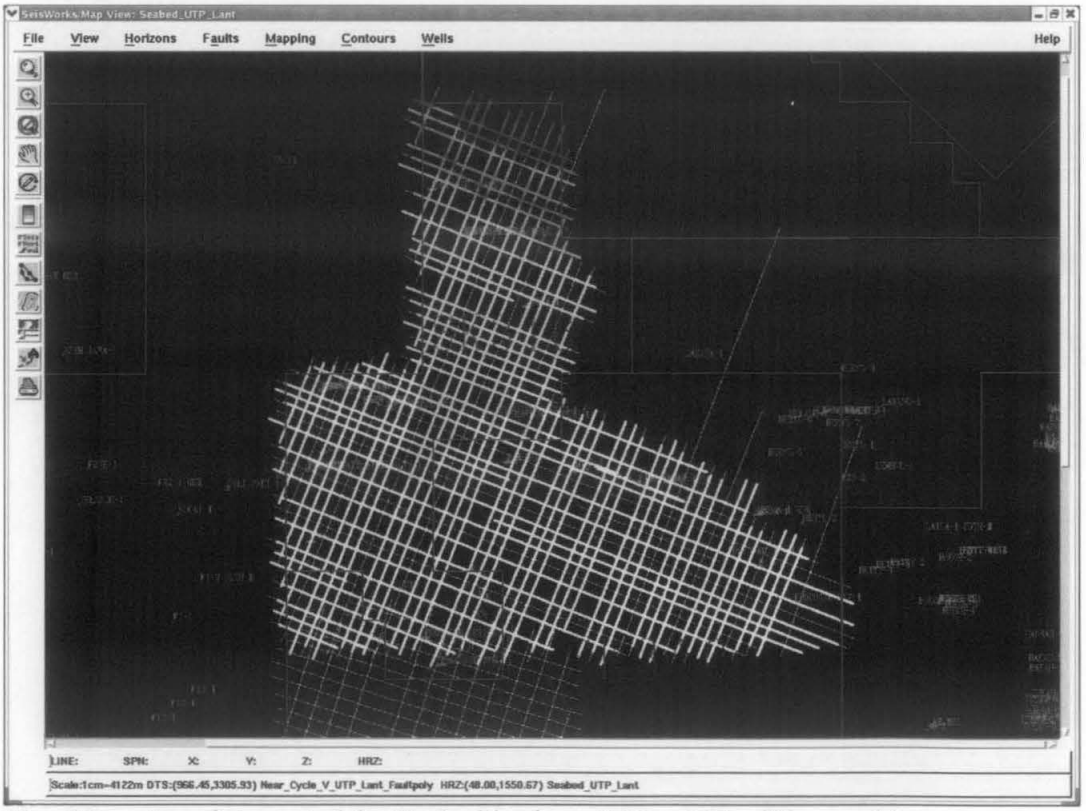

Fig. 4.1 Area interpreted for Seabed horizon (100 – 500 milliseconds).

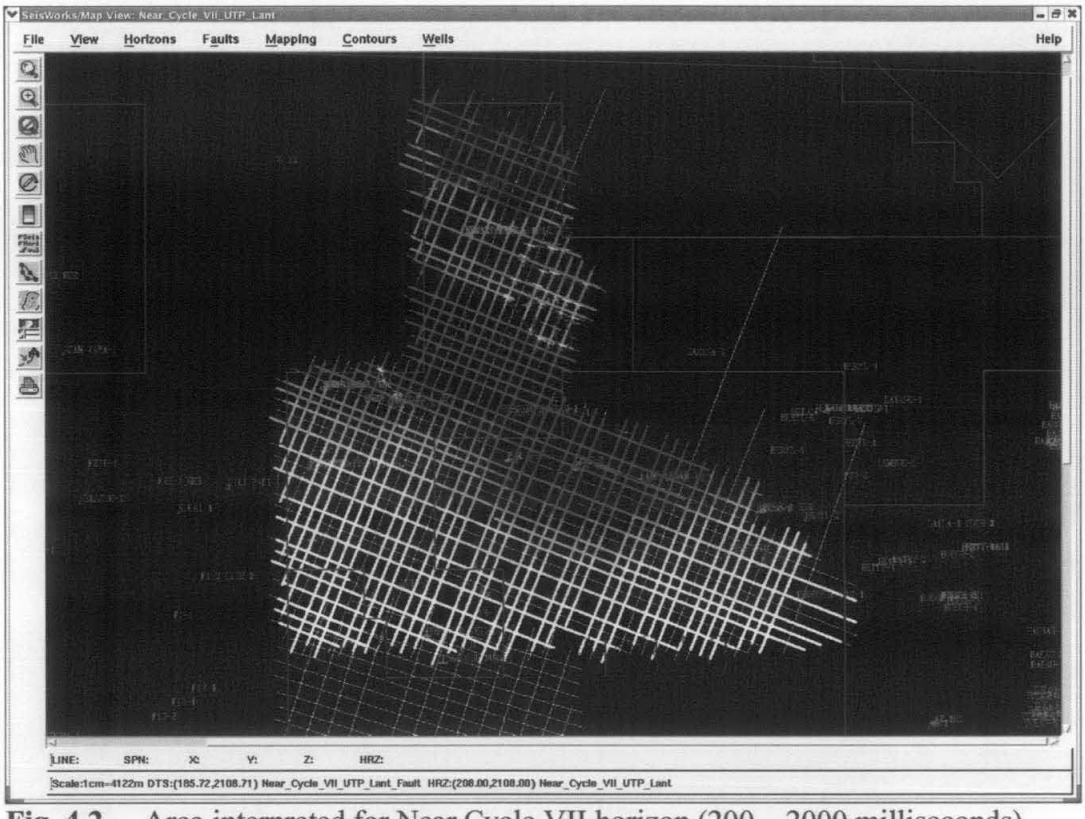

Fig. 4.2 Area interpreted for Near Cycle VII horizon (200 – 2000 milliseconds).

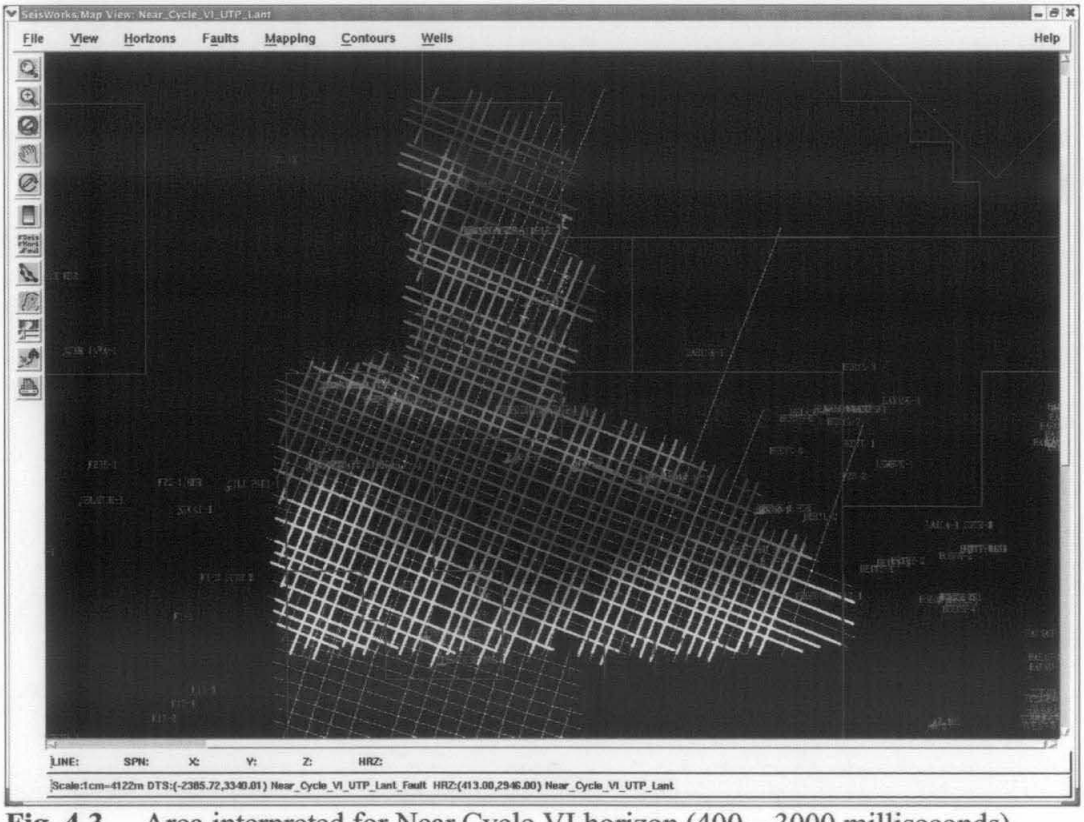

Fig. 4.3 Area interpreted for Near Cycle VI horizon (400 – 3000 milliseconds).

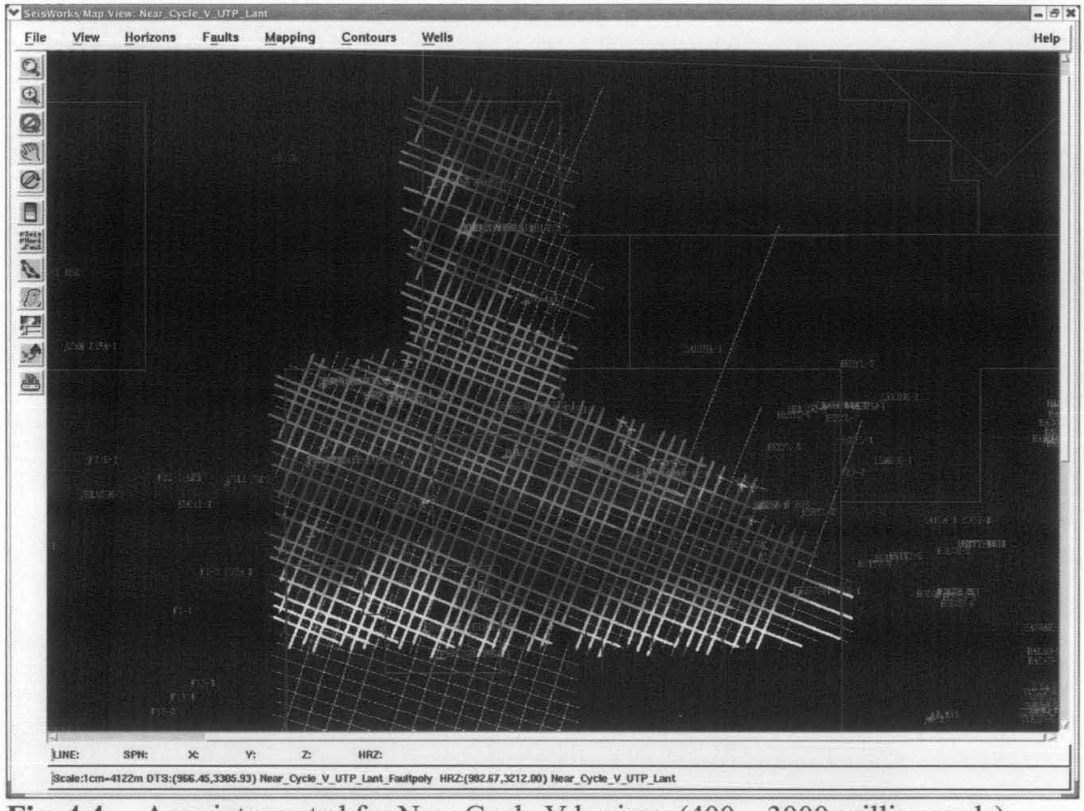

Fig. 4.4 Area interpreted for Near Cycle V horizon (400 – 3000 milliseconds).

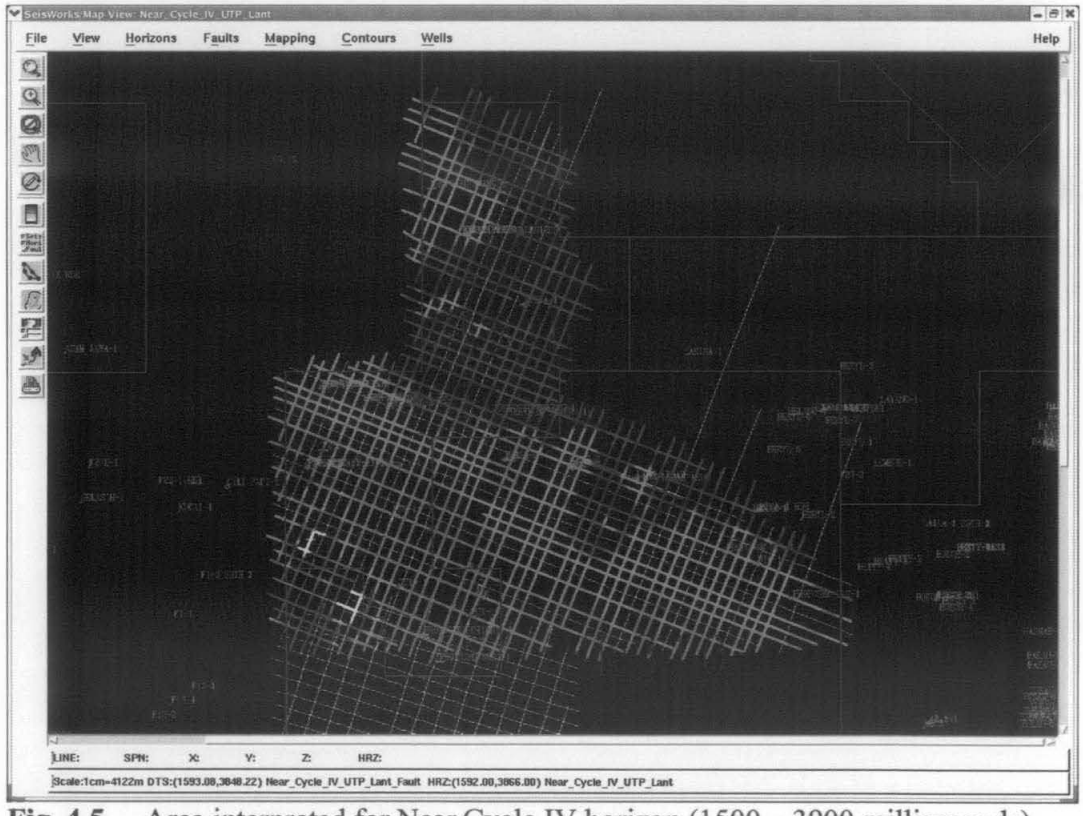

Fig. 4.5 Area interpreted for Near Cycle IV horizon (1500 – 3900 milliseconds)

4.2 TWT CONTOUR MAP

Below are two-way-time (TWT) contour maps of each interpreted horizon (Fig. 4.6 – Fig. 4.10). Please refer to Fig. 2.2 for the workflow.

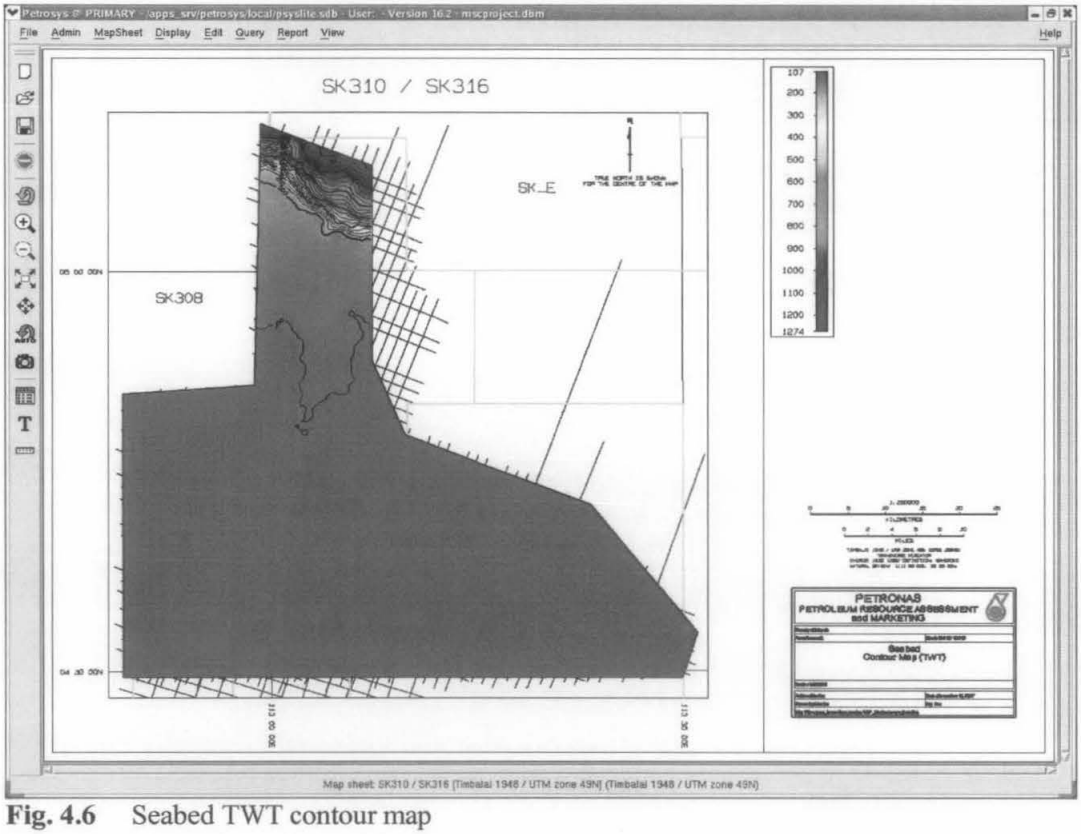

Fig. 4.6 Seabed TWT contour map

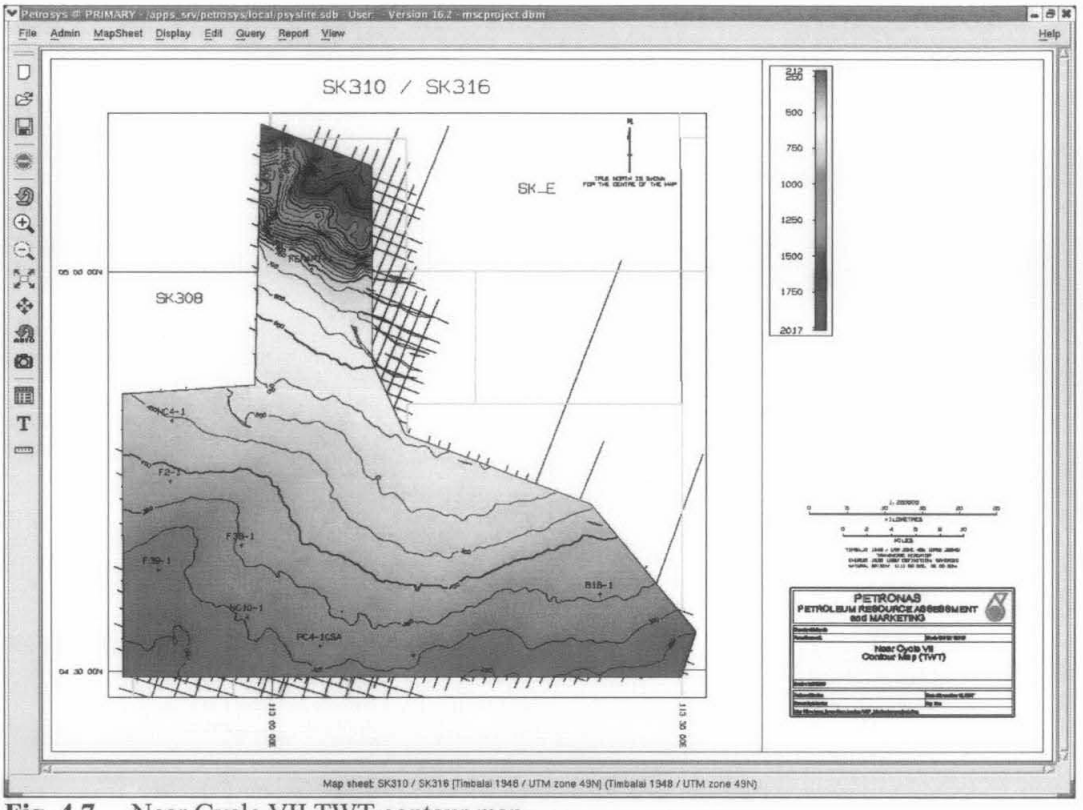

Fig. 4.7 Near Cycle VII TWT contour map

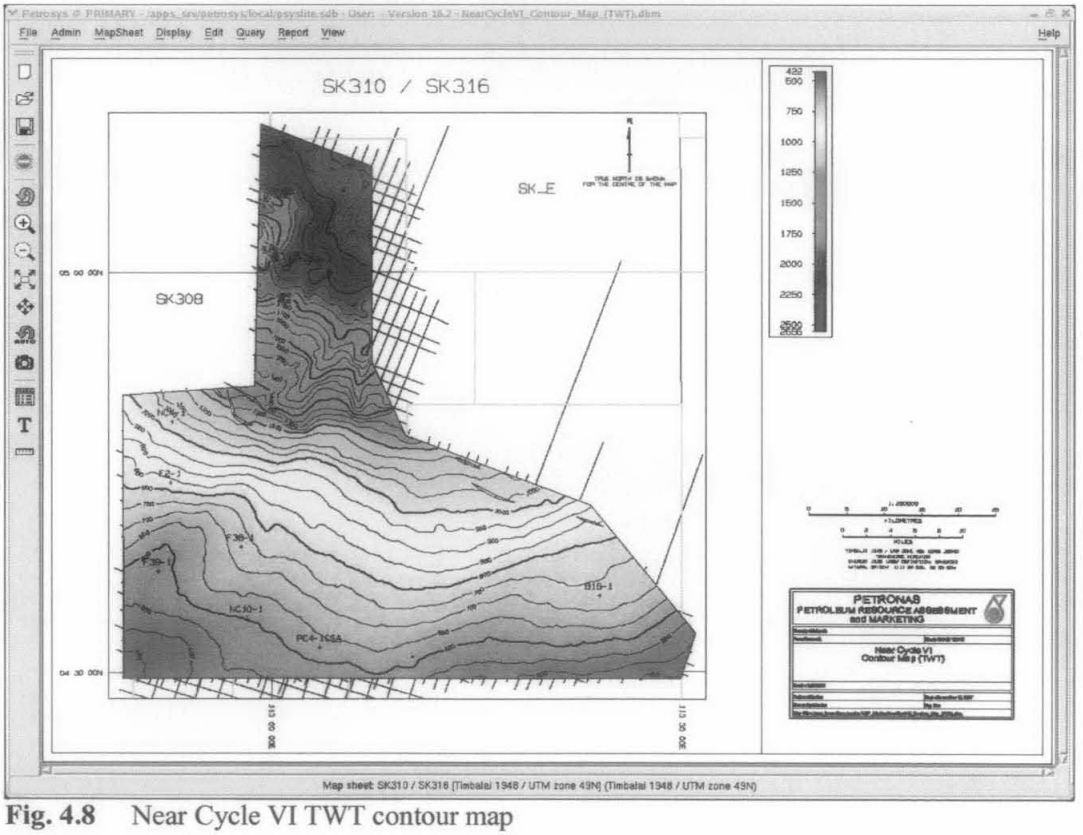

Fig. 4.8 Near Cycle VI TWT contour map

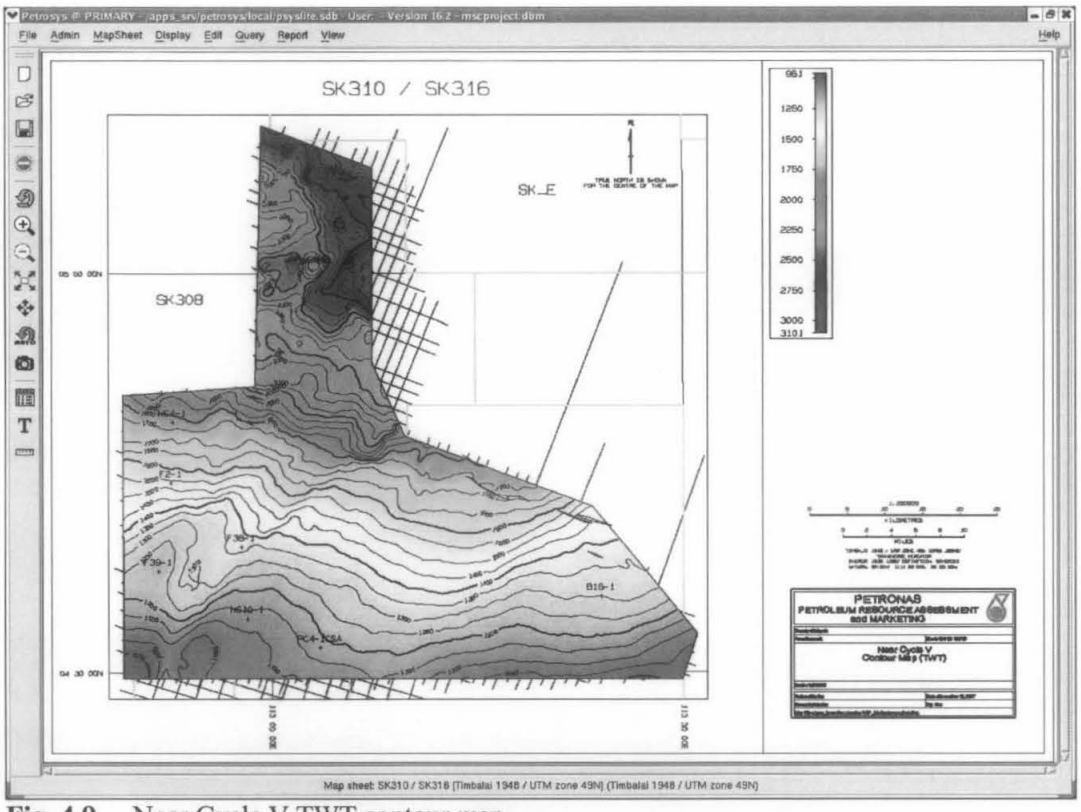

Fig. 4.9 Near Cycle V TWT contour map

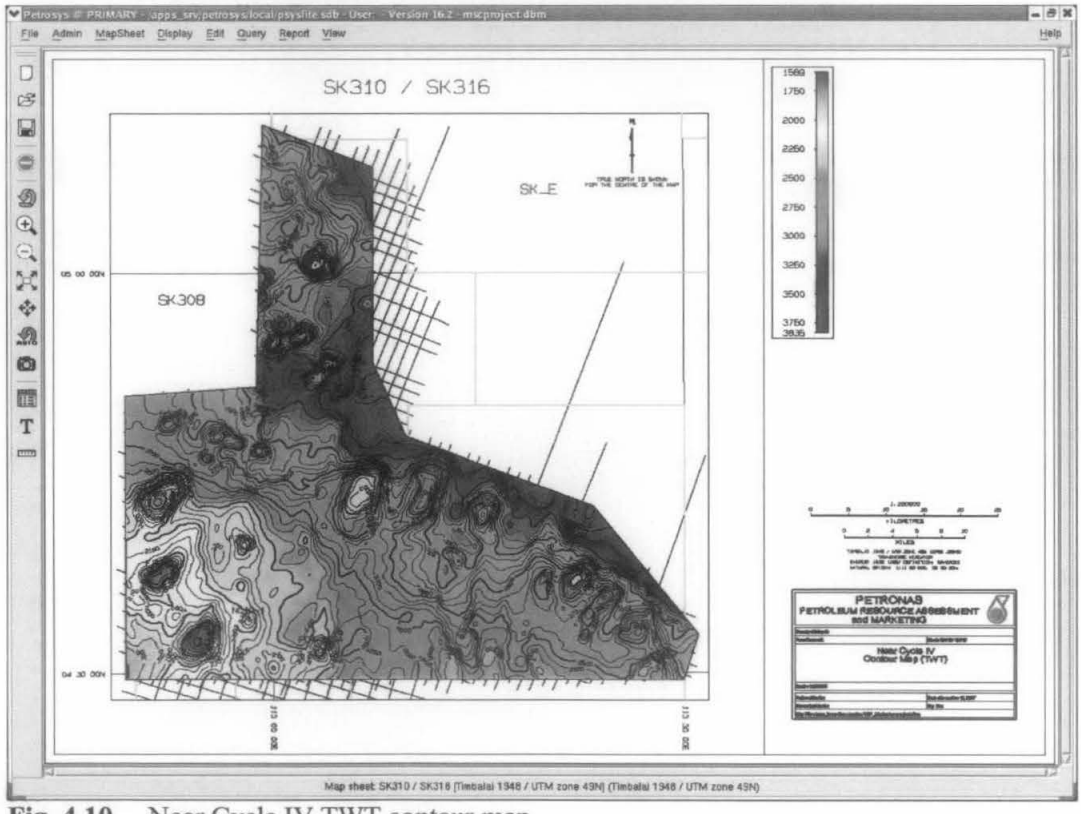

Fig. 4.10 Near Cycle IV TWT contour map

4.3 ISOCHRON CONTOUR MAP

Isochron (thickness in time domain) contour map is a contour map that displays the variation in time between two seismic events or reflections. It can be generated using the Petrosys software easily. Below are the isochron contour maps of each layer (Fig. 4.11 – Fig. 4.14).

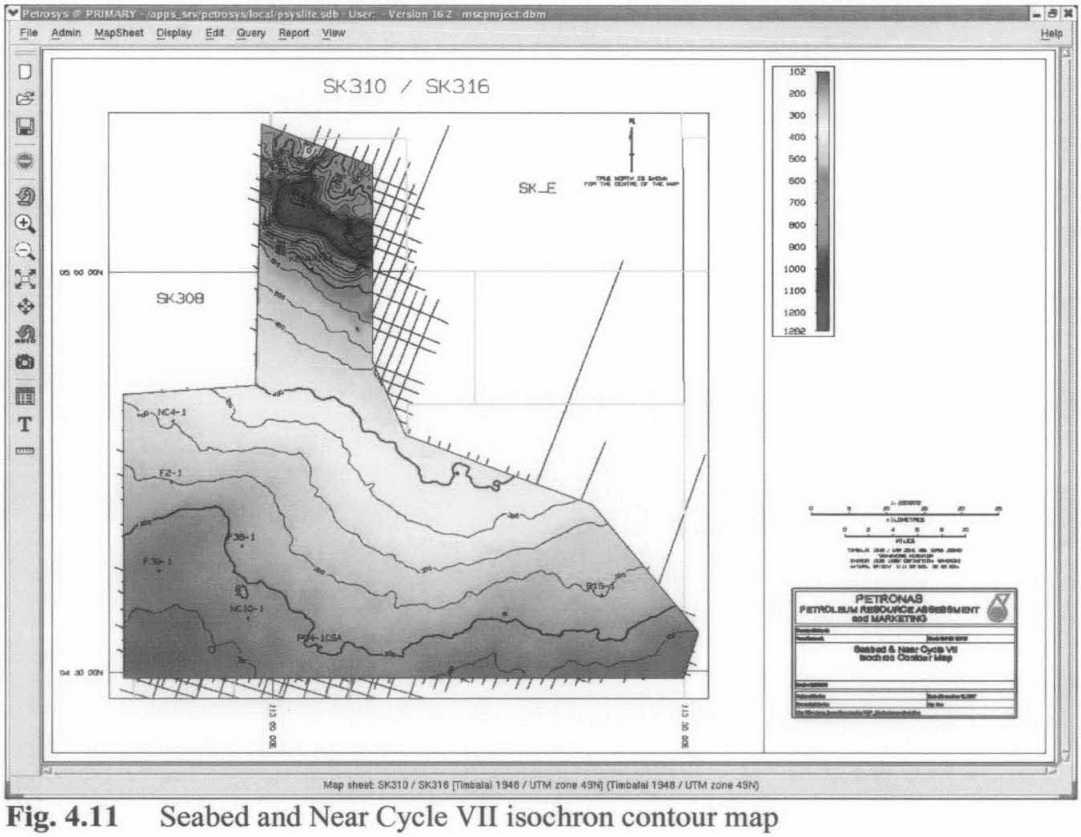

Fig. 4.11 Seabed and Near Cycle VII isochron contour map

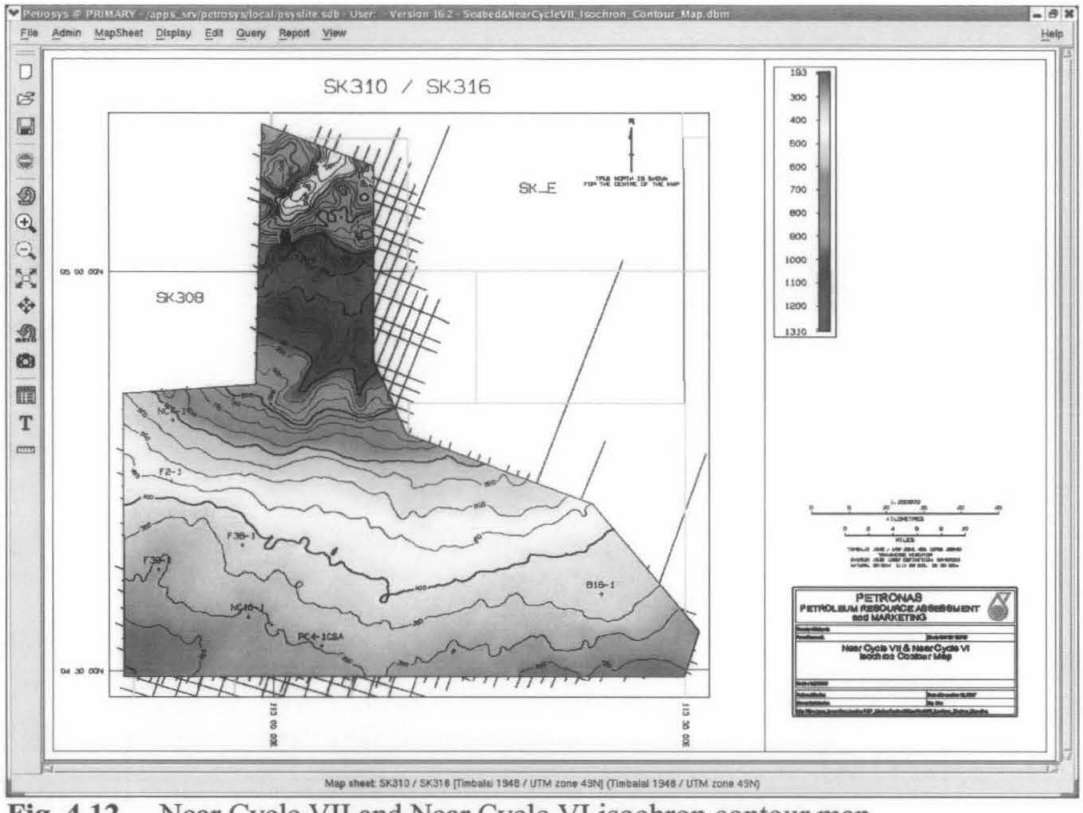

Fig. 4.12 Near Cycle VII and Near Cycle VI isochron contour map

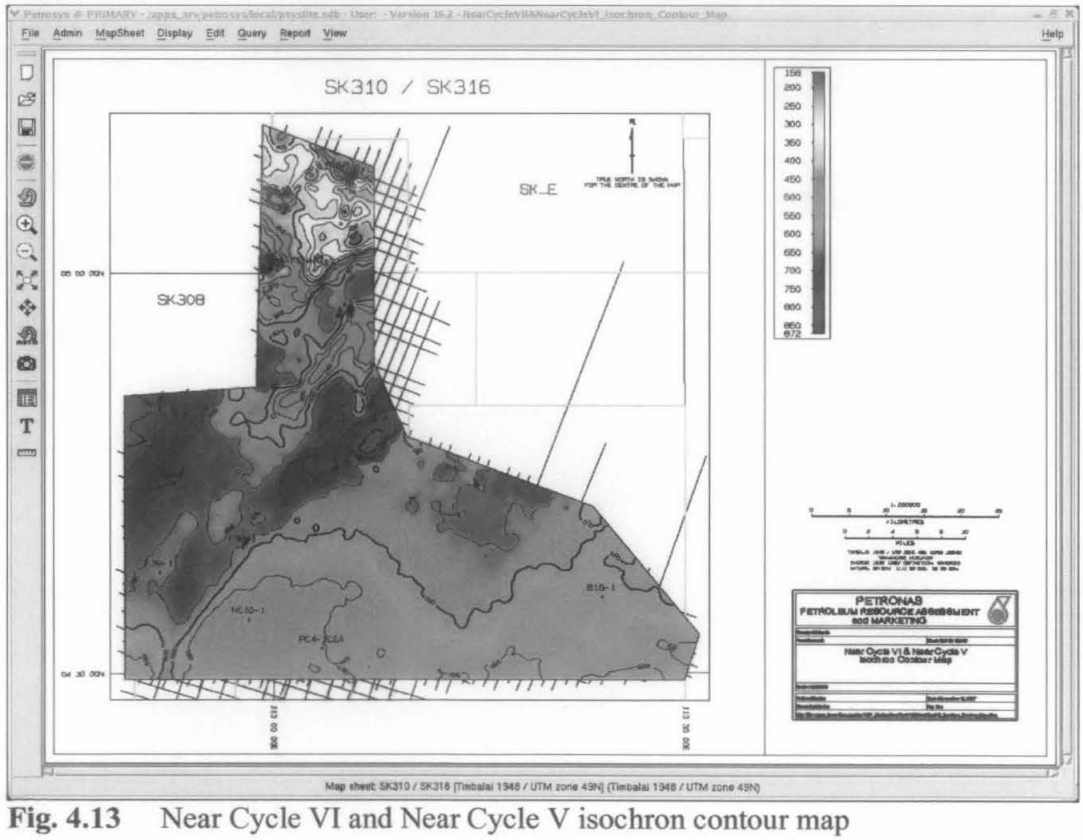

Fig. 4.13 Near Cycle VI and Near Cycle V isochron contour map

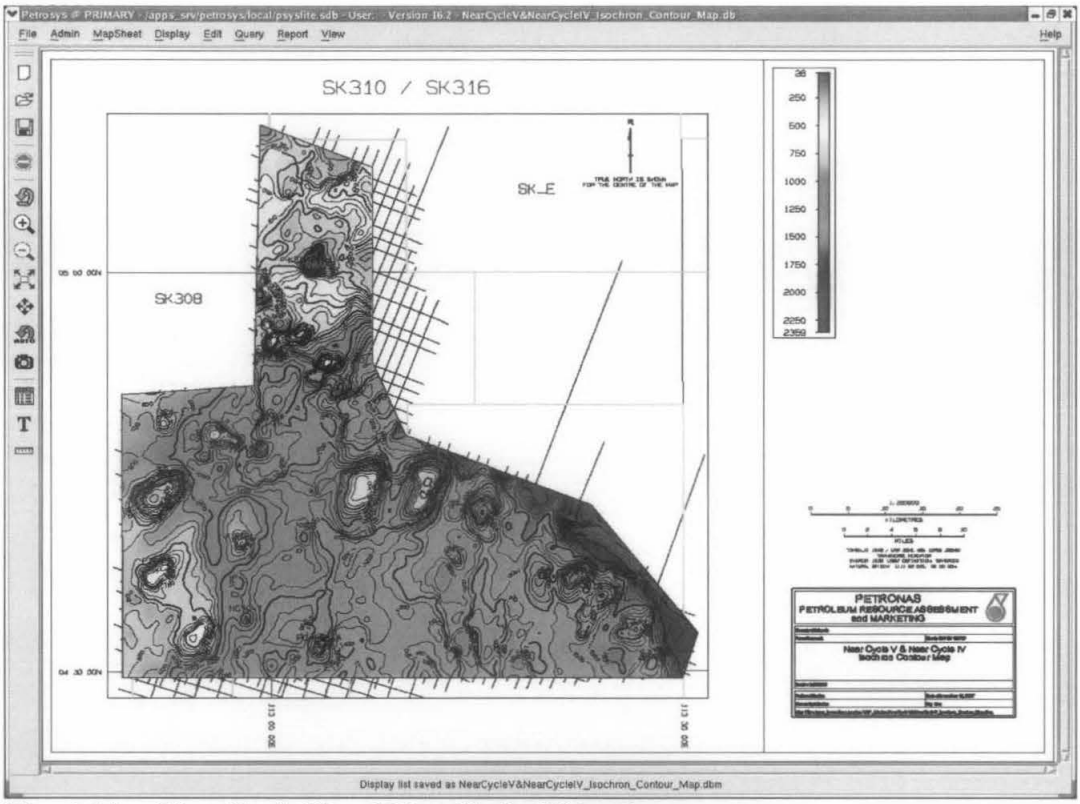

Fig. 4.14 Near Cycle V and Near Cycle IV isochron contour map

4.4 INTERVAL VELOCITY CONTOUR MAP

From the interval velocity calculation in the spreadsheet WDF, we can generate the interval velocity contour map for each horizon. Below are the interval velocity maps (Fig 4.15 – Fig. 4.18).

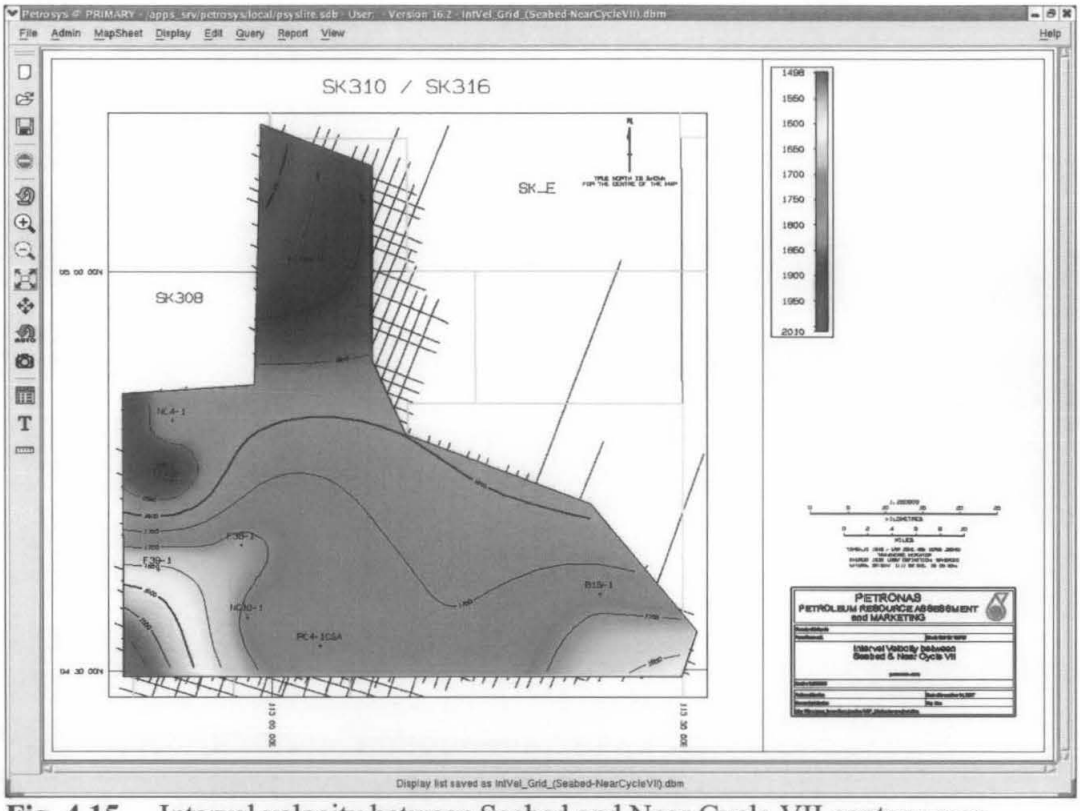

Fig. 4.15 Interval velocity between Seabed and Near Cycle VII contour map.

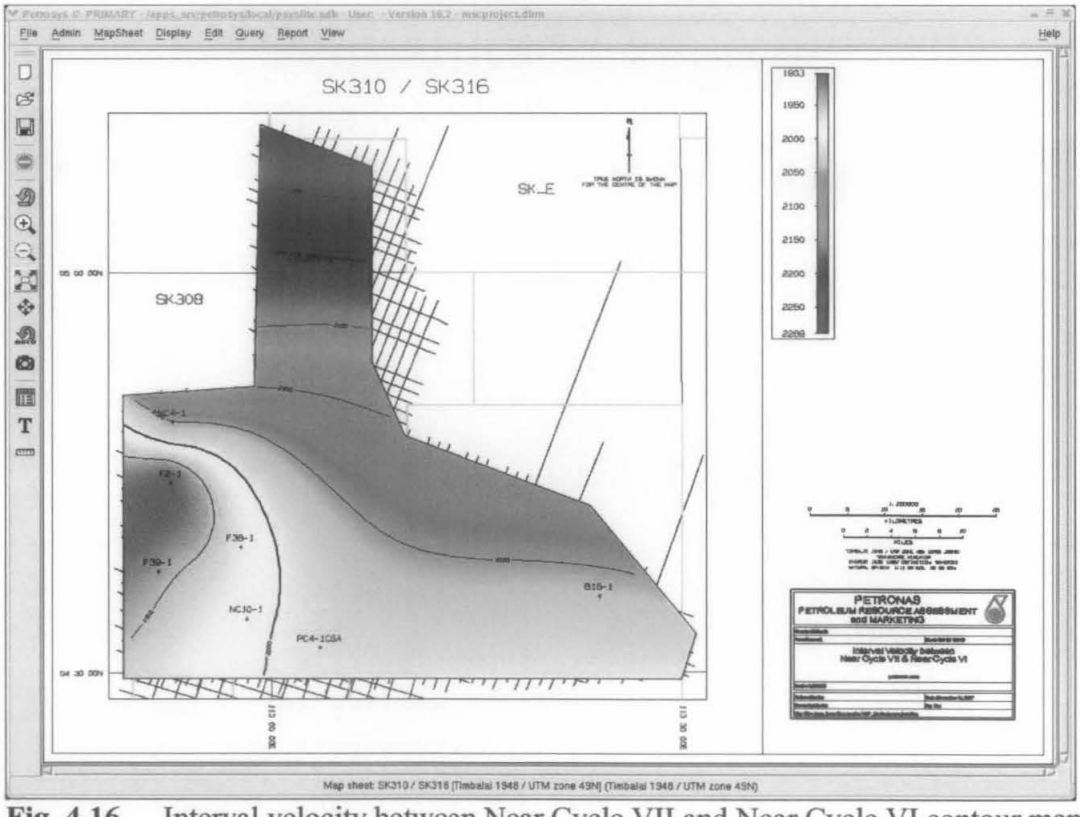

Fig. 4.16 Interval velocity between Near Cycle VII and Near Cycle VI contour map.

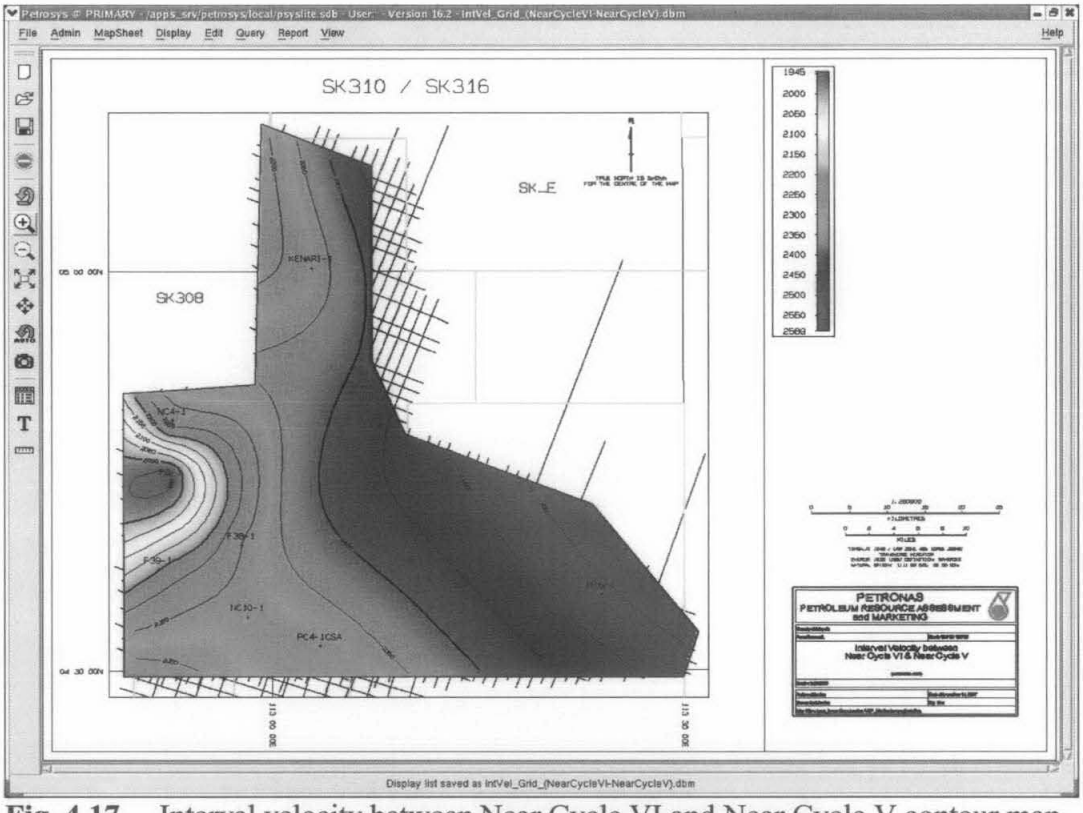

Fig. 4.17 Interval velocity between Near Cycle VI and Near Cycle V contour map.

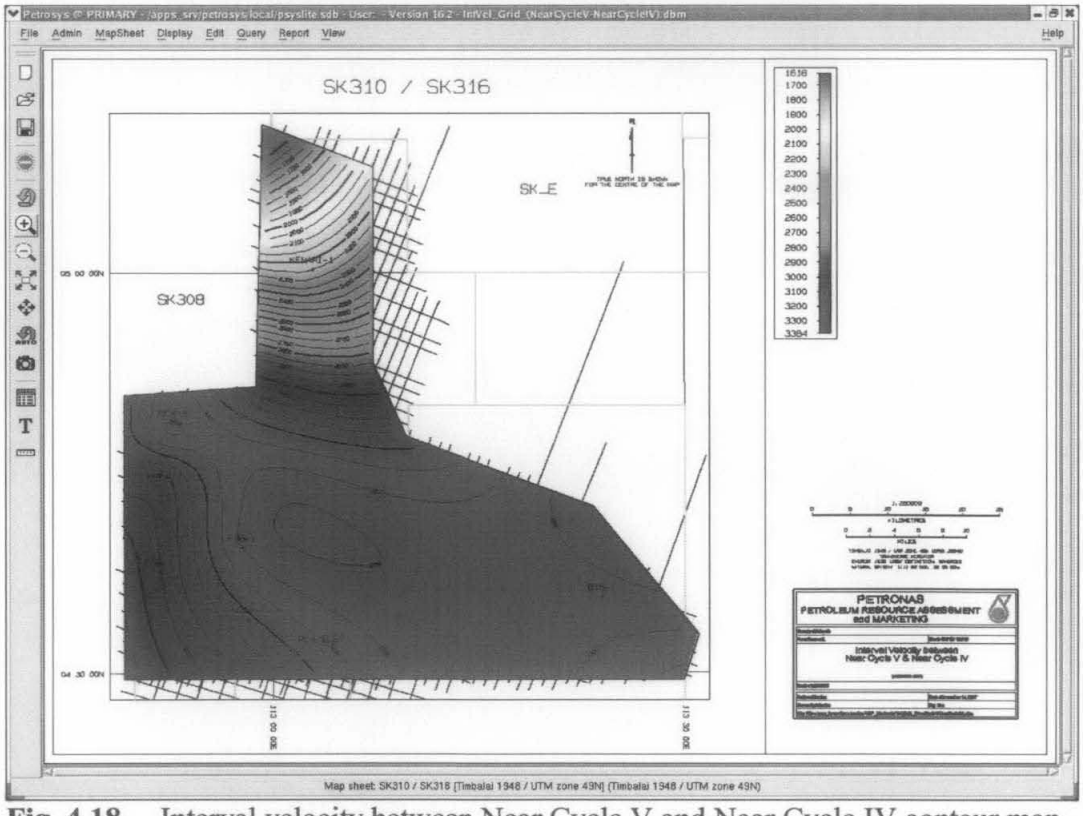

Fig. 4.18 Interval velocity between Near Cycle V and Near Cycle IV contour map.

4.5 ISOPACH CONTOUR MAP

By knowing the TWT contour map and value of the interval velocity, we can generate the isopach (depth thickness or true stratigraphic thicknesses; i.e., perpendicular to bedding surfaces) map of the layer. Below is the formula (Fig. 4.19) that been used to generate the isopach contour map in Petrosys software.

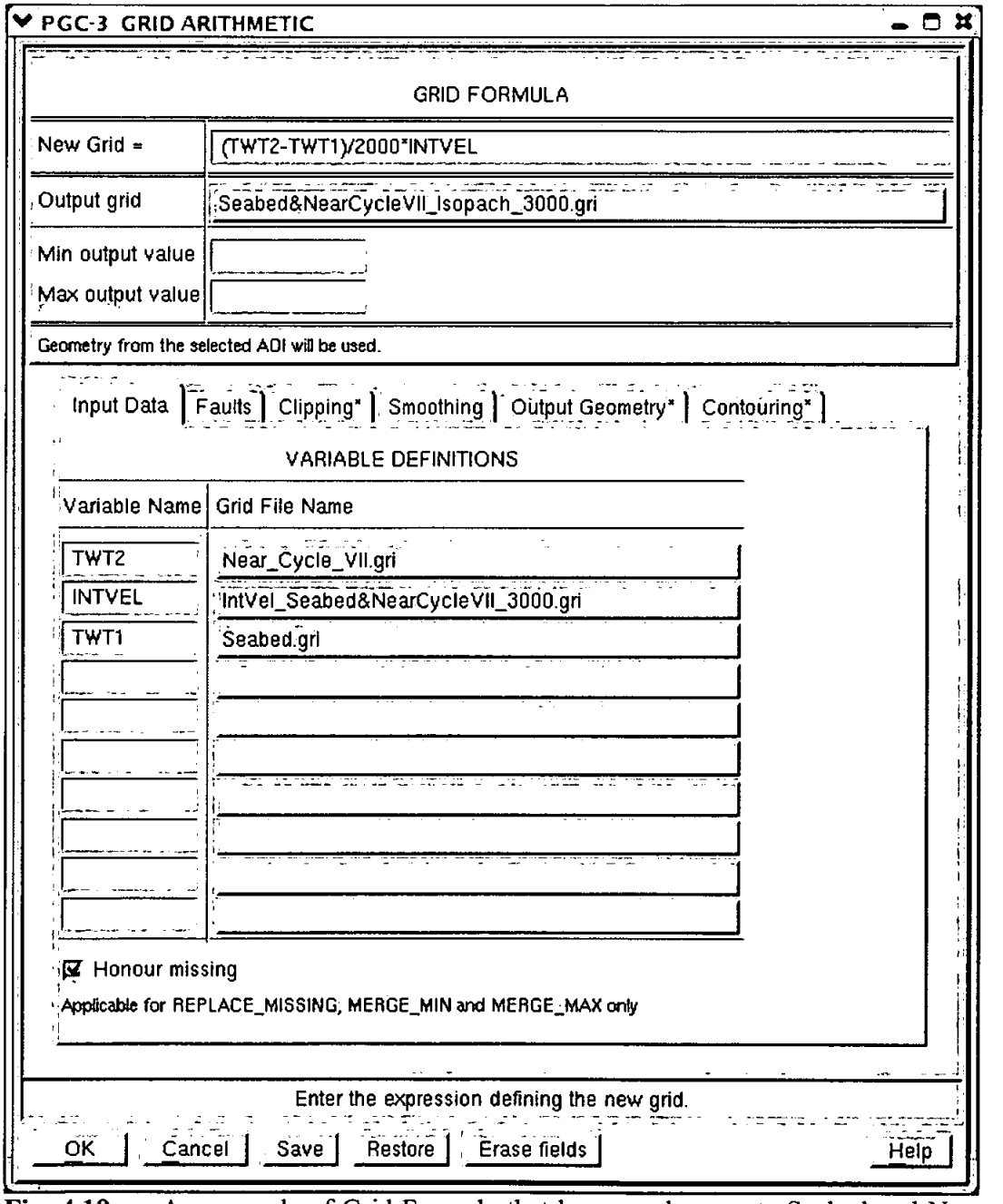

Fig. 4.19 An example of Grid Formula that been used generate Seabed and Near Cycle VII isopach contour map in Petrosys software.

Fig. 4.20 – Fig. 4.23 are the isopach contour map of each layer.

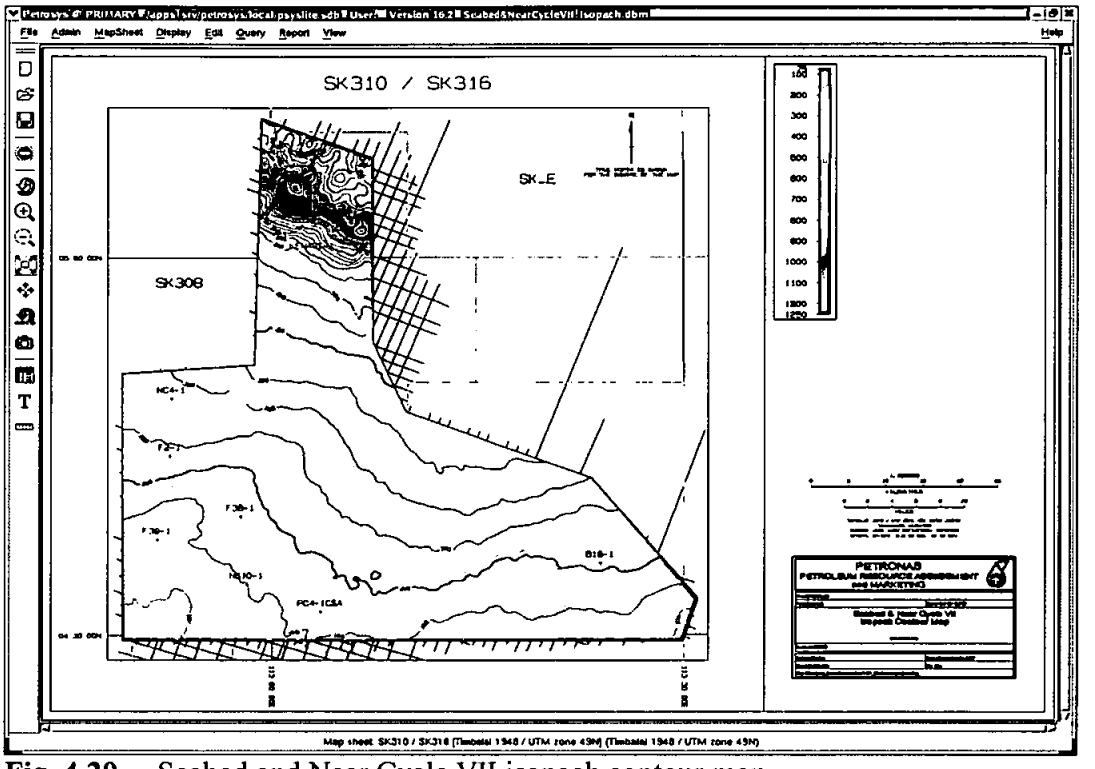

Fig. 4.20 Seabed and Near Cycle VII isopach contour map.

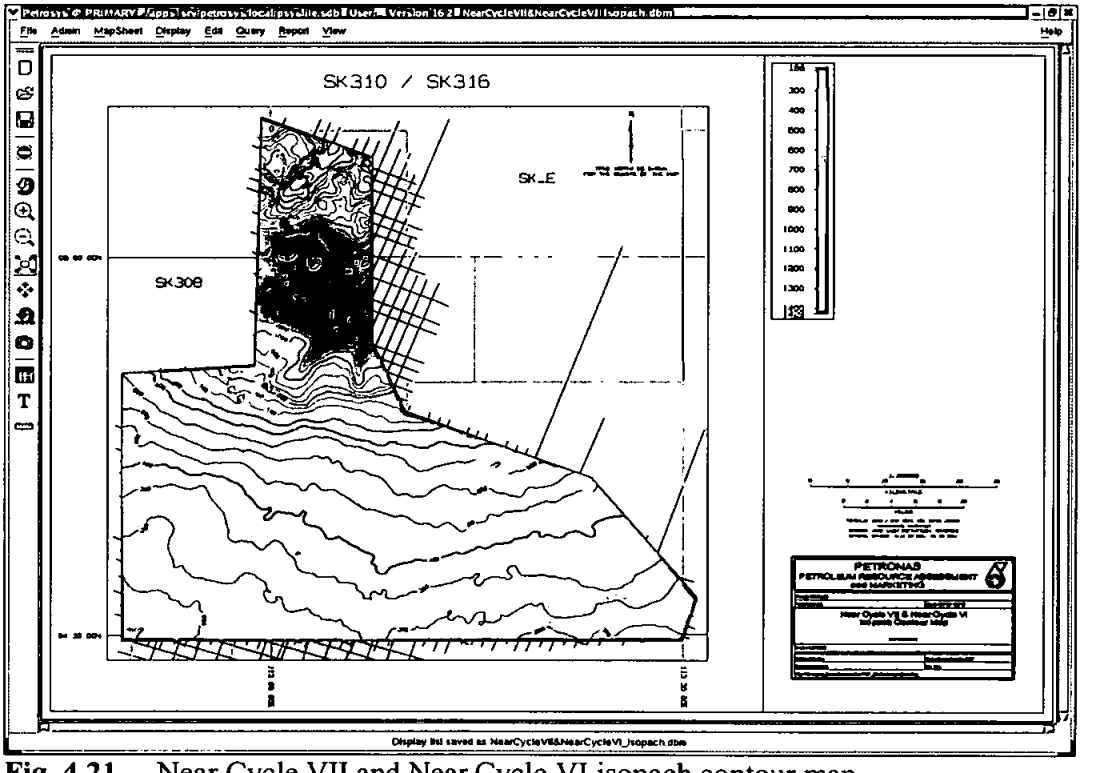

Fig. 4.21 Near Cycle VII and Near Cycle VI isopach contour map.

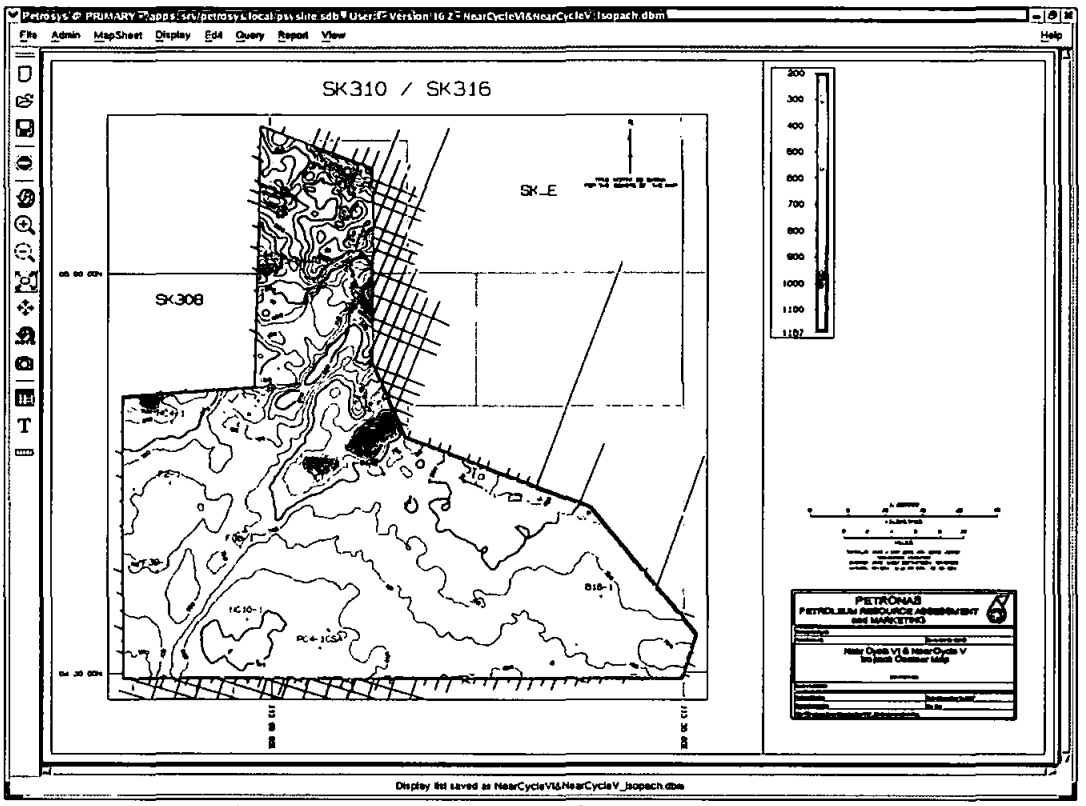

Fig. 4.22 Near Cycle VI and Near Cycle V isopach contour map.

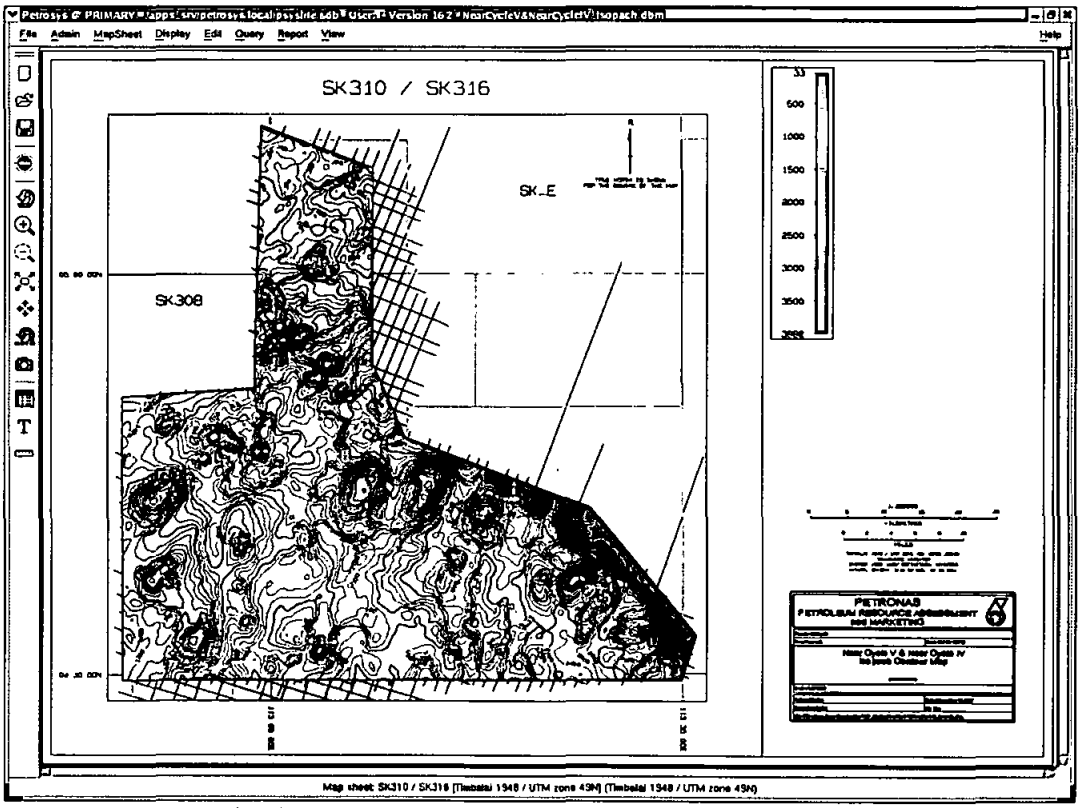

Fig. 4.23 Near Cycle V and Near Cycle IV isopach contour map

4.6 DEPTH CONTOUR MAP (NOT TIED TO WELL)

Refer to Fig. 3.3, we need to generate the depth contour map after we had done the isopach contour map. Following figure shows how seabed depth contour map (Fig. 4.29) generated by using constant value of wave velocity in water (1475 ms^{-1})

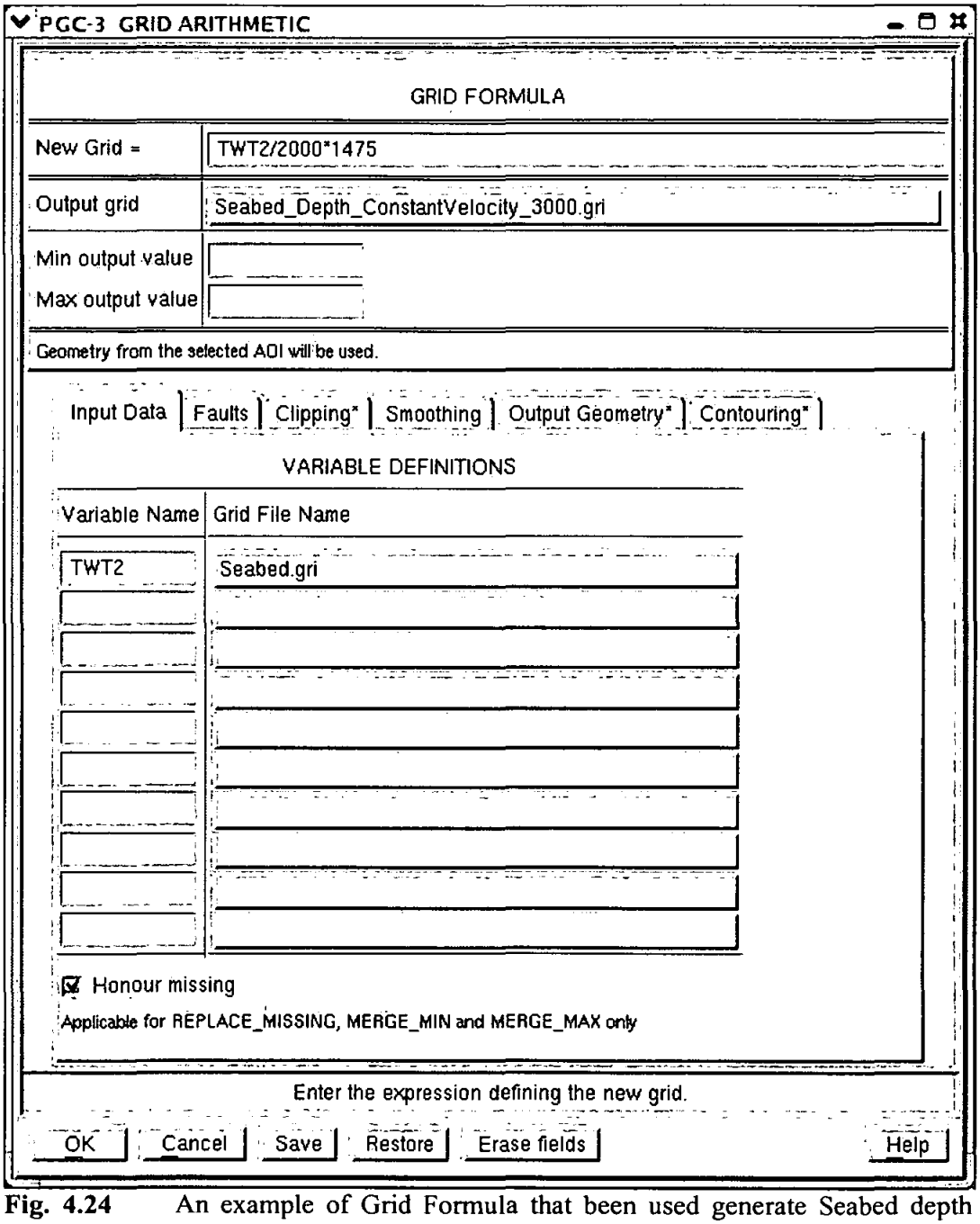

Fig. 4.24 An example of Grid Formula that been used generate Seabed depth contour map in Petrosys software.

Figure 4.25 is the seabed depth contour map generated from grid arithmetic process in Petrosys.

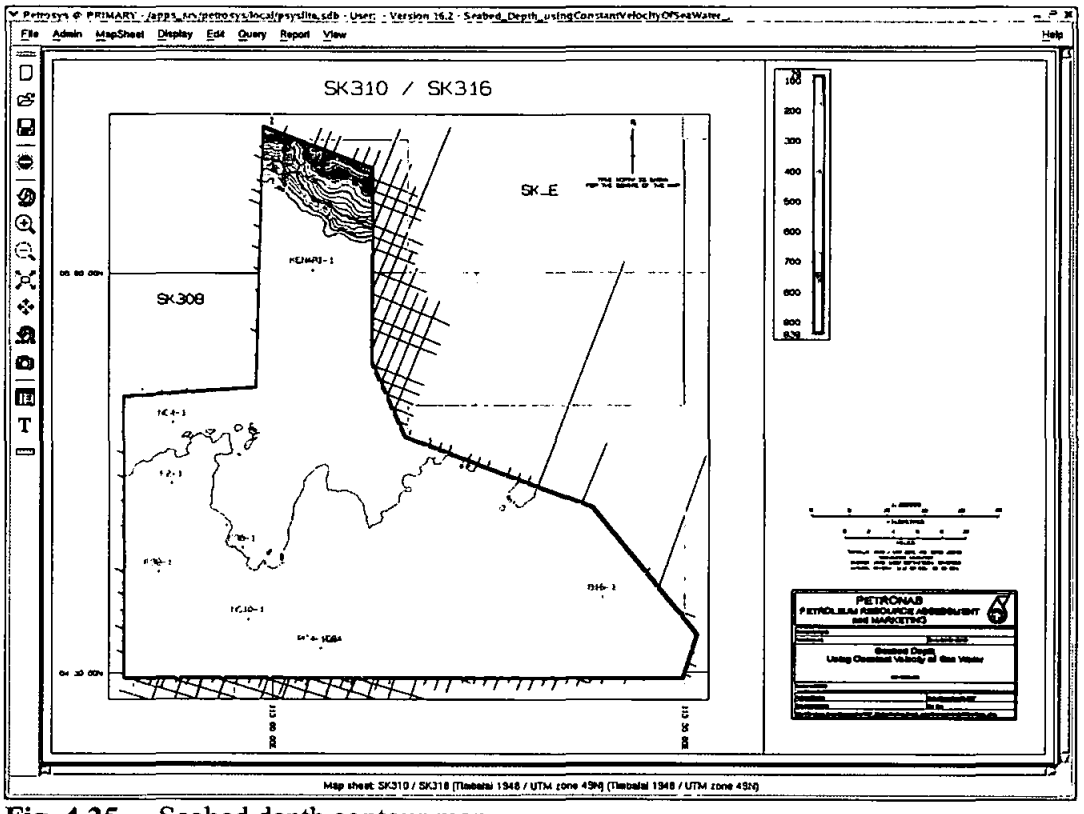

Fig. 4.25 Seabed depth contour map

Then, from here we can computed and generate each horizon depth contour map. Remember! Here each horizon contour map is still not yet tie to the well data. Figures below are the horizon contour map (not tied to all wells) (Fig. 4.26 – 4.29).

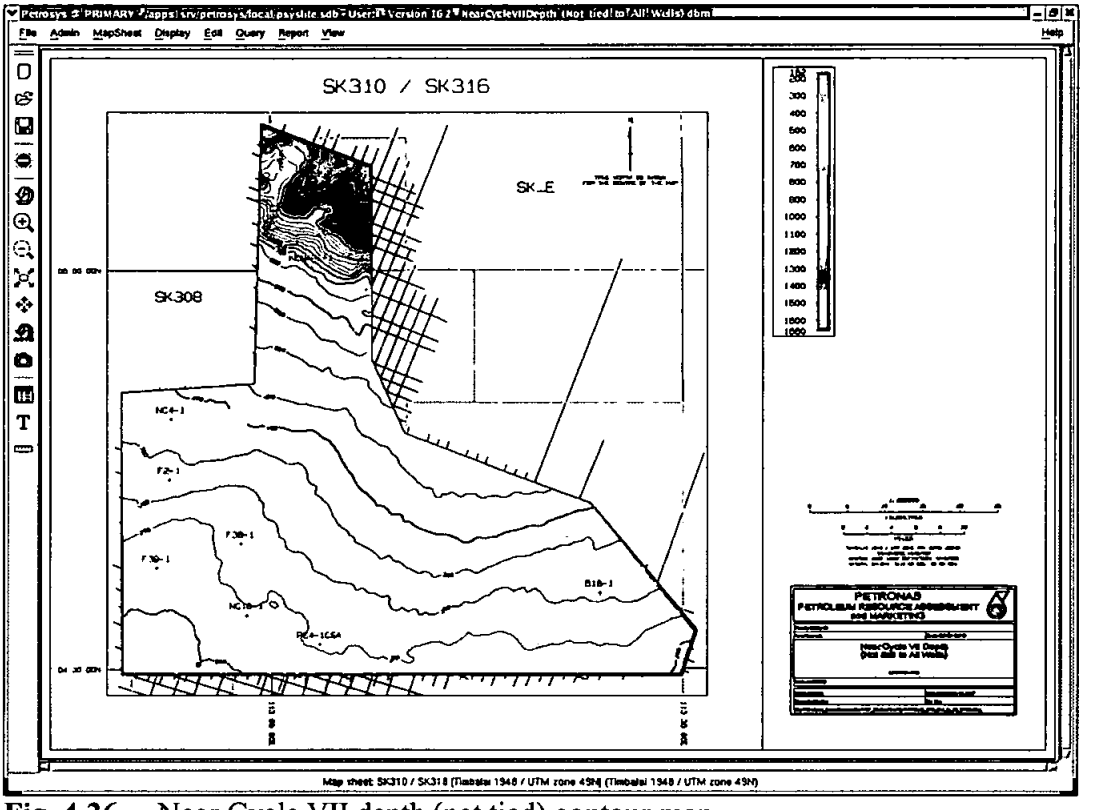

Fig. 4.26 Near Cycle VII depth (not tied) contour map.

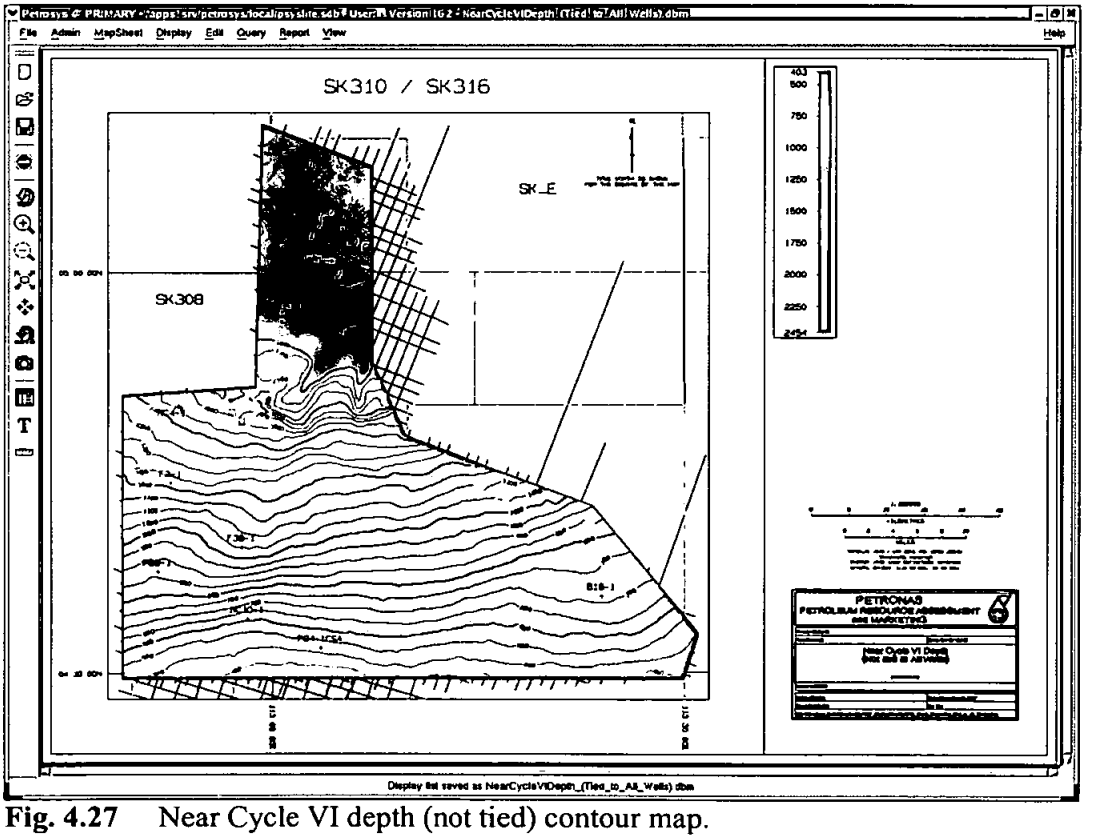

Fig. 4.27 Near Cycle VI depth (not tied) contour map.

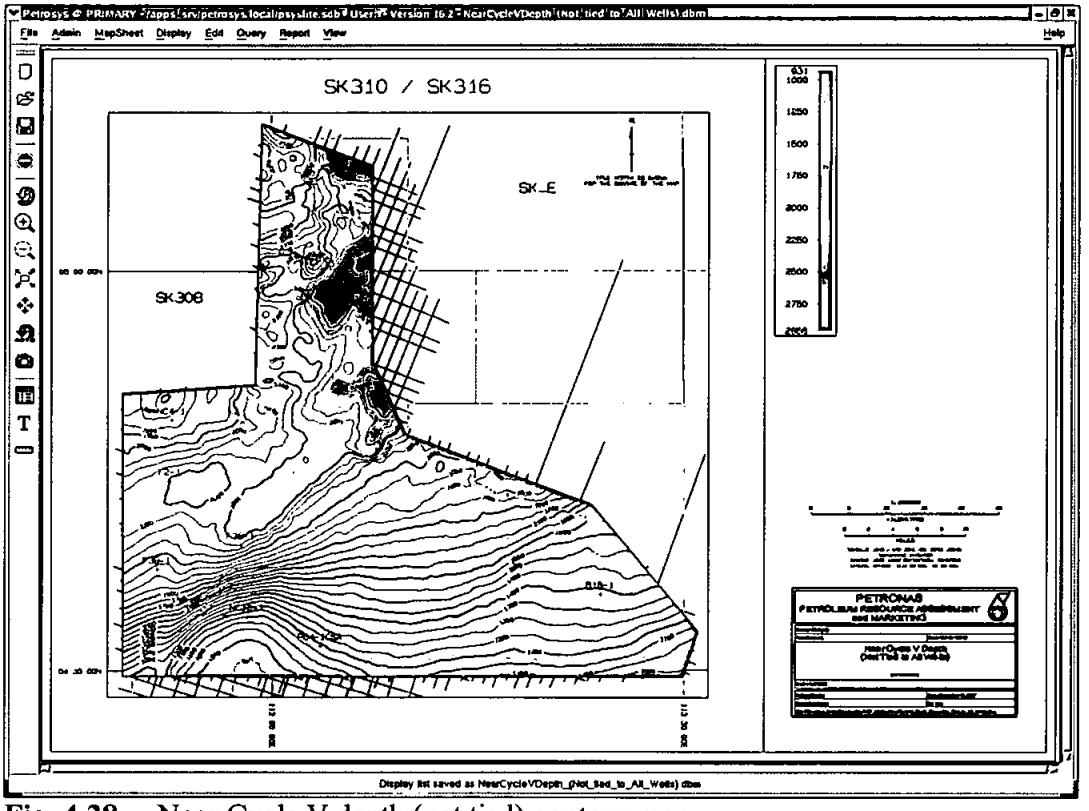

Fig. 4.28 Near Cycle V depth (not tied) contour map.

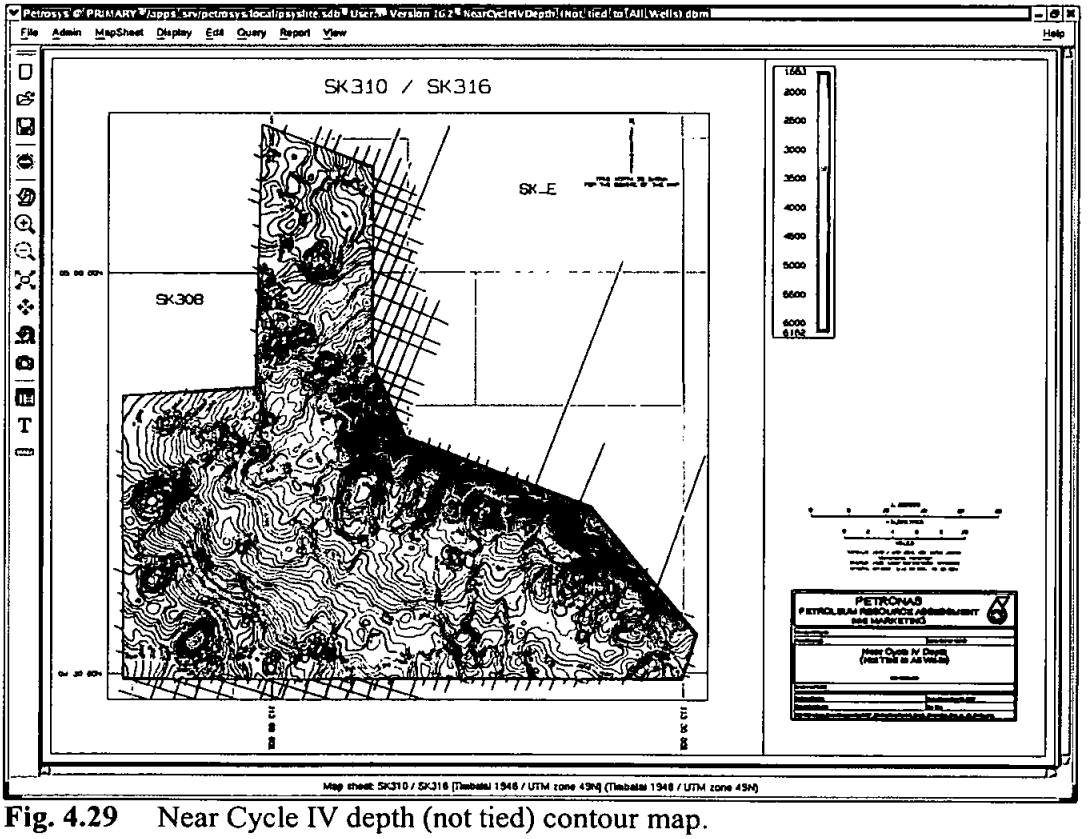

Fig. 4.29 Near Cycle IV depth (not tied) contour map.

4.7 DEPTH CONTOUR MAP (TIED TO WELL)

Before computing the depth contour map (tied all wells), we need to generate WDF spreadsheet containing actual depth data for each horizon in all wells. Below figure is the example of the WDF spreadsheet (Fig. 2.33).

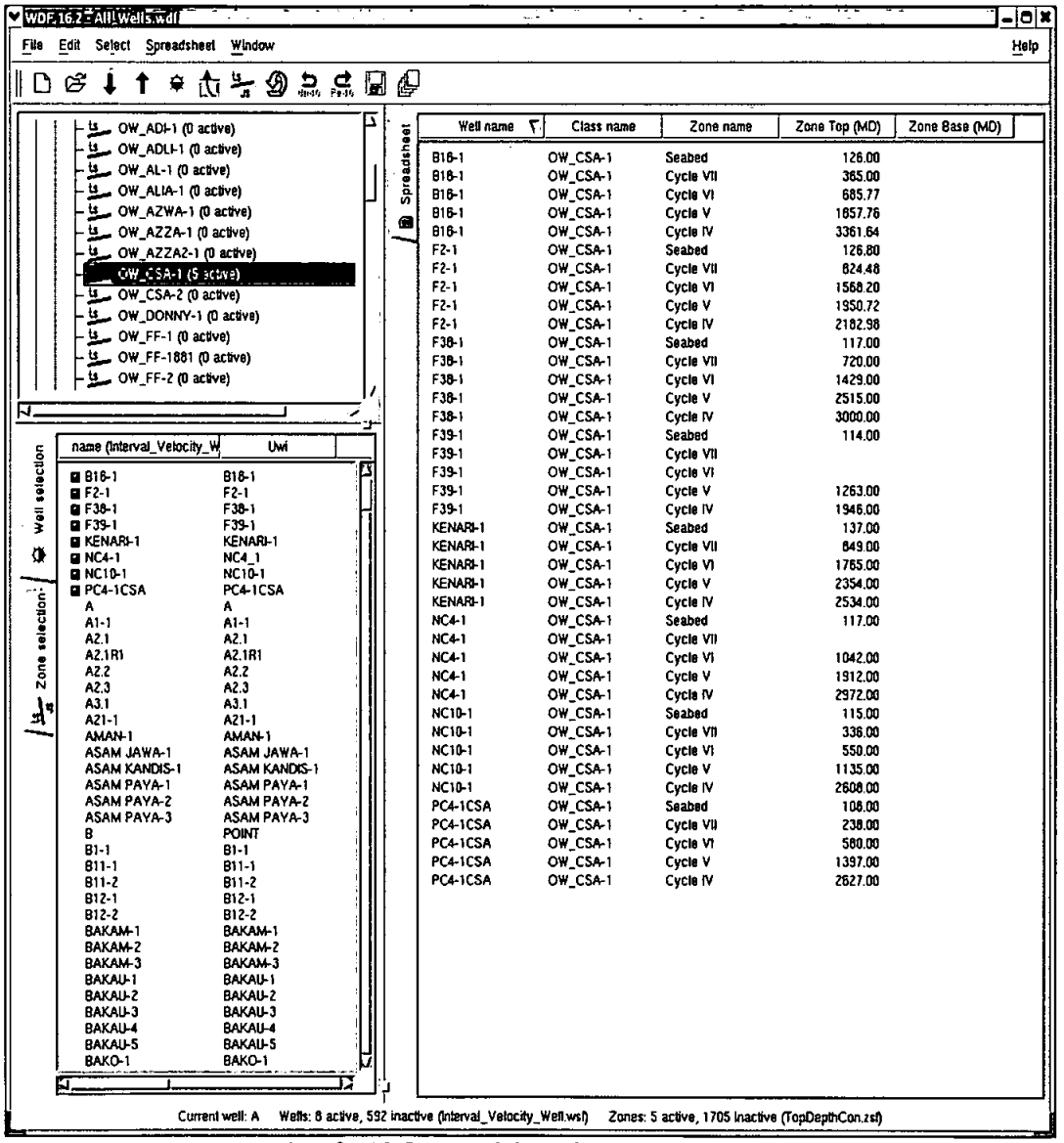

Fig. 4.30 An example of WDF spreadsheet in Petrosys that shows actual depth data on each horizon in all wells in Block SK316 and SK310.

Thus, each horizon depth contour map that had been generated can be tie to all 8 wells (Fig. 4.31 – 4.35).

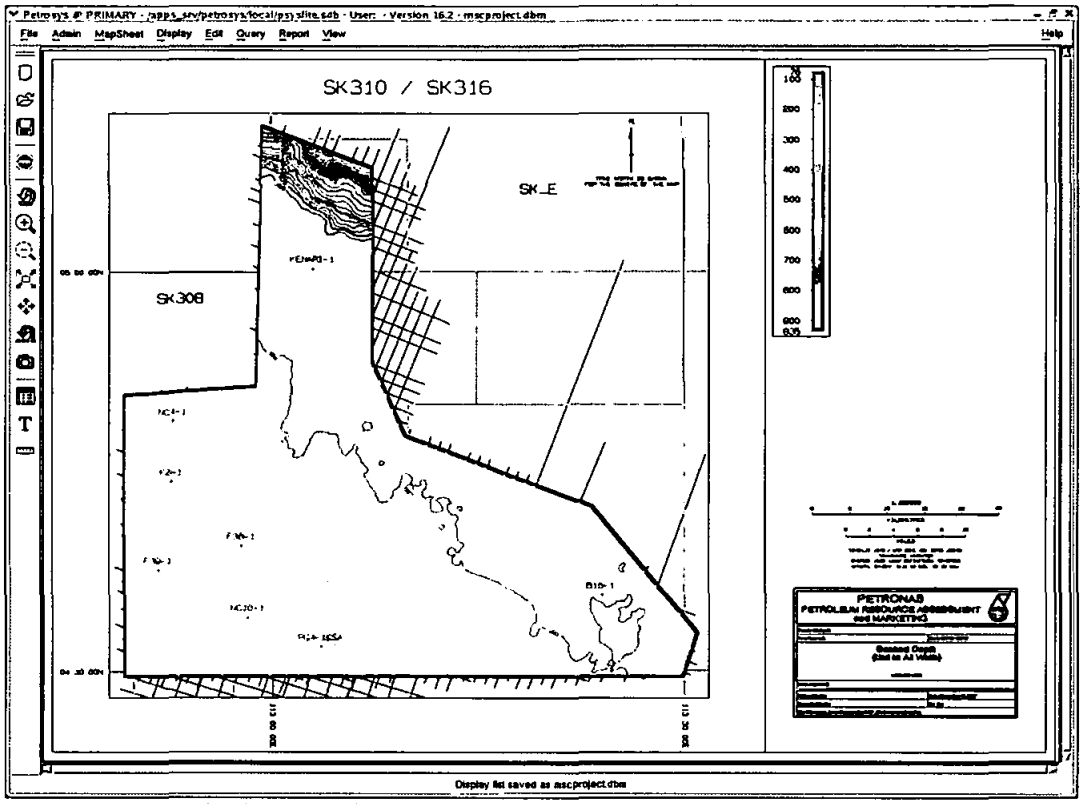

Fig. 4.31 Seabed depth (tied to all wells) contour map.

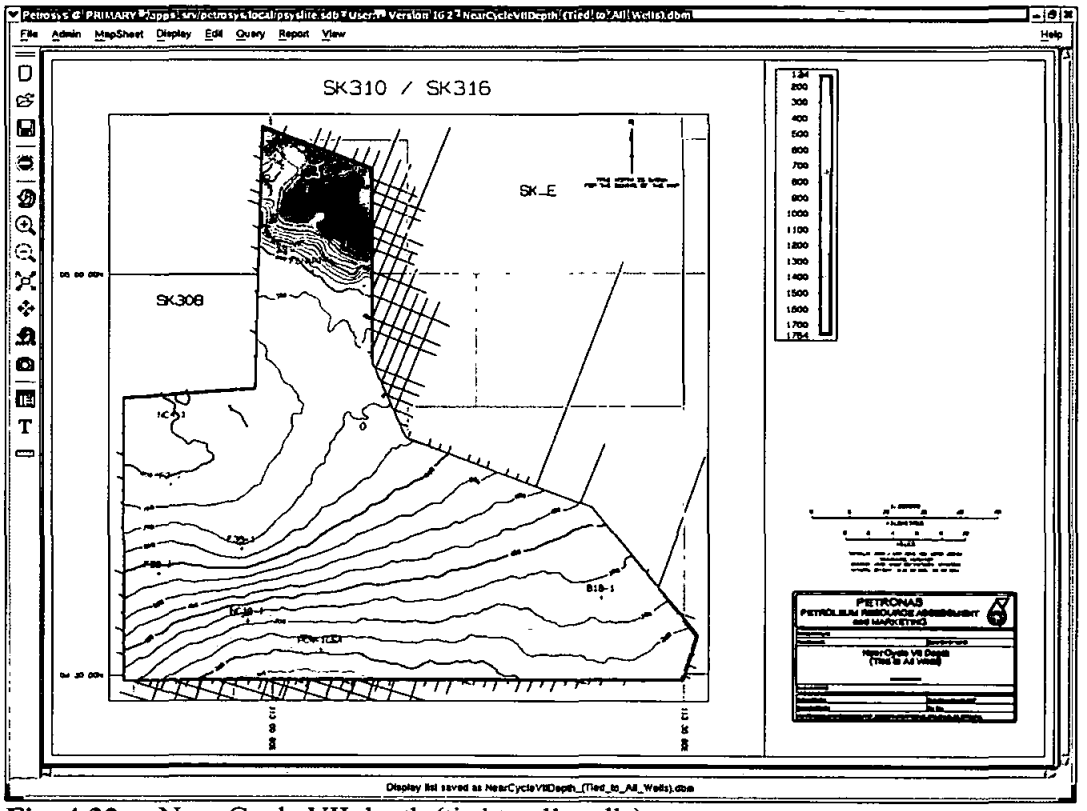

Fig. 4.32 Near Cycle VII depth (tied to all wells) contour map.

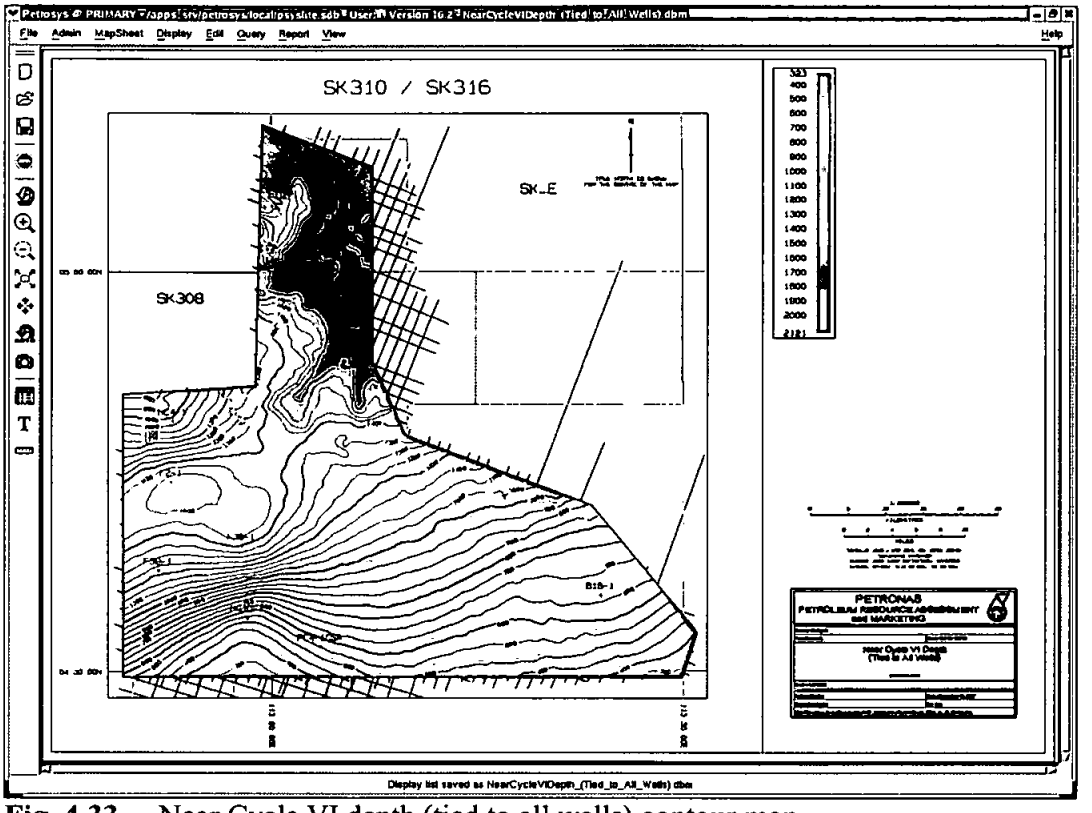

Fig. 4.33 Near Cycle VI depth (tied to all wells) contour map.

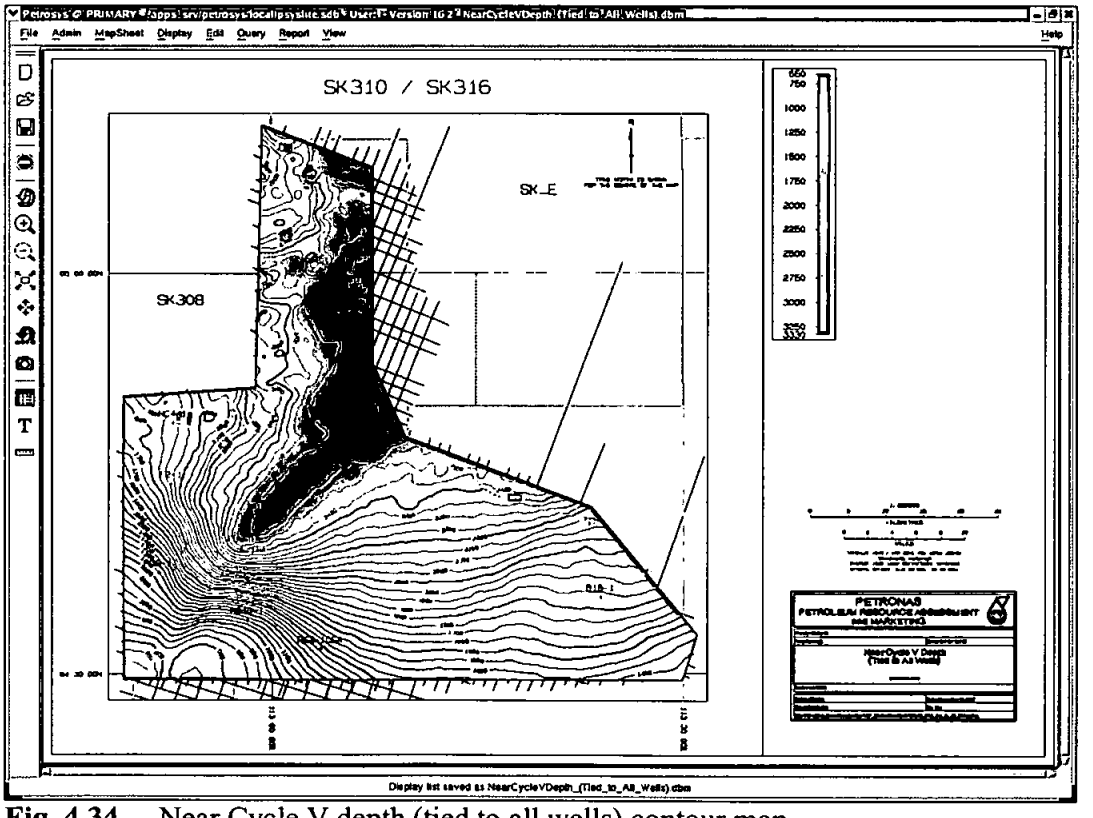

Fig. 4.34 Near Cycle V depth (tied to all wells) contour map.

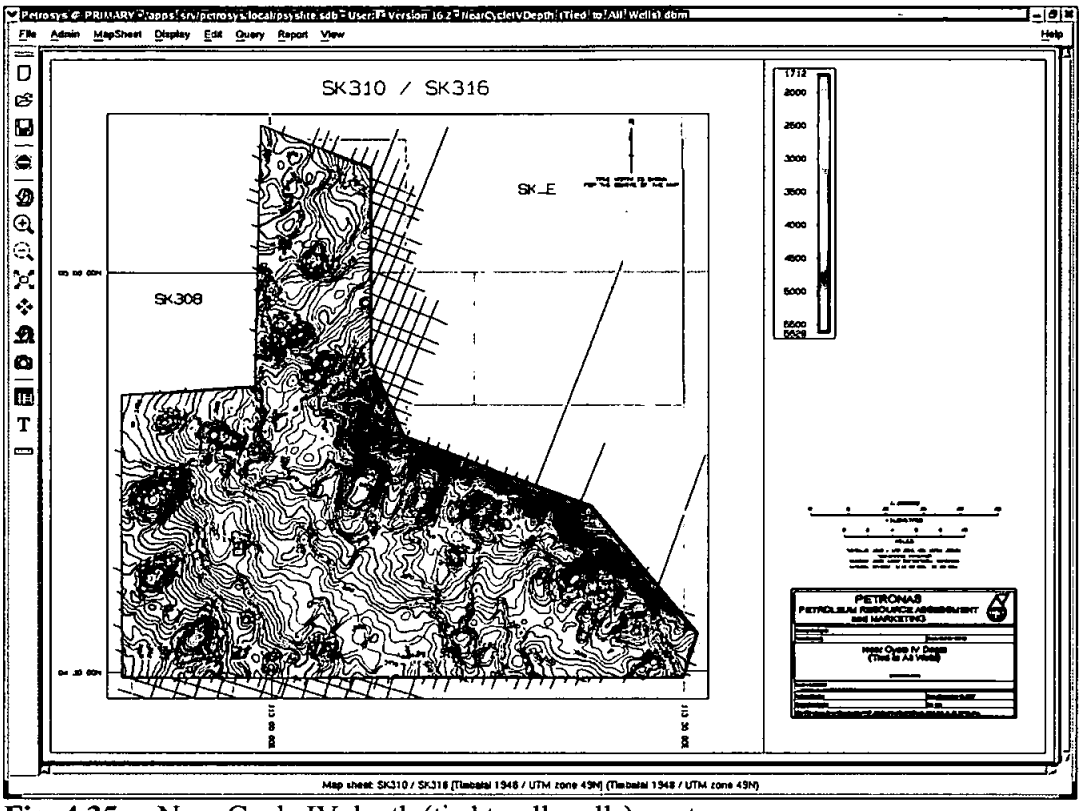

Fig. 4.35 Near Cycle IV depth (tied to all wells) contour map.

4.8 DEPTH CORRECTIONS

Some correction had been applied to the map. This is to get a good result in generating each horizon depth contour map. Below figures are the correction that been implemented (Fig. 4.36 –Fig. 4.39). Noticed that the correction area was also applied outside of the clipping polygon.

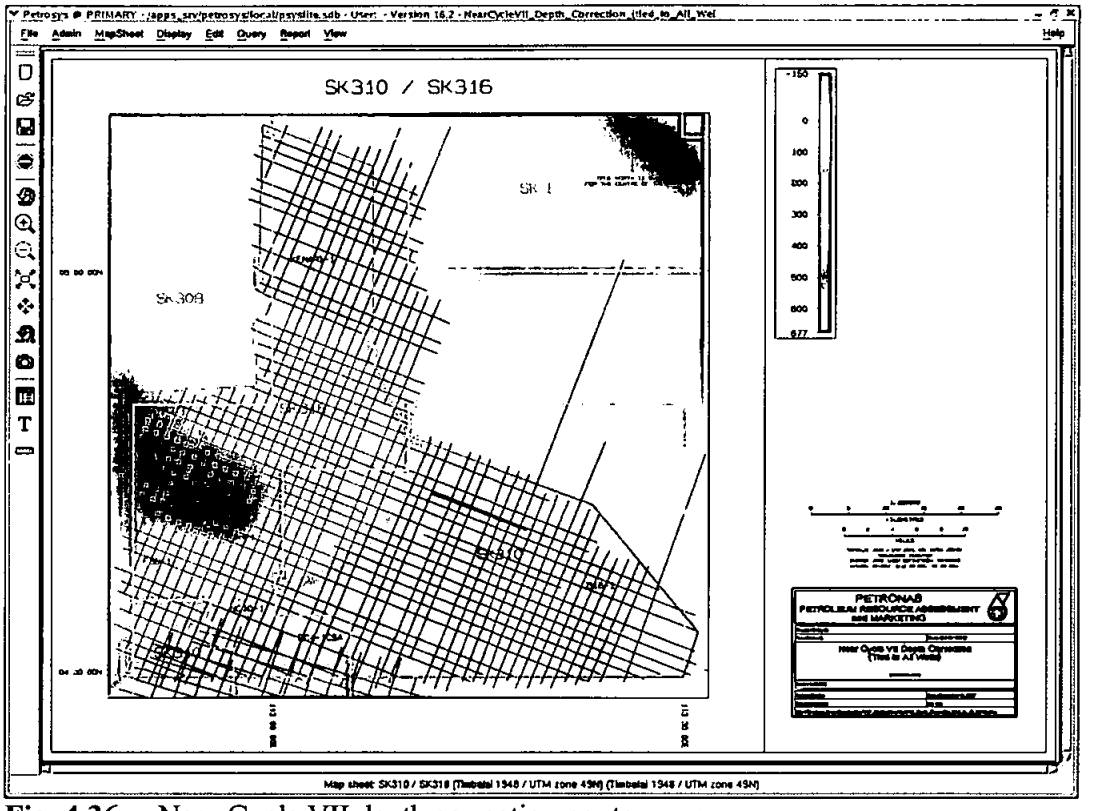

Fig. 4.36 Near Cycle VII depth correction contour map.

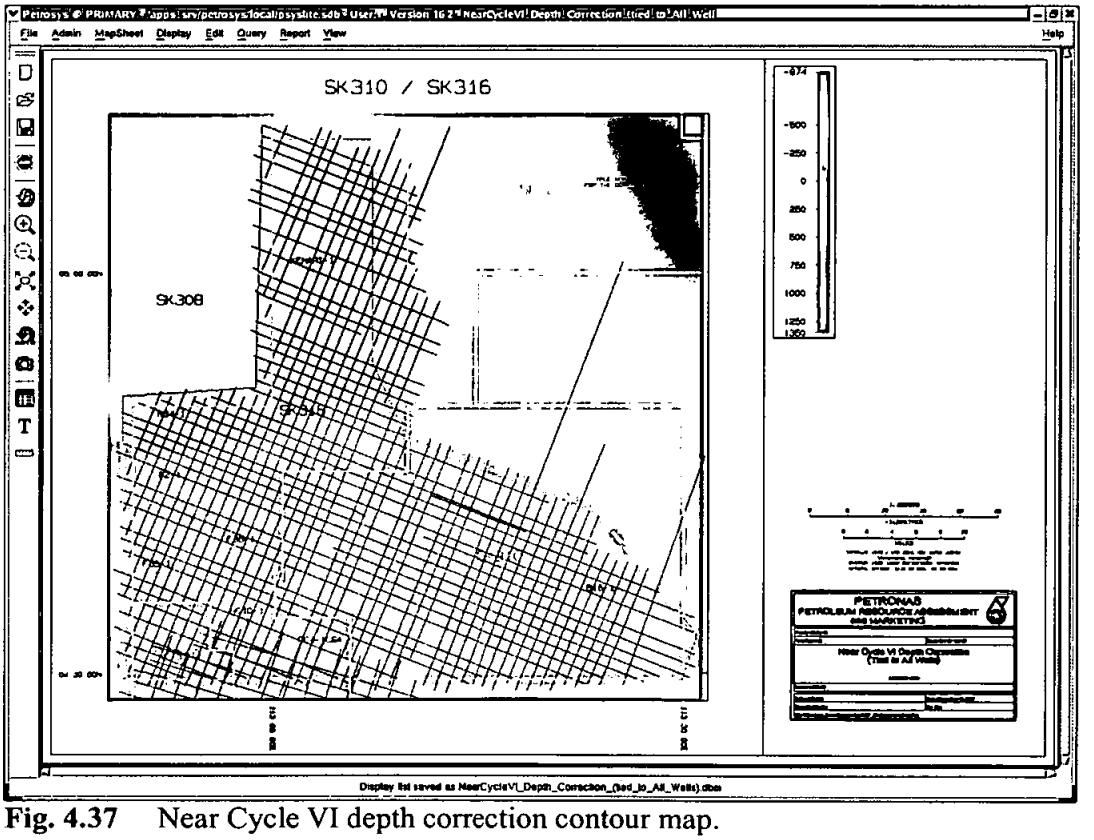

Fig. 4.37 Near Cycle VI depth correction contour map.

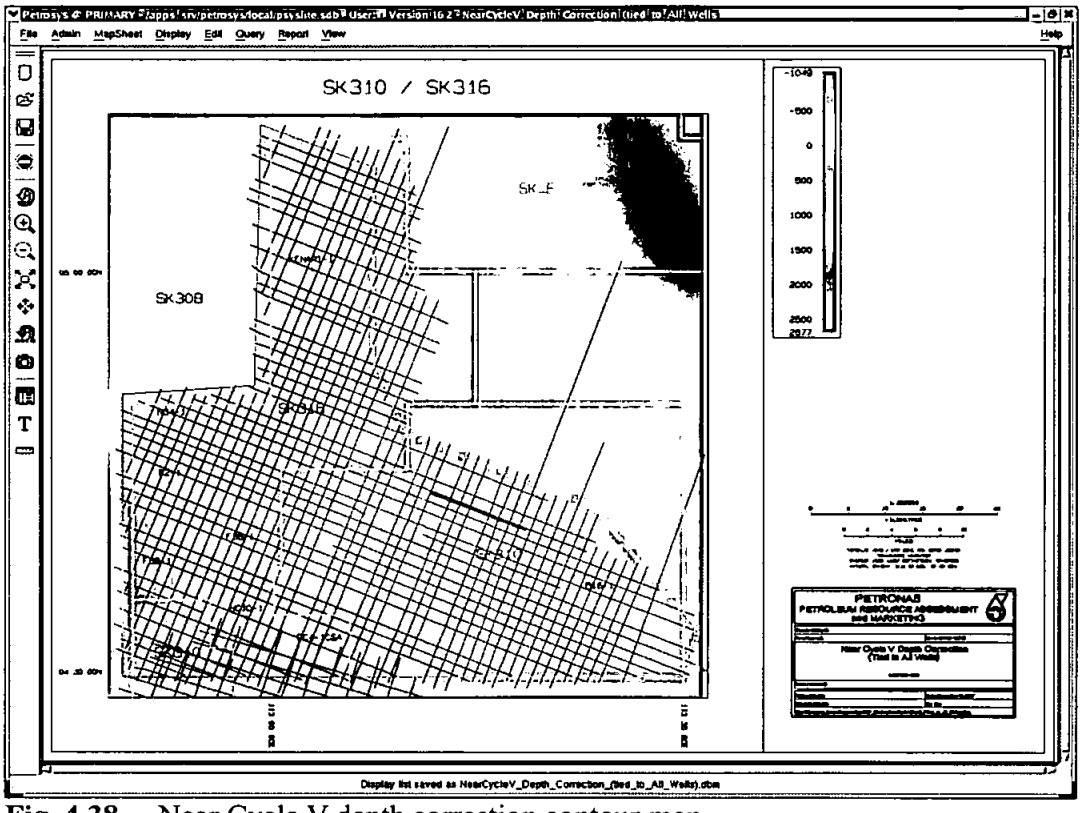

Fig. 4.38 Near Cycle V depth correction contour map.

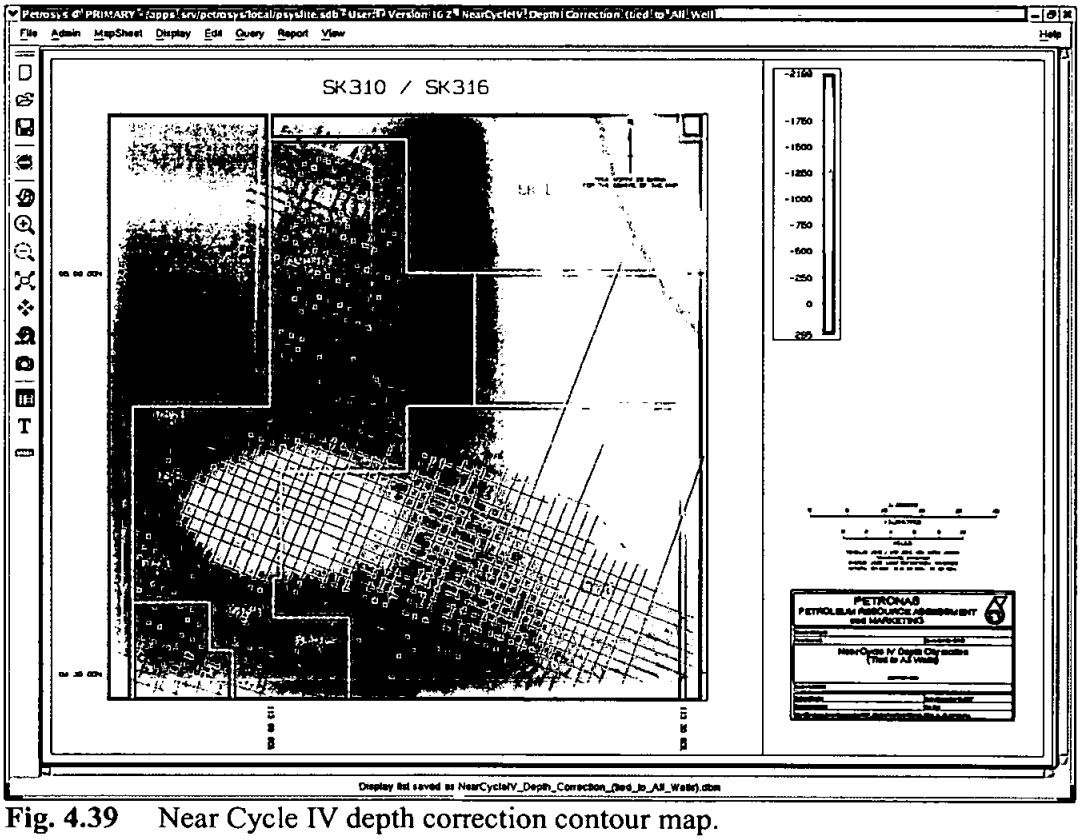

Fig. 4.39 Near Cycle IV depth correction contour map.

4.9 RESULTS

The expected results are:

1. Interval velocity models for the major stratigraphic sequences: maps and gridded models
2. Depth structure map of the target reservoir

4.9.1 INTERVAL VELOCITY MODELS

Figure 3.1 is the interval velocity maps that been computed and generated for each horizon. Workflow 1 (Figure 2.2) is utilized.

Interval Velocity between Seabed & Near Cycle VII Contour Map

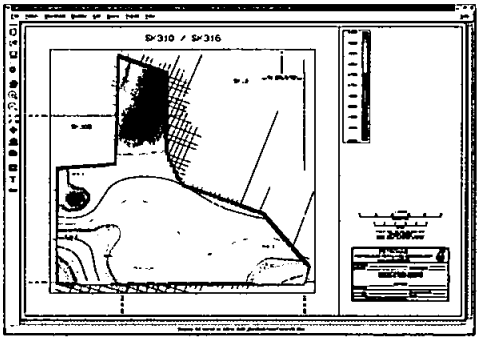

Interval Velocity between Near Cycle VII & Near Cycle VI Contour Map

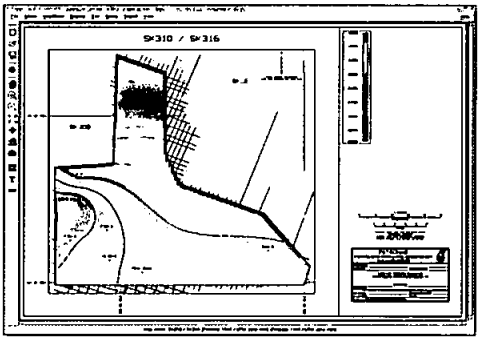

Interval Velocity between Near Cycle VI & Near Cycle V Contour Map

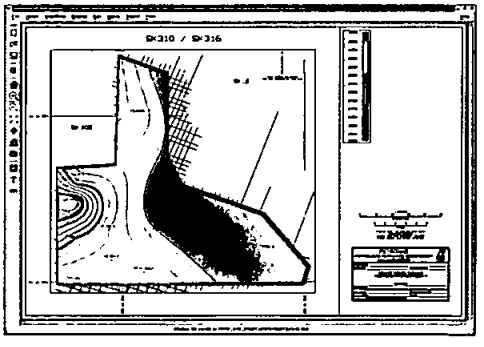

Interval Velocity between Near Cycle V & Near Cycle IV Contour Map

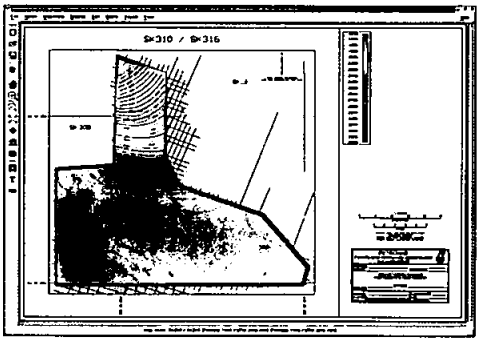

Fig. 4.40 Interval velocity contour map of each layer; Seabed & Near Cycle VII, Near Cycle VII & Near Cycle VI, Near Cycle VI & Near Cycle V and Near Cycle V & Near Cycle IV.

Noticed that there is velocity anomaly in Fig. 2.20 and Fig 2.21. This anomaly will be discussed later in following chapter.

Figure 3.1 is the interval velocity maps that been computed and generated for each horizon. Workflow 1 (Figure 2.2) are followed.

Noticed that there are some anomalies (red bull eye) had been identified at the interval velocity contour map (Fig. 4.16 – Fig. 4.17) especially between Near Cycle VII & Near Cycle VI and between Near Cycle VI & Near Cycle V. These anomalies is located at well F2-1.

The reason of this anomaly are due to high faulted block topography on the underlying lower Cycle IV/V clastic-carbonate shelf. This platform is surrounded and overlain by a thick sequence of clastics raging in age from Cycle V to recent that might have migrated from the Baram Depocenter. The thicker of carbonate section in the F2-1 also maybe contribute to these anomalies.

4.9.2 DEPTH STRUCTURE MAP OF THE TARGET RESERVOIR

Refer to Workflow 2 (Fig. 2.3), we can compute and generate the depth contour map of the target reservoir. Figure below is the best result for the depth contour map of the carbonate structure in Central Luconia Province, offshore Sarawak.

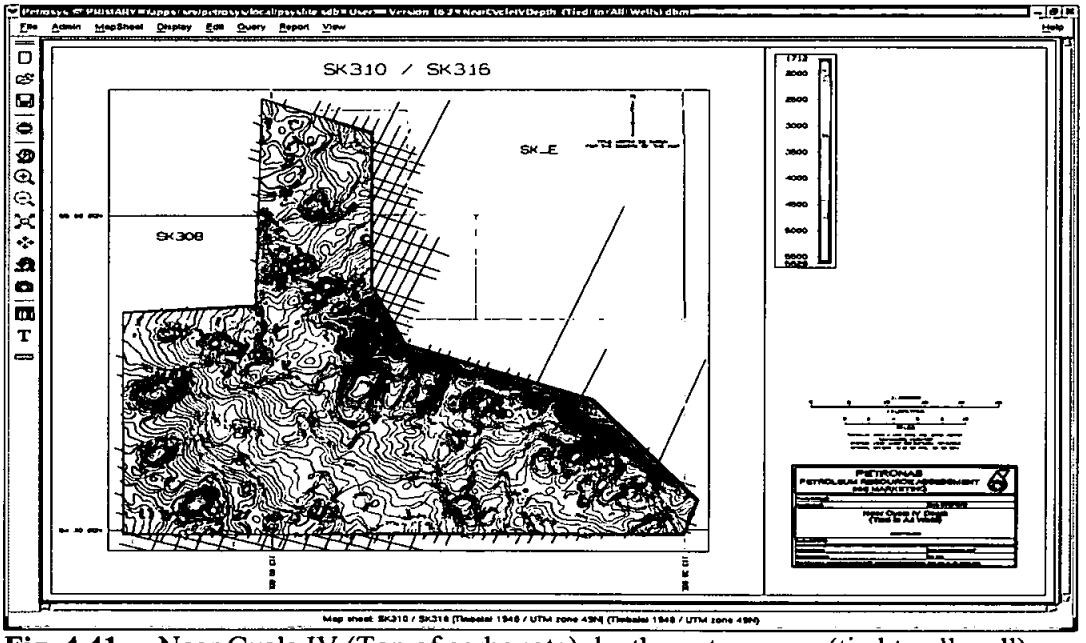

Fig. 4.41 Near Cycle IV (Top of carbonate) depth contour map (tied to all well).

4.10 COMPARISON IN DEPTH CONTOUR MAP USING DIFFERENT TYPE OF VELOCITY

Some comparison in depth contour map using different type of velocity had been done for this case study.

Below figure shows workflow for depth contour map generated from interval velocity models and average velocity models (Fig 4.42).

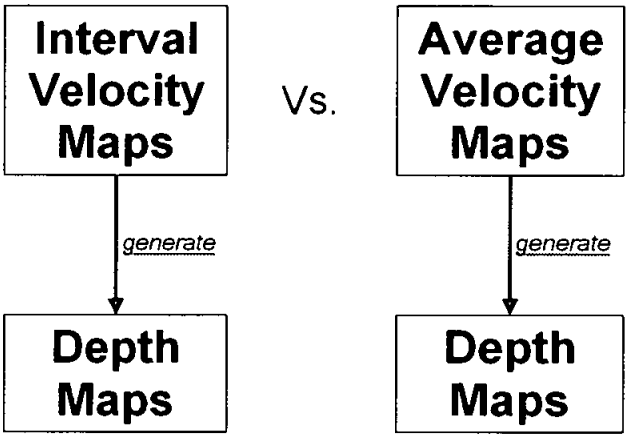

Fig. 4.42 Workflow for depth map generated from difference type of velocity.

Table 4.1 and Table 4.2 are the comparison in depth contour map generated from interval velocity models and average velocity models.

Generally, depth contour map generated from average velocity models is shallower than depth contour map that generated from interval velocity models in this case study. It shows that if we using depth contour map of the target reservoir generated from the average velocity models is totally wrong. This will affect the well depth forecasts and prospect evaluation later. It is better to use the depth contour map generated from interval velocity models. This is to avoid the error in depth prediction and volumetric calculation.

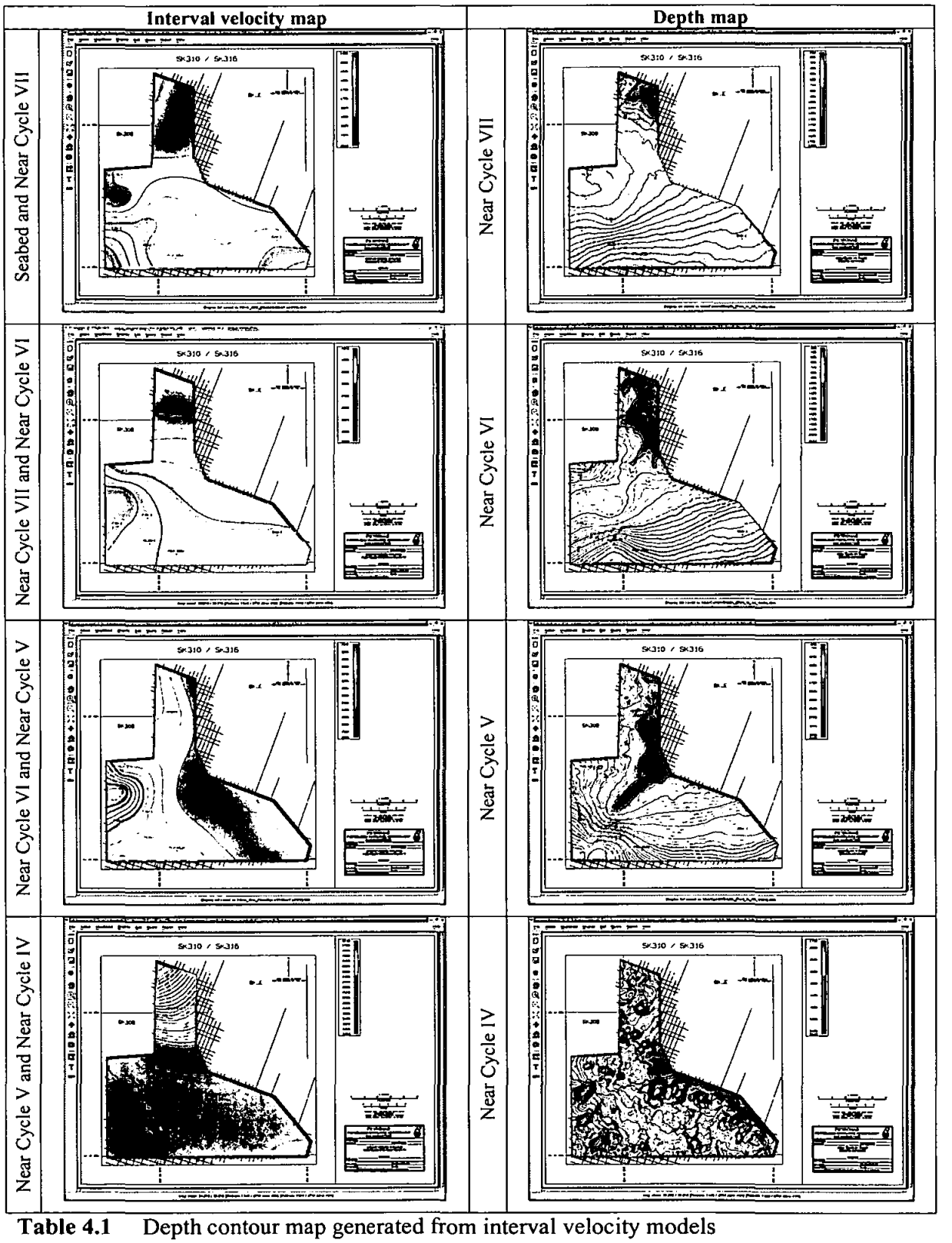

Table 4.1 Depth contour map generated from interval velocity models

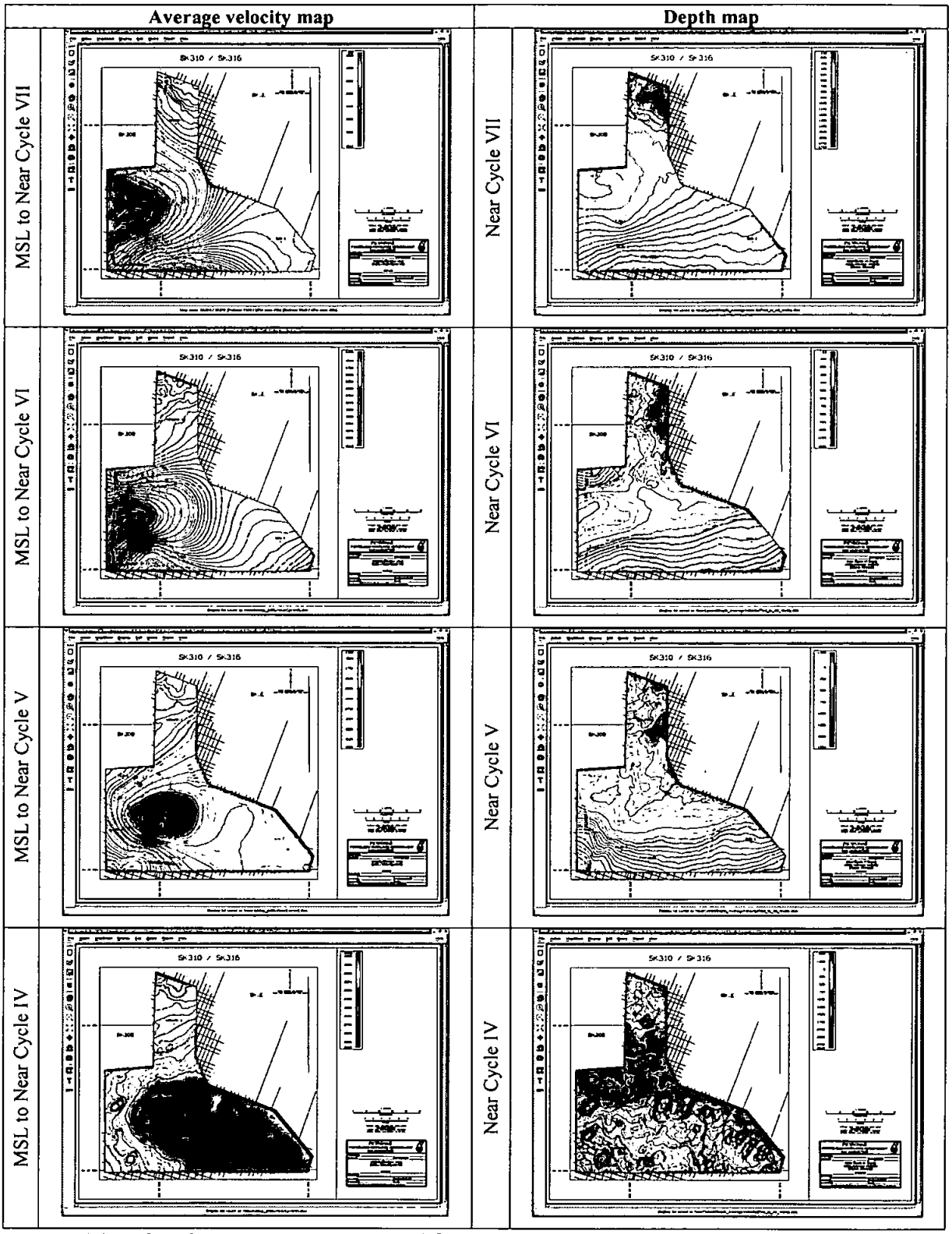

Table 4.2 Depth contour map generated from average velocity models

4.11 BLIND WELL TEST

Below coordinate had been chosen to the blind well test using the depth contour map generated from the interval velocity models.

Coordinate: [113° 00′ 00″ E, 4° 45′ 00″ N]

Horizon	V_{int} (ms^{-1})					OWT_{int} (s)					$Depth_{int}$ (m)					Accumulative Depth (m)
MSL	1475					0.7350					108.41					0.00
Seabed		1763					0.1446					253.98				108.41
Near Cycle VII			2025					0.2969					601.26			362.39
Near Cycle VI				2330					0.3523					820.93		963.65
Near Cycle V					3310					0.1735					2361.82	1784.58
Near Cycle IV																4146.40

Table 4.3 Depth calculation using interval velocity models in blind well location

In Table 4.3, the depth of Near Cycle IV is calculated at 4146.40 m. However, the result from this case study shows that the depth at the blind well coordinate is slightly deeper at 4150 m, based on depth contour map generated from the interval velocity models. It depicts a negative variance of 3.60 m between these values, giving 99.91% accuracy in depth prediction.

Thus, interval velocity models in this case study is the optimum velocity models generated in refining the accuracy of depth prediction and improve the depth structure mapping of the carbonate reservoir.

CHAPTER 5

CONCLUSION & RECOMMENDATION

5.1 CONCLUSION

This case study shows that by finding the optimum velocity model, we can refine the accuracy and alleviate the uncertainties of depth prediction and improve the depth structure mapping of the target reservoir. In this case, the target reservoir is the carbonate structure.

With these depth structure maps, we also can use it help to determine for:

1. **Well forecasts**
   Improve the wildcat well depth forecast in exploration.

2. **Prospect evaluation (volumetric)**
   Reduce the uncertainties in hydrocarbon volume estimation.

3. **Structural Interpretation and Modelling**
   Improve the depth structure map of the carbonate pinnacle reservoir in interpretation and modelling.

4. **Basin Analysis**
   Help in sedimentary basin analysis whether to determine the possible presence and extent of hydrocarbons and hydrocarbon-bearing rocks in a basin or concerned with any or all facets of a basin's evolution.

5.2 RECOMMENDATION

It is best to add more well control in generating the best optimum velocity models. This can help in refine the accuracy for generating the depth contour map later.

To enhance this case study, it would be best if the method can be tested to some other carbonate area to further test the applicability of the method.

REFERENCES

Aigner, T., Doyle, M., Lawrence, D., Epting, M., and Van Vliet, A., 1989. Quantitative modelling of carbonate platforms : some examples. In: Crevello, P.D., Wilson, J.L., Sarg, J.L., Srag J.F., and Read, J.F., eds., Control on carbonate platform and basin development, Society of Economic Paleontoligists and Mineralogists Special Publication No. 44, 27-37.

Baldwin, B. and Butler, C., 1985. Compaction curves: AAPG Bulletin, v. 69, No.4.

Caline B. and Mohammad Yamin Ali, 1991. Depositional and diagenetic cyclicity in a Miocene carbonate built-up (F23) Central Luconia gas province, offshore Sarawak. A contribution to Carbonate Research Workshop, 28 Oct. to 2 Nov. 1991, 1-16.

Doust, H., 1981. Geology and exploration history of offshore central Sarawak. In: Halbouty, M.T., ed., Energy Resources of the Pacific Region. American Association of Petroleum Geologist, Studies in Geology Series, 12, 117-32.

Epting, M., 1980. Sedimentology of Miocene carbonate buildup, Central Luconia, offshore Sarawak, Bulletin of the Geological Society of Malaysia, 12, 17-30.

Gardner, G.H.F., Gardner, L.W. and Gregory, A.R., 1974. Formation velocity and density - The diagnostic basics for stratigraphic traps: Geophysics, 39, p. 770-780.

Ho, K.F., 1978. Stratigraphic framework for oil exploration in Sarawak. Bulletin of the Geological Society of Malaysia, 10, 1-13.

Homewood, P.W., 1999. Best practices in sequence stratigraphy for exploration and reservoir engineers. Elf EP- Editions, Mémoire 25, 34-44.

Magara, K., 1986. Geological models of petroleum entrapment, Elsevier Applied Science. Keith, L.A. and Rimstidt, J.D., 1985, A numerical compaction model of overpressuring in shales: Mathematical Geology, v. 17, No.2.

Mohammad Yamin Ali, 1994. Reservoir development in the Miocene Carbonate, Central Luconia Province, Offshore Sarawak. American Association of Petroleum Geologists International Conference (Abstract), Kuala Lumpur, 21-24 August, 1994.

PETRONAS, 1999. The Petroleum Geology and Resources of Malaysia. Petroliam Nasional Berhad, Percetakan Mega Sdn Bhd., 371-391.

Schlager, W., 1981. The paradox of drowned reefs and carbonate platforms: Geol. Soc. Am. Bull., 92, p. 197-211.

Schlumberger, 1991. Schlumberger Wireline and Testing. 225 Schlumberger Drive, Seventh printing, 3-1 – 3-7, 5-1 – 5-9.

APPENDIX 1

Workflow – Landmark

28 November, 2007

Summary

These notes are intended to compliment the Petrosys online help and Training manuals – not replace them. For more information on importing data, using the WDF editor, mapping and gridding please consult the training manual.

Procedure

1. Execute Petrosys from OW menu – Applications/Petrosys
2. Select an existing Petrosys project from the list, or create a new project as outlined below
3. Import and QC the 2D seismic data – navigation and interpretation
4. Import the 3D seismic data – surfaces and survey outlines
5. Import and QC the well data – well header, directional survey and tops
6. Map the data
7. Grid the data and display the grids / contours

Preparation in Landmark (SW / OW)

Petrosys cannot import or read fault polygons stored in the Landmark mapit file, so before loading the fault polygons into Petrosys you need to make sure that they have been written to the OW database:

1. Execute SeisWorks
2. In the map view, select Applications/Write to database
3. Write the fault polygons to the database

You do not need to worry about doing any preparation of the seismic navigation, interpretation, or the well data as this will have already been written to OW / SW and accessible within Petrosys.

Execute Petrosys

Select the Applications/Petrosys option from the OW start menu. If the option is not available ask Rozilan or Yusmaizi.

Select the appropriate team when prompted.

Create or Select a Project

Select an existing project from the list or Create a new Petrosys project using one of 2 approaches:

1. Use *Project/New* to create a new project
2. If you have MASTER / EXAMPLE projects available in the list use the *Project/Copy* command to copy the example project to a new project.

When creating new projects:

1. Change the Filter to the correct directory:
   a. Petronas Carigali projects should be created under:
      /petrosys_data01/<TEAM>
   b. PMU projects should be created under:
      /pmu_common/PETROSYS_DATA/<Team>
2. Enter the name of the new project after the full path name at the bottom of the file selection filter.

<TEAM> is the name of your group, for example SKO, TRAINING etc

Default Coordinate Reference System (CRS)

When you first run Petrosys in a new project you will be asked to define the Coordinate reference system. This should match the datum / projection set in your OW project. Note that all the data that you import to a Petrosys project should be in the same CRS.

For example:

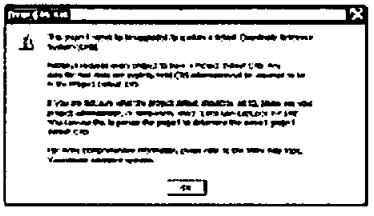

Click on OK and then select the CRS:

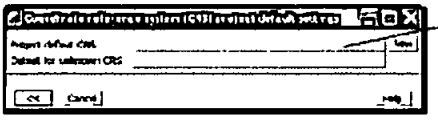

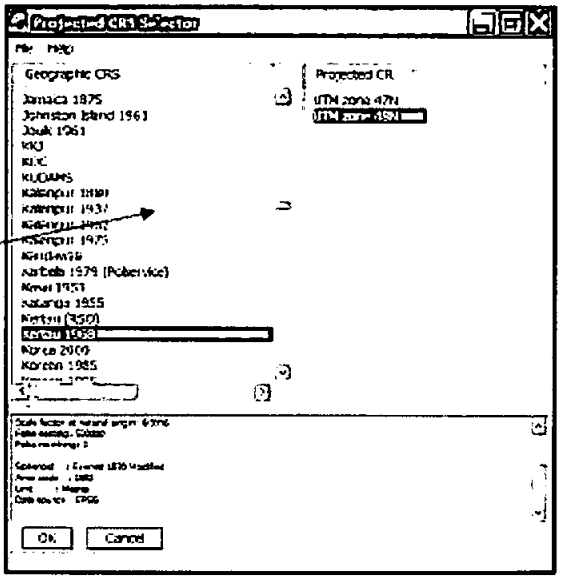

2D Seismic Data – Import and QC

2D seismic data is loaded into a Petrosys SDF as follows:

1. Import the 2D Seismic Data (coordinates, interpretation, fault polygons and cultural data) using *FILE/Import/Landmark/Seisworks direct link*:
    a. Select the project
    b. Import the coordinates and the interpretation:
        i. Create a new SDF using *Create new SDF*, or select an existing SDF. You must define at least 2 new horizons but you can add more horizons at a later date.
        ii. Select the lines to load (you may need to switch off duplicates)
        iii. Select the horizons to load by clicking on the tick box.
        iv. Double click on the selected horizons to translate them to Petrosys codes. If the Petrosys code does not exist then use the *Edit horizons* option to add new horizons.
        v. Import the coordinates using the *Import coordinates* button. Compress and Create new lines should be ON. You only have to do this once per SDF.
        vi. Import the horizons using the *Import horizon data* option. Compress should be OFF, and select the correct data types. If you want to load amplitude, phase and other data types then you should create new Petrosys horizons with appropriate names.
    c. Import the fault polygons using the *Import fault polygons* option. Load Z values should be OFF, and Close fault polygons should be ON.

    You must make sure that the faults have been written to the OW database before you can import them to Petrosys. See note on Page 1.
2. QC the seismic data:
    a. *SEISMIC/Project Manager*
        i. Compute line intersections using the *Coordinates/Compute intersections* option and make sure that *Line activity to honour* is set to LINE
        ii. Generate a mistie report using *Reports/Mistie* and view the report using the text browser.
    b. *SEISMIC/Edit/Seismic data* – QC the interpreted data values
        i. Select a line using *Line/Select*
        ii. Use *Display/Profiles* to highlight TWT / Intersections and Misties
        iii. Scroll from line to line to see that the data has loaded correctly and that there are no bad misties

3D Seismic Data – Import

3D data is only loaded into an SDF if you want to use stacking velocities to do a depth conversion. In general most people convert the 3D surface to a grid and then regrid the grid. Even if you want to use stacking velocities, there are ways around loading the interpreted data to an SDF. To import the 3D surface and associated fault polygons use the *FILE/Import/Landmark/Seisworks direct link* option:

1. To load 3D surfaces:
    a. Select the horizons to load by clicking on the tick box.
    b. Select the *Import 3D surfaces to Petrosys grids* option. The 3D surfaces will be converted to Petrosys grids.
2. To load fault polygons:
    a. You must make sure that the faults have been written to the OW database before you can import them to Petrosys. See note on Page 1.
    b. Create a new SDF using *Create new SDF*, or select an existing SDF. You must define at least 2 new horizons but you can add more horizons at a later date.
    c. Select the horizons to load by clicking on the tick box.
    d. Double click on the horizons to translate them to Petrosys codes. If the Petrosys code does not exist then use the *Edit horizons* option to add new horizons.
    e. Import the fault polygons using the *Import fault polygons* option. Load Z values should be OFF, and Close fault polygons should be ON.
3. To load the 3D survey outline:
    a. Click on the *Save 3D survey outline as polygon* option and enter the name of the polygon file to contain the survey outline polygon.

<u>QC Data</u>

The best way to QC the grids created at the time of import, is to display them in mapping:

1. *MAPPING/Interactive*
2. *Display/Grid/Values* – display ALL the symbols and no values
3. *Display/Grid/Values* (again) – display the Non-missing symbols and no values in a different colour

You can now see the bin locations (all symbols) and the interpreted lines (non-missing)

<u>Dealing with 3D Stacking Velocities</u>

If you plan on working with 3D stacking velocities, the coordinates for the 3D inlines / xlines must exist in an SDF:

1. Create a new SDF using *Create new SDF*, or select an existing SDF. You must define at least 2 new horizons (even though you may not be loading the interpretation)

2. Select the 3D survey to load. If you are planning on loading more than one 3D survey into the same SDF then you should assign prefix/suffixes to the line names (RMB/Assign prefix/suffix)
3. Import the coordinates using the *Import coordinates* button. Compress and Create new lines should be ON. You only have to do this once per SDF.
4. You could (not recommended) import the horizon data using the same procedure as we have done for 2D data, but you are probably better off back-interpolating the 3D grids to the SDF prior to doing the velocity analysis, as follows:
    a. Load the stacking velocities using the *FILE/Import/Velocities* option. You may need to reformat the velocity file and you need to make sure that the line name in the SDF matches the line names in the ascii file (contact Petrosys support for details)
    b. Create the TWT grids from the 2D or 3D data
    c. Back interpolate the grids to the SDF using the *PGC/Grid/Back interpolate/SDF* option
5. Use the *SEISMIC/Velocities-Depth/Velocites/Compute from Stacking* options to convert the stacking velocities to average or interval.

Import the Well Data and QC

Well data (header, directional survey and tops) is loaded into a Petrosys WDF as follows:

1. *FILE/Import/Landmark/OW → WDF*
2. Create a new WDF:
    a. You must define the Units (and this should match the units in Landmark) and the Coordinate Reference System (and this should also match the CRS in Landmark)
3. Select the OW project and the OW well list
4. Highlight the wells and formation tops to import
5. Import the well data:
    a. Load Common well name
    b. Filter by Interpreter if appropriate
6. QC the data under MAPPING/Wells:
    a. Use the appropriate icons to display the well header and directional survey data for the current well. Select the appropriate wells from the list of wells displayed in the bottom left hand corner.
    b. Open up the tree widget for the current well or for the selected wells / zones and display the data in a spreadsheet view. Check the BH / TH locations and see if they are correct.
    c. See the training notes for more information on editing / viewing the well data in a WDF

Mapping

Now that you have imported and QC'd the data you can start mapping:

1. *MAPPING/Interactive*
2. *File/Preferences/Datum conversion* – set the appropriate datum
3. **If this is a new project with no existing mapsheets**, then you will need to create a mapsheet:
    a. *Mapsheet/Create/Coordinate range*
        i. Use the SDF as the input data source, leave the template blank and set the coordinate type to Rectangulars
        ii. OK
    b. Make sure that you select the coordinate reference system (CRS)
    c. Change the min / max East/North as required (maybe round the numbers up and down).
    d. Change the scale and other parameters as required
    e. OK
4. If this is an existing project then you can select the appropriate mapsheet, using the *Mapsheet/Select* option.
5. Display the seismic data as follows:
    a. Display the seismic lines using the *Display/Seismic/Lines and data* option. Create selection files / line style files as required
    b. Post the interpretation using the *Display/Seismic/Ribbon maps* option
6. Display the well locations using the *Display/Wells* option
7. Display ply files created using the *Display/Polygon* option
8. Display the fault polygons using the *Display/Faults* option. If the fault polygons need editing use the *Edit/Contours, Faults, Polygons* option to do so. Only edit the **fault polygons** (not the contours, polygons)
9. Display the 3D surfaces using the *Display/Grid/Colourfill* option

Grid the Data

You can grid the well data, 2D interpretation and 3D surfaces; do arithmetic operations, handle faulted surfaces, tie the resulting grids to wells and merge grids together. This information is outlined in the Petrosys online help and training manuals and will not be repeated here.

This section outlines 2 typical workflows:

- Gridding of 2D seismic data
- Re-Gridding of a 3D surface

Gridding 2D Seismic Data

There are 3 questions to ask:

1. What is the AOI (Area of interest) of the grid – display data, select / create mapsheet
2. What cell size to use – 1/5 to 2/5 average spacing
3. What clipping to use if any – do you use a clipping distance or create a clipping polygon using the *Edit/Create single polygon* option.

Use the following procedure:

1. Display the seismic lines and the interpretation as a ribbon map
2. If necessary create a smaller mapsheet around the area of interest using the *Mapsheet/Create/Using mouse/EN* option (this will be the AOI)
3. Use the distance-Measure icon to work out the average spacing between lines and select an appropriate cell size eg 1/5-1/3 average line spacing
4. If necessary, create a clipping polygon using the *Edit/Create single polygon* option. Save all the clipping polygons to one file (eg clipping.ply) and create polygons for each formation. If you can get away with one polygon then that is great.
5. If necessary create selection files containing the wells and seismic lines to grid – not generally required.
6. *Grid, Contour, Volumetrics*
7. *Grid/Create grid*
    a. Define the output grid, the input data, the fault file, clipping polygon etc.
    b. Important parameters include Cell size, Area of interest – mapsheet for 2D; Fault file – no to Z value; Contouring – 10 for faulted cells and contour up to faults set to Y
8. Display the Grid / Contours on map:
    a. *Display/Grid/Colourfill* to display the grid – select an appropriate increment
    b. *Display/Contours*
    c. *Display/Colour bar* to post the colour range
    d. *Edit/Gradient* if you want to edit the gradient

e. *Display/Map base* to display the mapsheet on top of the grid

9. Display the grids in the 3D viewer

Gridding 3D Seismic Data

1. Display the 3D survey outline on a map using the *Display/Polygon* option
2. Display the interpreted values using *Display/Grid/Values* and make sure:
   a. Symbols = Non-missing
   b. Values = N

   This will display only the interpreted values / traces
3. If necessary, create a clipping polygon around the actual interpreted values using the *Edit/Create single polygon* option. Otherwise the resultant grid will cover the entire 3D survey outline

   Save all the clipping polygons to one file (eg clipping.ply) and create polygons for each formation. If you can get away with one polygon then that is great
4. *Grid, Contour, Volumetrics*
5. *Grid/Create grid*
   a. Define the output grid, the input data (3D surface grid), the fault file, clipping polygon etc.
   b. Set the AOI to the input grid
   c. Set the *Cell size* to a multiple of the cell size of the original grid (or leave exactly the same)
   d. Make sure *Snap to cell size* is set to *N*
   e. Other parameters include - Fault file – no to Z value; Contouring – 10 for faulted cells and contour up to faults set to Y
6. Display the Grid / Contours on map:
   f. *Display/Grid/Colourfill* to display the grid – select an appropriate increment
   g. *Display/Contours*
   h. *Display/Colour bar* to post the colour range
   i. *Edit/Gradient* if you want to edit the gradient
7. Display the grids in the 3D viewer

Fault Handling

There are a number of ways to deal with fault polygons. The recommended approach is as follows:

1. Grid/Create grid and grid the data as described above, but make sure:
   a. Select the fault file
   b. Set the *Keep inside faults* field under the Faults tab to *N*

   This will create a grid with no data in the fault polygons
2. Re-grid the grid using the same cell size, and the AOI set to the grid, but do not include the fault file. This will result in the values in the "fault polygons"

being interpolated between the existing grid values. Because the AOI matches the existing grid, nothing will change away from the faults. You can even use a different gridding method if so desired.

3. Load the fault file back into the new grid using the *../Grid/Load fault file* option. This assumes that the fault plane between the top and bottom surfaces is linear. It will not work if you have listric faults (for example).

APPENDIX 2

Increasing interpretation accuracy:

A new approach to interval velocity estimation

By DAVID HADLEY, JEFF THORSON and SHANNON MAHER
Sierra Geophysics, Inc.
Seattle, Washington

A crucial paradox exists in the discrepancy between the accuracy to which arrival times of seismic events are routinely picked by interpreters (a few tenths of a percent) and the accuracy inherent in the use of interval velocities for depth conversion (10-20 percent). In addressing this full 10 000 percent (or full factor of 100) difference in accuracy, a new approach for velocity determination has been developed. This approach directly addresses three major problems that degrade interval velocity analysis: complex overburden structure; uncertainty in the location, strike and dip of the depth-point reflector; and depth-point smear along the reflector.

The new approach greatly improves upon the industry's standard techniques. Tests show that the derived interval velocities depart from the model velocities by about 1-2 percent in shallow horizons and by 2-4 percent in the deeper horizons. For the same models computed with the Dix equation or from the dip-corrected Dix equations (standard technique), the interval velocities varied by 20-50 percent. In addition, tests have shown that the approach is stable in the presence of typical noise levels and interpretation uncertainties.

Conceptually, the determination of interval velocity is a simple geometric problem. With increasing offset, the raypaths within the interval of interest change path length, and the observed traveltimes show a characteristic moveout. For geologic models with constant interval velocities and simple flat-lying interfaces, the observed moveout is sufficient to solve for interval velocities. Fortunately, exploration plays are generally much more interesting, and (unfortunately) simple assumptions can prove woefully inadequate. Figure 1 shows a slightly more interesting 2-D geologic model and the seismic raypaths associated with one reflection event that contribute to the common midpoint gather. Accurate resolution of the interval velocity for the zone immediately above the reflector requires an analysis procedure that accounts for the complex overburden, the location and dip of the reflector and the depth-point smear.

The geologic overburden can introduce uncertainty and complexity in two distinct ways. First, lateral structural variations alter path lengths in an irregular fashion that cannot be easily predicted from the basic data contained within a single gather. Next, the overburden may contain interval velocities that vary both laterally and vertically. Clearly, these effects conspire to degrade resolution of the component of the observed moveout that should be attributed to the target interval.

The second major problem, the true location of the reflector, is particularly important and difficult. Path lengths in the target interval are directly dependent on the position of this reflector; however, without a good estimate of the interval velocity we cannot correctly position the reflector. It is a bit like saying that a very good analysis of interval velocity could be provided if the correct answer were available at the beginning of the analysis.

For geologic structures with dip, either at the target horizon or in the overburden, the effects of depth-point smear can further complicate analysis. As seen in Figure 1, the far offsets tend to reflect from a shallower portion of the dipping reflector, thus changing path lengths from those of the ideal case with a single reflection point.

The previous observations may provide some insight into why the resolution of interval velocity has remained one of the more elusive problems confronting accurate depth conversion. It should not be too surprising to conclude that a satisfactory solution requires bringing to bear every bit of information available to the interpreter: CMP gathers, time maps and accurate estimates of the overburden velocity structure.

Figure 2 provides a graphic overview of a method that overcomes the problems discussed. For clarity, the method is presented as a 2-D analysis, but the method is equally applicable to 3-D geometries. For argument's sake, assume that Horizons 1 and 2 (Figure 2A) have already been depth converted (Figure 2B) and that the task is the computation of the interval velocity between Horizons 2 and 3. The argument remains unchanged for any number of intervals, including the simple first interval.

For any position along the zero-offset section, such as location A, the slope of the time pick can be used to compute the direction that seismic energy approached the CMP (combination of the slope or apparent velocity, Snell's law and the surface velocity at point A). The seismic ray then can be shot into the earth model, refracting at each interface encountered. When the ray reaches the bottom of the model, there is a bit of a problem—the velocity is not yet known for the next interval. However, as with conventional stacking velocity analysis, there is some geologically reasonable range that should be scanned. For each velocity in the scan, the raypath can be extended through the bottom of the model until the total path length corresponds to the observed traveltime from the section.

In general, for the minimum velocity there will be a minimum refraction angle and a shallow reflection point (point B on Figure 2B). Similarly, the highest velocity will, in general, be associated with the largest refraction angle and the deepest reflection point (point C on Figure 2B). Hence, by scanning a range of velocities of interest, the location of the reflection depth point can be computed, thus partially overcoming the second major problem of degrading velocity analysis.

Estimation of the reflection depth point is only part of the solution. The local shape, or at least the dip, of the reflector in the vicinity of the reflection point must be estimated. However, if the seismic section being analyzed corresponds to stacked data (i.e., not time migrated), then the reflector at depth must be perpendicular to the normal incidence raypath associated with each trial velocity. Thus, for each trial interval velocity, a trial planar reflector (D on Figure 2B) may be incorporated into the model, normal to the associated raypath and passing through the corresponding depth point.

Finally, the raypaths and associated traveltimes that connect each source-receiver pair within a CMP gather and that reflect from the dipping plane can be computed (Figure 2B). By repeating this process for a range of velocities, a family of traveltimes versus offset curves (Figure 2C) can be computed. The curves are fully corrected for all of the effects of overburden structure and velocity, location of the depth point and the local dip of the reflector.

This paper was presented before the Geophysical Society of Houston, January 18, 1988.

Note that these curves are, in general, nonhyperbolic.

As a final step, the nonhyperbolic moveout curves must be combined with the CMP gathers to select the best estimate of the interval velocity. This is a fairly easy task; the computed moveout curves are ideally suited for stacking the gathers, computing semblance and assessing which curve optimizes the power in the stack. The simple identification is made that the curve which optimizes the stack corresponds to the correct average interval velocity for the zone above the depth-point estimate (point D on Figure 2B).

Implementation of this approach requires a few additional considerations. Although the interpreter can provide a time pick or time map for estimating the reflection point, in practice there will always be some uncertainty in the absolute reliability of the time. Were the peaks, troughs or zero crossings picked? Was the map smoothed or edited in some way that may introduce minor but significant errors?

The solution to this problem is simply to scan a range of times (say ± 150 ms) around the pick time and compute a range of target reflection points and associated moveout curves for each velocity at each time. Finally, the semblance can be computed for each moveout curve as a function of pick time and average interval velocity.

As might be expected, the raytracing consumes a majority of the CPU time in this approach. Without careful implementation, one could find that the computation of several hundred moveout curves, corresponding to each velocity-time pair, would render this attractive approach unfeasible. Experience has shown that they generally change shape rather predictably with changes in traveltime and interval velocity.

Computation of about 15 curves, corresponding to two to three traveltimes centered around the pick time, and five to seven velocities spanning the range of interest, is usually sufficient to describe the behavior of the moveout curves as functions of pick time and interval velocity. This set of moveout curves can then be interpolated to a more dense set, as functions of time and velocity, to obtain higher resolution for picking semblance peaks.

The algorithm makes the explicit assumption that the overburden structure, in terms of traveltime effects, is known. This requirement can be met if the velocity algorithm is used with a map migration algorithm that also accounts for the overburden. The depth conversion process is then "top-down," which is as follows: First the near-surface velocities are derived (starting model has no horizons). Next the shallowest traveltime map is migrated to depth. For marine prospects, the process starts with the first layer defined by the velocity of water and the bathymetry map. The velocity algorithm is then used to solve for the next deepest interval velocity, and the migration routine uses this derived velocity map for depth conversion of the next deepest traveltime horizon. This process is repeated until all time horizons have been converted to depth.

Figure 3 shows a convenient layout for presenting to the interpreter the results of the interval velocity analysis for a single CMP gather. On the left is the semblance plot showing the power in the semblance spectrum as a function of pick time and average interval velocity. Note that the spectrum is time windowed around the pick time, which is indicated by the bold horizontal tick at 2.125 s. A velocity pick of 3880 m/s, indicated by the vertical bars on the velocity axis, has been made by the interpreter. The seismic gather has been flattened using the complex moveout curve appropriate for the interval velocity-time pick, as described. By picking various velocity-time pairs and redisplaying the gather with the appropriate moveout curve, the interpreter can quickly assess accuracy. Inappropriate velocities will do a poor job of flattening the event. The flattened gather has been summed to produce a "zero-offset" trace, which is displayed in the center of the figure.

The summed trace provides a convenient reference for correlating the event arrival time with interval velocity. The gather shown on Figure 1 was associated with a very strong velocity peak that was well correlated with the picked event. However, over one portion of the play, bounded by two growth faults, it

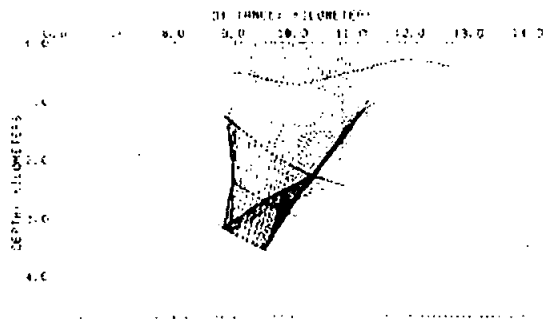

Figure 1. Traveltimes on a CMP gather in structurally interesting areas cannot be predicted by the simplistic Dix flat-layer model.

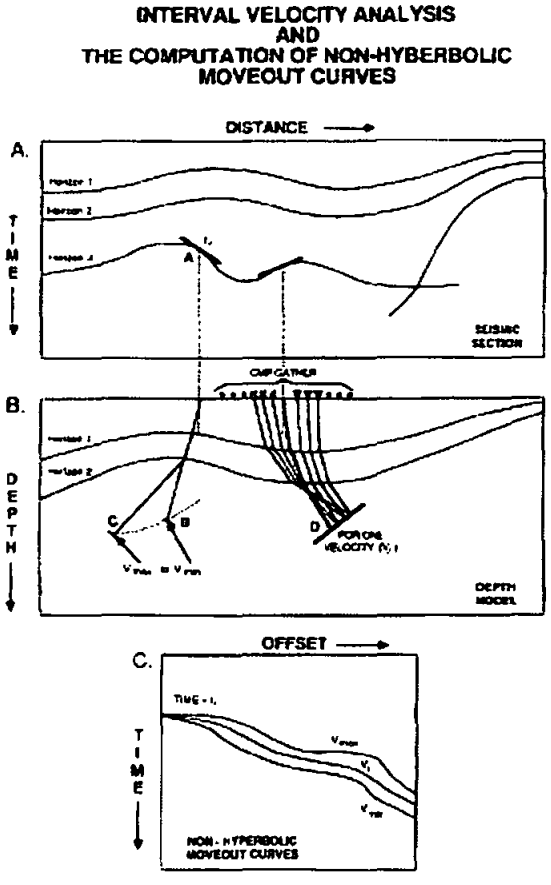

Figure 2. Basic elements of the model-based velocity estimation algorithm for single CMP analysis.

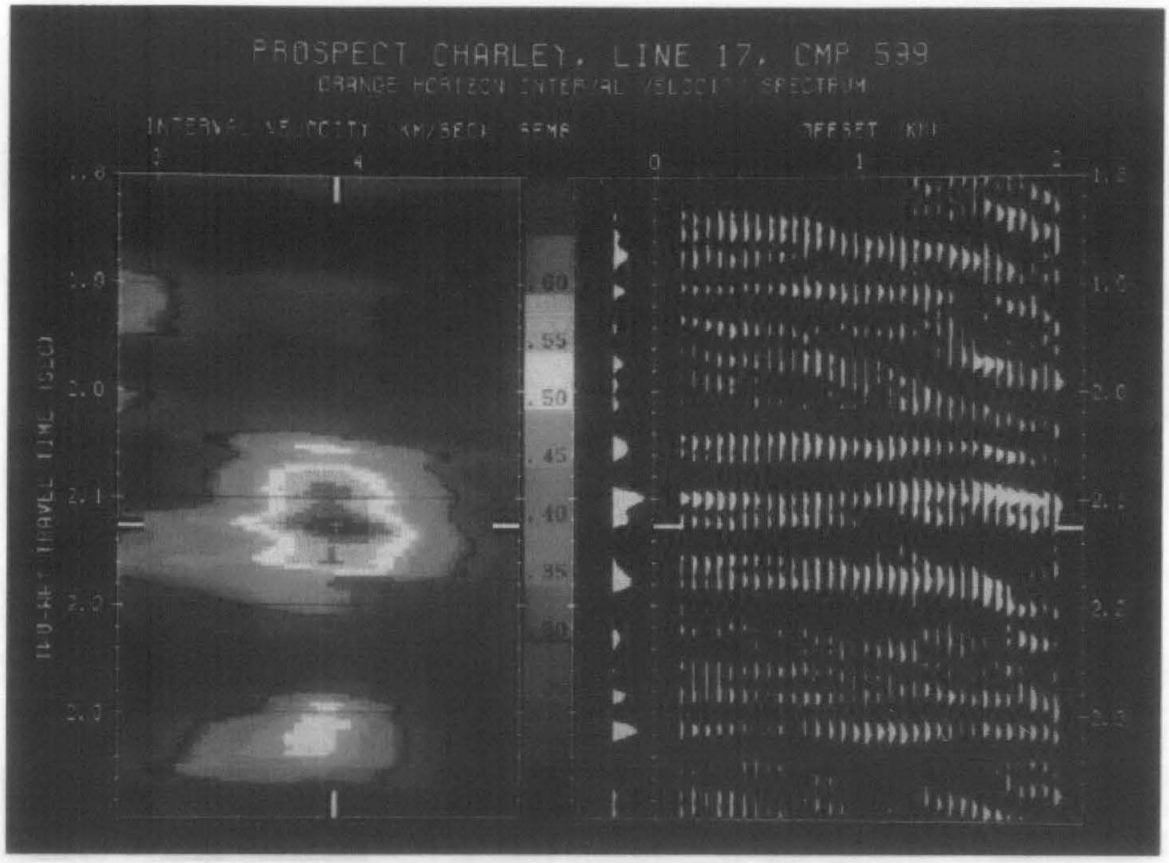

Figure 3. Results of the interval velocity analysis for a single CMP gather.

was noticed that the velocity peak and the interpreted pick times differed by about 35-40 ms. Reexamination of the sections suggested that the interpreter had skipped a cycle over this portion of the map. The joint presentation of the stacked trace and the velocity spectrum provides a good mechanism for the integration of event picking and interpretation with velocity analysis.

The stacked trace is also extremely important for maintaining consistency between the depth conversion (map migration) process and the solution for interval velocities. A recent test with data from the North Sea provided an interesting example. The sections contained strong reflected events with a wavelet shape that appeared to be a doublet (i.e., two distinct reflections that were closely spaced), even though the sections had been processed with deconvolution operators.

Several gathers were analyzed and displayed in the format shown in Figure 3. Each display showed two closely spaced velocity peaks associated with the doublet; the later velocity peak was always associated with an interval velocity that was systematically lower than the first peak by about 4-6 percent. The second semblance peak was interpreted as a peg-leg multiple from a shallow low-velocity zone that reduced the derived interval velocity estimate by the contribution from the lower velocity peg-leg path. Again, the joint display of the velocity analysis and the stacked trace provided a powerful combination for high-resolution velocity analysis. If the velocity analysis had averaged the semblance over the time gate of the doublet, the interval velocity maps would have been systematically biased toward low values, and the depth migration would have underestimated the true depth of the target horizon.

As noted, the proposed algorithm is a top-down process that cycles between velocity estimation and map migration. It is important to note that seismic noise will add uncertainty to the velocity analysis of CMP gathers, and time maps usually reflect both hard data and interpretation judgement. The final geolgic model is developed in a series of steps that proceed from the shallowest horizon to the deepest. Obvious questions arise: What happens when some error is made in the shallow structure? Does the algorithm diverge to unstable or unreliable depth estimates?

A simple geometrical argument shows that the process is somewhat self-correcting for the usual uncertainties and noise levels typically encountered; however, the method cannot compensate for major interpretation blunders. Consider the case in which the interval velocity has been underestimated. The depth conversion process will then underestimate the true depth of the associated reflector. However, the moveout information contained within the gathers remains unchanged, regardless of the derived model, and controls the selection of the "optimum" interval velocity. Hence, the interval velocity analysis for the next deeper zone must automatically select a velocity that is slightly higher than the true interval velocity to compensate for the error in the overburden. Depth conversion using the derived velocity will

then produce an interval that is slightly too thick, compensating for the error in the overburden.

This geometrical argument has been checked with several synthetic model data sets in which large velocity variations were "hidden" in the analysis. These models typically contained five to seven horizons. The goal of these tests was to simulate the real-world case where significant velocity variations might occur within an overburden seismic sequence that was not mapped and, hence, not captured in the velocity analysis-depth conversion process. The results of these tests were both surprising and encouraging: the derived interval velocities departed from the model velocities by about 1-2 percent in the shallow horizons and 2-4 percent in the deep horizons. For the same models, interval velocities computed from the Dix equation or from the dip-corrected Dix equation varied by 20-50 percent.

The algorithm is a top-down approach that integrates with the depth conversion of each mapped horizon and is used to first estimate the interval velocity of the shallowest horizon. Map migration is next used to depth convert the first time map. The derived overburden structure is used, in conjunction with the next deepest time map and the CMP gathers, to estimate the interval velocity for the second horizon. This process continues, alternating between interval velocity analysis and depth conversion, until all time maps have been depth converted.

This approach significantly increases accuracy when working with interval velocities. And because it also reduces the time spent on such estimates, it is cost-effective. LE

David M. Hadley is a cofounder of Sierra Geophysics and has served as senior vice-president since the company's beginning (1978). His current responsibilities include directing all research and software product development. Prior to founding Sierra, Hadley was a research fellow at California Institute of Technology. He received a doctorate in geophysics from CalTech and a master's in geophysics from the University of California, Riverside.

Jeff Thorson is a senior staff geophysicist at Sierra Geophysics. Before joining the firm, he worked as an interpretation geophysicist in the International Division of Getty Oil in Los Angeles. While working on a doctorate in geophysics from Stanford University (1984), Thorson did basic research in seismic processing as a member of the industry-sponsored Stanford Exploration Project. He received a B.S. in geology from the University of Washington (1973) and a M.S. in geophysics from the University of Houston (1975).

Shannon Maher is senior research manager at Sierra Geophysics where he is responsible for management of the company's forward and inverse modeling efforts. Prior to his current position, he worked for the USGS, Branch of Petrophysics and Remote Sensing (1979-81). Maher earned a B.S. in electrical engineering and computer sciences from M.I.T. (1978) and an M.S. in geophysics from the University of Colorado (1982).

APPENDIX 3

Interval velocity estimation using iterative prestack depth migration in the constant angle domain

By N. D. WHITMORE and J. D. GARING
Amoco Production Company
Tulsa, Oklahoma

This article discusses a technique which a number of people at Amoco have been working on since the early 1980s.

We begin by answering two questions: *What is the constant angle domain?* and *Why would anyone want to use it?*

First, although the concept has been around for the better part of two decades, the term "constant angle" is not widely known (for example, it is not included *in* SEG's *Encyclopedic Dictionary of Exploration Geophysics)* probably because seismic exploration has traditionally used a point source which generates rays in all directions. The constant angle technique, on the other hand, uses an extended source which produces a plane wave that has a single ray parameter along its entire length.

This is not just a mathematical convenience; it could be done in the field. Amoco actually performed such an experiment in the late 1970s by simultaneously igniting a series of sources. But, of course, such field work cannot be done routinely because it's far too expensive. However, constant angle data can be produced with computers by superposition of a series of point sources initiated sequentially with a linear time delay (Figure 1).

Second, the major reason to use this domain is that it can handle a large suite of imaging algorithms, from exact moveout on the low end to full f-x migration at the high end. There are ways to actually do elastic migration with ray precision. For the most part, this is the only domain where all these algorithms exist. Their availability makes this domain suitable for migration velocity analysis because it allows the use of very fast f-k methods, phase shift migrations, Kirchhoff migrations when more complicated media are encountered, and then f-x migrations to handle more arbitrary media where the Kirchhoff algorithms start to break down. In addition, this domain allows the use of interval velocity models which are not bound by assumptions of a horizontally stratified earth or by the rms approximation.

Constant angle prestack processing requires two major steps: 1) constant angle plane wave synthesis and 2) iterative constant angle depth migration.

The first is achieved by a tau-p transform of common receiver seismograms, followed by a sort into fixed ray pa-

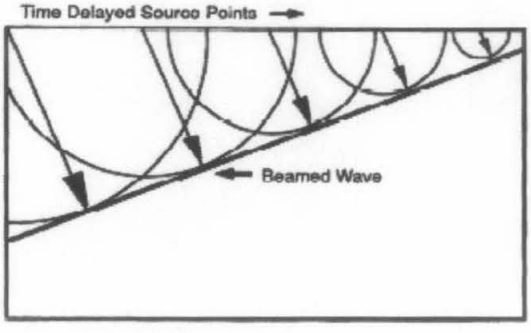

Figure 1. Forming a beamed plane wave.

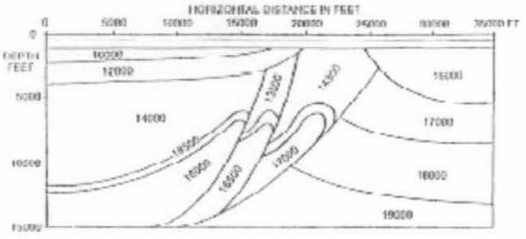

Figure 2. Geologic model showing compressional wave interval velocities.

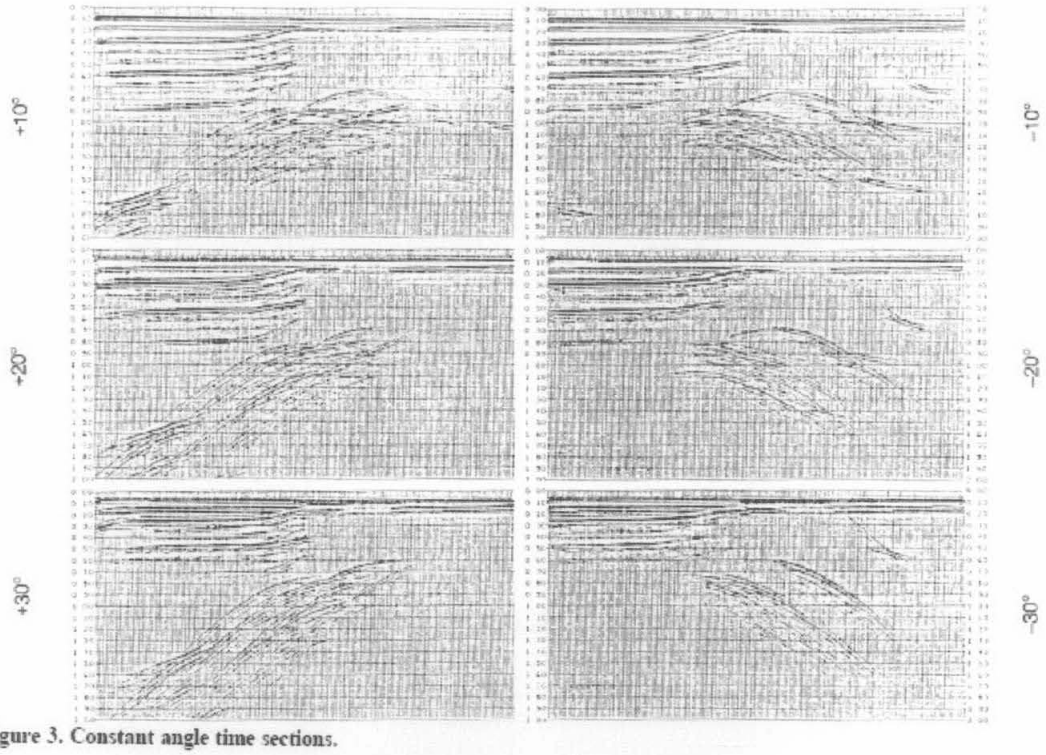

Figure 3. Constant angle time sections.

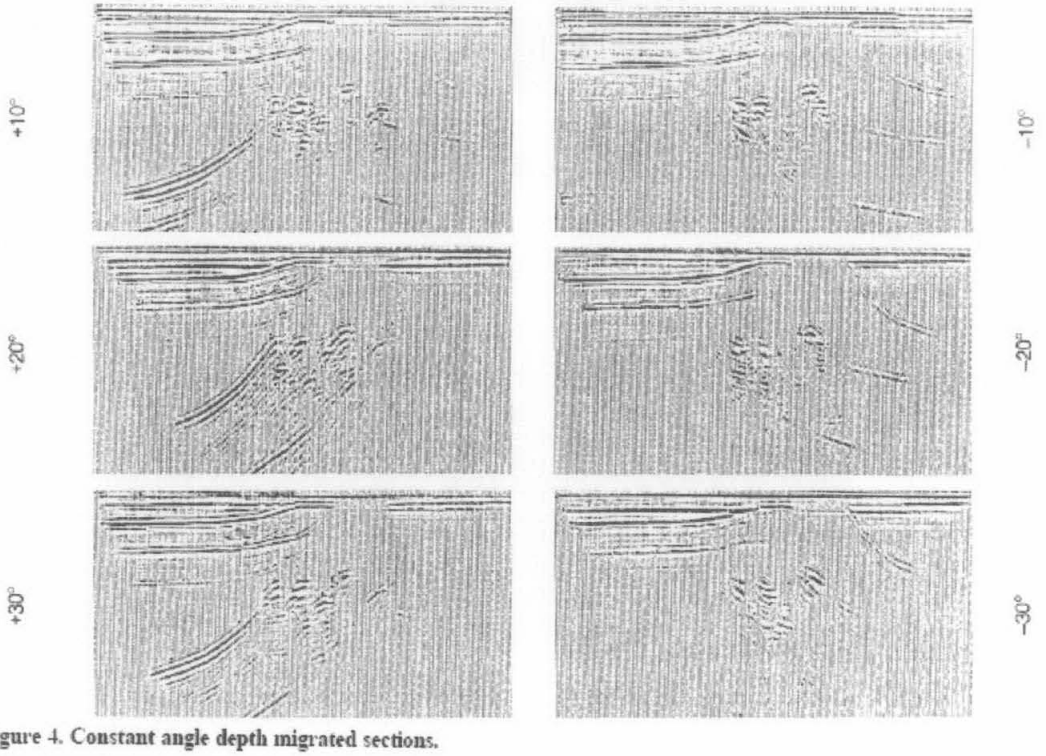

Figure 4. Constant angle depth migrated sections.

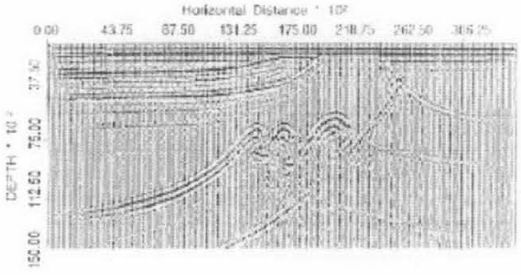

Figure 5. Vertical stack of depth migrated common angles.

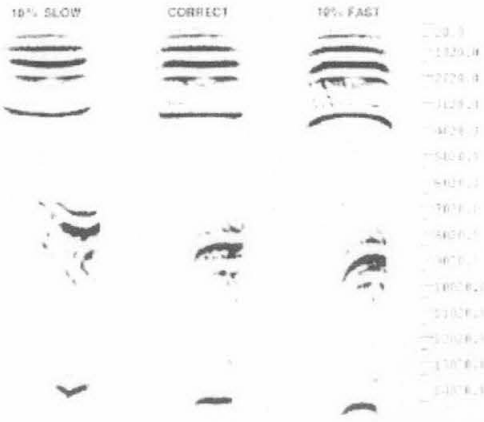

Figure 6. Prestack migration quality control gathers.

rameter constant angle gathers. The tau-p transform is performed in the f-x domain and the result is then transformed back to time.

To demonstrate this, consider the model in Figure 2. A series of finite-difference shotpoint synthetics was processed to produce the constant angle seismograms shown in Figure 3. Note that each of these constant angle seismograms illuminates a different portion of the subsurface.

If a simple linear delay is applied to each trace in a constant angle seismogram, the resulting seismogram can be considered as the surface wavefield response due to a plane wave source spanning the length of the line and, as a consequence, a variety of depth migration algorithms can be applied to the data. In this case, f-x downward continuation operators were applied to produce the constant angle depth migration seismograms shown in Figure 4. Again, each illuminates a portion of the subsurface and their stack (Figure 5) renders a good

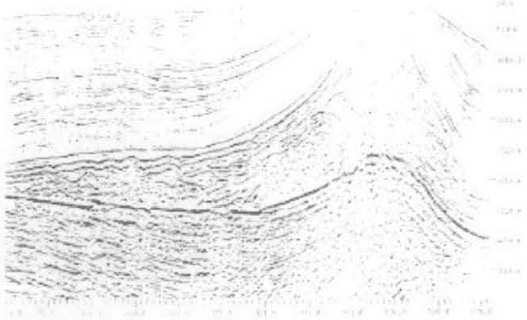

Figure 7. V(z) poststack depth migration.

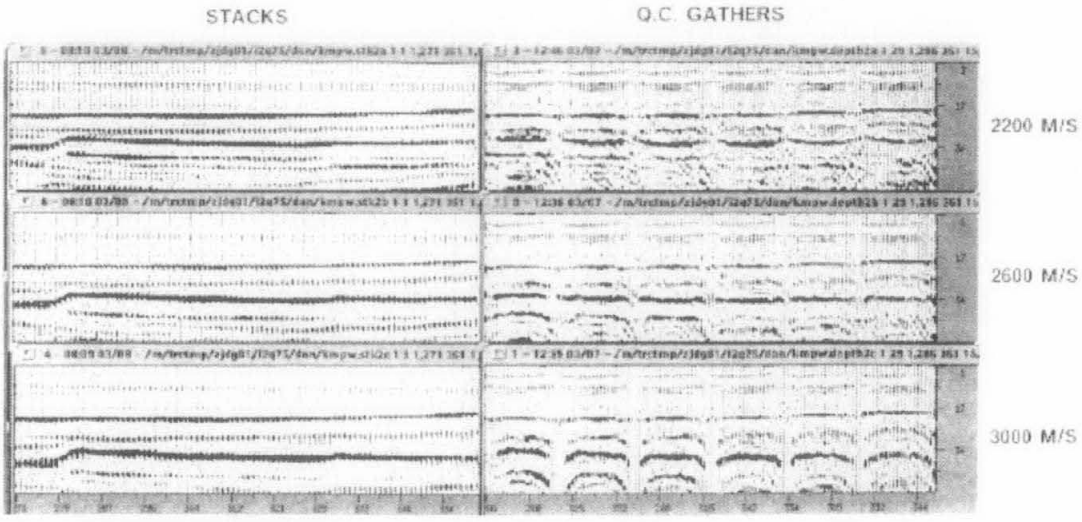

Figure 8. Velocity iterations for layer 2.

approximation of the starting model.

So, this technique produces an output similar to that of conventional migration. Its advantages are that a larger number of migration algorithms are available and that it gives considerable "leverage" for velocity analysis. That leverage is the ability to pinpoint correct velocities on the consistency-or lack of curvature-of the data across a constant angle section.

Figure 6 is an example; note that slow velocities curve upward (or "smile") across the velocity gather, fast velocities curve downward ("frown"), and correct velocities are constant accoss the entire gather.

We have used this leverage to develop a technique for interval velocity determination that could be termed "prestack layer stripping." It can be implemented as follows:

1) Make an initial estimate for the interval velocity and gradients in the first layered sequence.

2) Prestack migrate the constant angle data down to a sufficient depth to encompass the velocity model in step 1.

3) Inspect the prestack sort and sum to determine the viability of the velocity estimate.

4) If the estimate is incorrect, perturb the model appropriately and return to step 2.

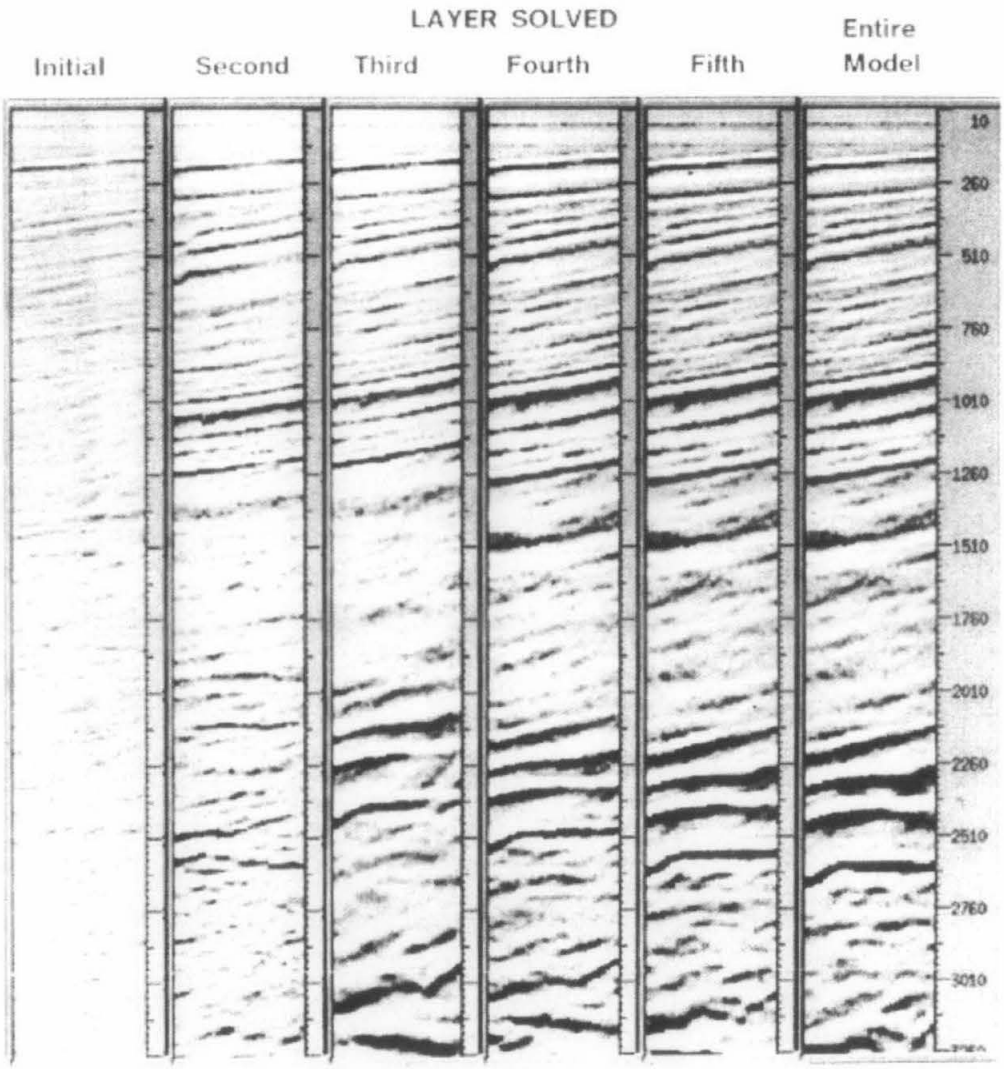

Figure 9. Velocity model evolution stack changes.

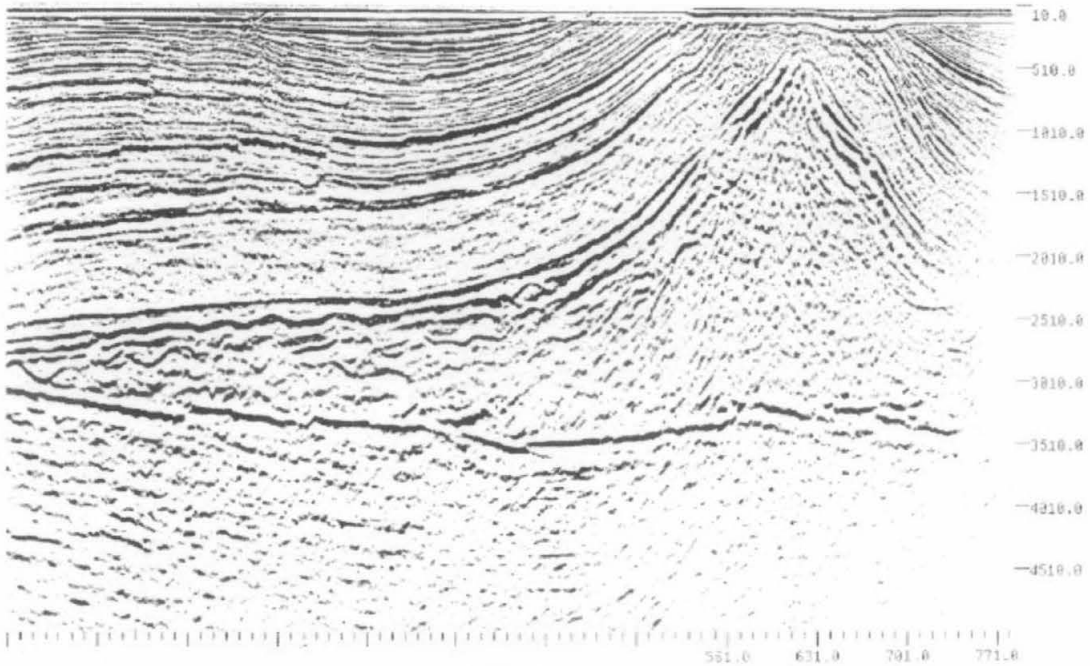

Figure 10. Prestack depth migration using layer stripping $V(x,z)$ model.

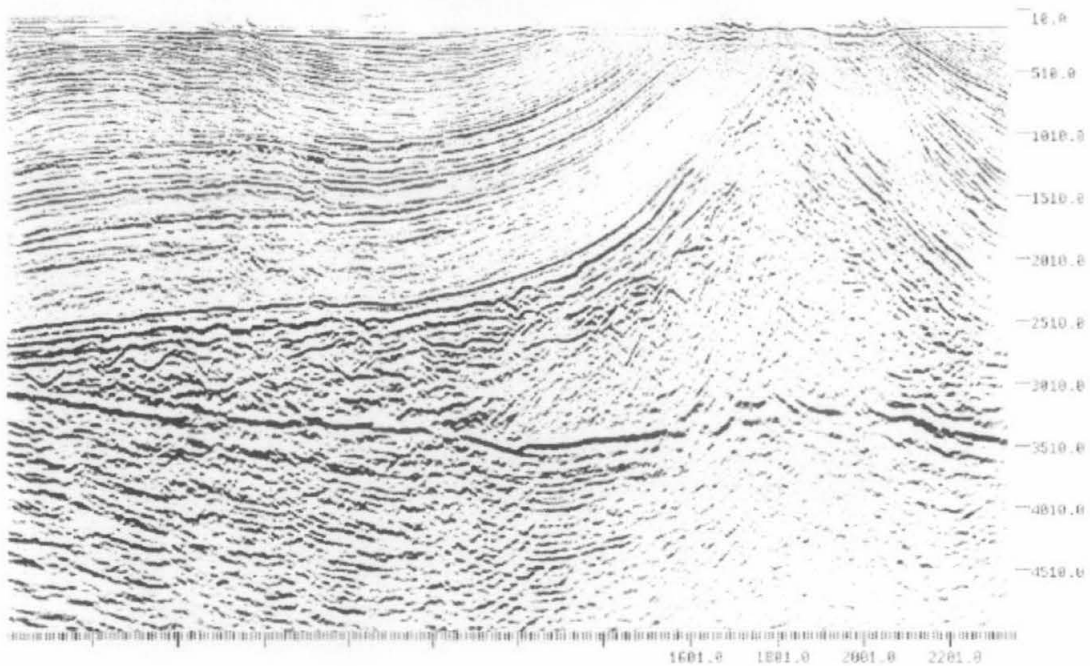

Figure 11. Poststack depth migration using prestack $V(x,z)$ model.

5) When the velocity estimate is correct, extend the interval velocity and gradient estimates to the next layer and return to step 2.

The accuracy and advantages of this method can be illustrated by comparison with a conventional stack on a real data example.

Figure 7 shows a conventional poststack migration of a salt conglomerate. There is a high in the sands below the salt and it generates the key question: *Is this just velocity pull up or is it structure?*

This is difficult, if not impossible to determine, from Figure 7. Let us see if the answer is clearer in the constant angle domain with interval velocities iteratively determined from the top downward.

We know the top layer is water and is flat at the surface, so we put that in and continue to the second layer. Figure 8 shows some of the iterations for the second layer where the "smile/frown versus flat" criterion implies a correct velocity of 2600 m/s.

The evolutions of the velocity model are shown in Figure 9. Figure 10 shows the prestack depth migration using the velocity model derived from the constant angle layer stripping technique and Figure 11 shows the poststack depth migration based on the interval velocities obtained from the prestack velocity model.

In both Figure 10 and Figure 11, most of the high under the salt that was present in Figure 7 has vanished. There is no closure here so the decision was made not to proceed in this area.

As this article demonstrates, this approach has proved viable with both model and real data. The cost is dependent on the algorithm used and the number of iterations required. If simple trial and error is used at each stage, the number of iterations can become large and the process tedious. However, the number of iterations can be reduced by inserting a velocity estimation step at each iteration. The velocity estimation step is generally based on a residual correction to the depth migrated data.

Multiples, out-of-plane events from three-dimensional structures, and poor signal-to-noise ratio have all been found to complicate the process. On the other hand, the efficiency of the method is generally improved when a knowledgeable interpreter helps perform the iteration process.

Suggestions for further reading. Constant angle processing of seismic data has been discussed by many authors. The relevant titles can be found in Rick Ottolini's *A Tau-p bibliography* (Stanford Exploration Project Report #51,1987).E

Acknowledgments: I wish to thank Larry Lines for encouraging me to submit this paper.